Department of Chemistry, Material Chemistry Division

Faculty of Science

University of Helsinki

Helsinki

Ionic Liquids in the Chemical Valorisation of Pulps and in their Chemical Analyses

Daniel Rico del Cerro

DOCTORAL DISSERTATION

Doctoral thesis, to be presented for public examination with the permission of the Faculty of Science of the University of Helsinki, in Auditorium A129, Chemicum Building, on the 10th of August, 2021 at 12 o'clock.

Helsinki 2021

Supervisor

Professor Ilkka Kilpeläinen

Department of Chemistry

University of Helsinki

Helsinki, Finland

Reviewers

Professor Henrikki Liimatainen

Fiber and Particle Engineering

University of Oulu

Oulu, Finland

Professor Jan Deska

Department of Chemistry

Aalto University

Espoo, Finland

Opponent

Professor Jouko Vepsäläinen

School of Pharmacy

University of Eastern Finland

Kuopio, Finalnd

ISBN 978-951-51-7325-6 (paperback)

ISBN 978-951-51-7326-3 (PDF)

Unigrafia

Helsinki 2021

The Faculty of Science uses the Urkund system (plagiarism recognition) to examine all doctoral dissertations.

ABSTRACT

The overall aim of this thesis is to understand the chemistry of different types of ionic liquids (ILs) and their application in cellulose processing, as well as in the chemical analyses of pulp. ILs are applied either on their own or as electrolytes with dimethyl sulfoxide (DMSO) or gamma valerolactone (GVL) as co-solvents. All of the ILs utilised in this work were synthesised in our laboratory via Menshutkin reaction followed by metathesis to different counter anions or via acid-base chemistry.

The beginning of our work focused on the investigation of the C2 chemistry of imidazolium ionic liquids (IMILs), one of the first class of ionic liquids utilised in biomass processing, resulting in the understanding of the C2 chemistry of IMILs under neutral and acidic conditions, which complete the comprehension on the mechanistic scenario of the C2 chemistry of IMILs. In this investigation, the importance of the quality of the ILs is remarked.

The studies continued to investigate the activation of the chemical reactivity of pulps using tetrabutylphosphonium acetate ([P_{4444}][OAc]), a more thermal stable ionic liquid. The non-dissolving pre-treatment of pulps by [P_{4444}][OAc] demonstrated a reduction in the crystallinity of the pulp to be directly related to its chemical reactivity enhancement. Additionally, [P_{4444}][OAc]:d_6-DMSO (20:80 wt.%) was also investigated in both the regioselectivity studies of acetylation reactions and the oxidised nanocellulose nuclear magnetic resonance (NMR) analyses. Quantitative heteronuclear single quantum correlation (HSQC) NMR was a suitable experiment for the quantitation of the oxidation level achieved in the nanocellulose, demonstrating the potential of this method for cellulose analyses.

Finally, the research concluded with the studies on other cellulose solvent systems, such as 1,8-diazabicyclo[5.4.0]undec-7-ene (DBU) with dimethylsulphoxide (DMSO), which resulted on the discovery of the unexpected reactivity of 1,1,3,3-tetramethylguanidinium acetate ([TMG][OAc]). Furthermore, this investigation led us to the design and synthesis of a novel task-specific ionic liquid (TSIL), so called 'TMG2sA'. This IL was investigated with regard to cellulose chemical modification, resulting in the high yield production of nanocellulose-type materials by a low demanding energy step, with a different approach than previously reported.

ACKNOWLEDGMENTS

First, I would like to thank Prof. Kristiina Wähälä, for hosting me as PhD candidate at the very beginning, when I originally started my PhD studies in ionic liquids. Unfortunately, the circumstances were not very appealing, so I chose not to continue with this research group.

After I left Wähälä´s research group, I noticed a vacant position in Prof. Ilkka Kilpeläinen's research group through a private company (UPM) for an industrial PhD, which I decided to apply for. I would like to thank Prof. Ilkka Kilpeläinen for providing me with the opportunity and space to develop myself as scientist and as member of his research group. I am extremely grateful to Prof. Ilkka Kilpeläinen for giving such a great opportunity at a very difficult and frustrating time of my life. I will never forget it. I greatly appreciate the freedom given to me to pursue my scientific interest and for the second chance to complete my PhD studies in Finland.

I would also like to thank Prof. Dage Sundholm for the great collaboration and for all of the encouragement while working toward the first publication. I tremendously appreciate your professional nature and all of the support given during the difficult times. At this point, I also want to thank Prof. Raúl Mera-Adasme, who together with Prof. Dage Sundholm, made my first publication in a high impact journal possible with their calculations. It was a great pleasure to work with both of you. Furthermore, I could not forget to mention Dr. Jesus Perea Buceta, who helped a lot in the elaboration of the introduction and in the formatting, especially in the images, of my first article and for all the support and help during my PhD studies.

Additionally, I want to give many thanks to Dr Alistair King for his co-supervision, input, scientific expertise and support. Despite the unpleasant situation during my second publication, we managed to professionally handle the situation. We all learned a lot and grew both professionally and personally.

I would also like to thank UPM-kymmene for financing my PhD studies, and especially Matti Ristolainen and Heikki Ilvespää for all of their support and interesting discussions during these years in the steering group meetings.

Furthermore, I would like to give my appreciation to all of my lab and office mates, group members and fellow chemists (past and present), who provided me with their scientific and technical support and good times during these years; this includes Eliza, Andreas, Alvaro, Mika, Niklas, Tiina, Gudrun, Sami, Gordon, Jesus, Eva, Alexander, Jussi, Matti, Jingwen, Maiju, Uula, Arno, Kalle, Hanna, Sofia, Marianna, Nicola and Ruth. Also, I want to thank the many other friends I made during my stay in Helsinki, like Virma, Fran, Ricardo, Filipe, Sara, Marta, Lady, Gali, Ismael, Luisa, Alvaro, Angela, Edu, Alex, Jonathan, Itziar, Foteini, Katharina, Vilma, Ines, Jacopo, Jaana, Miriam, Ana, and Tomasso. I want to apologise in advance if I have forgotten anyone, but the list is very long.

Here, I would like to remark upon the priceless and important work that the technical personnel are doing in the department of chemistry; for instance, Sami Heikkinen and Gudrun Silnnoinen, who are always available to give a hand with whatever is needed, even though it might not be directly connected to their daily duties. Many of the researchers and PhD candidates can perform their duties because people like Sami and Gudrun are there. I am sure that many of my work colleagues agree with this. Thank you very much for all of the help given.

To continue, I would like to make some special mentions to those who have been very important to me during this time in Finland.

1) I want to thank Mika, Gurdrun, Tiina and Niklas for all of the time we spent together in the labs and corridors, and at lunchtimes and social events we organised outside of the work environment. Even when I changed research group, we kept in touch and continued our scientific discussions, which we all enjoyed a lot. I miss our crazy lunch discussions. Thank you very much for all of these years!

2) I feel blessed to have had such a giver as Eliza Lambidis in Kumpula. She is a very good friend with a huge heart, and she is always ready to help and support in any matter at any time with her warm and tight hugs. It was extremely important to have your endless and beautiful friendship 24/7 just downstairs every day, not only in Kumpula. There are no words invented yet to appreciate it. Thanks a lot for everything! The white pigeon finally arrived!

3) I feel very lucky to have had the pleasure of meeting the German family (Dr Andreas Paulus, Katharina Franken and their daughter Vilma). They are pure love and a sign of that is their lovely cute daughter, Vilma. Unexpectedly, we ended up being in the same neighbourhood. The time we shared made me feel like I was at home. Big thanks for your true friendship. I miss our gatherings and dinners a lot. I wish you the very best back at home in Germany and I really hope to see you again soon.

4) I am extremely happy to have very good friends like Dr Andreas Kyritsakis and Foteini Andrikopoulou, who have also been there to help me and discuss anything I needed. I am extremely happy that we met. I enjoyed, and still I do, our meetings and the philosophical and scientific discussions, as well as all of the trips we have made together and those we will do in the future. Thank you for your Mediterranean friendship which I have been missing so much in Finland.

5) Last but not least, I want to thank Filipe Daniel Nunes Barbosa. Since we met in 2017, we have very often been together in many different situations; we could write a book about it! There are no words to describe what Felipe has been for me during this entire time.

Finally, I would like to show my appreciation and love to my whole family, but especially to my parents, brother, sister-in-law and nephews (Ana María, Jose Luis, Jose María, Yolanda, Raúl and Marcos) for their true love, trust and unconditional support since the very beginning, while I have spent all of this time abroad. Thank you for being there with all your unconditional support. Without them this would have been impossible.

CONTENTS

ABSTRACT 3
ACKNOWLEDGMENTS 4
LIST OF ORIGINAL PUBLICATIONS 9
AUTHOR CONTRIBUTIONS 10
ABBREVIATIONS 11
1. Background 15
1.1. Components of lignocellulosic biomass 15
1.1.1. Lignin 15
1.1.2. Hemicellulose 16
1.1.3. Cellulose 17
1.2. Cellulose solvents 21
1.3. Cellulose swelling and dissolution 23
1.4. Ionic liquids (ILs) 25
1.4.1. Classification of ILs based on their physical properties 26
1.4.2. ILs in biomass processing 28
1.5. Chemical modification of cellulose 30
1.5.1. Acetylation 31
1.5.2. Oxidation 31
1.5.3. Succinylation 31
1.6. Nanocellulose 32
1.6.1. Classification of nanocelluloses 32
1.6.2. Nanocellulose outlook 34
2. Aims of the study 35
3. Experimental & Methods 37
3.1. Cellulosic materials 37
3.2. Synthesis of ILs 37
3.2.1. Menshutkin reaction 37
3.2.2. Metathesis reaction 38
3.2.3. Acid-base chemistry reaction 39
3.3. IL pre-treatment of cellulose pulps 40
3.4. Cellulose acetylation 40
3.5. Cellulose oxidation 41
3.6. Analytical methods 41

3.6.1. Attenuated total reflection fourier transform infrared (ATR-FTIR) spectroscopy 41
3.6.2. Nuclear magnetic resonance (NMR) spectroscopy 42
3.6.3. Conductometric titration 44
3.6.4. Computational studies 45
3.6.5. Wide angle x-ray scattering (WAXS) 45
3.6.6. Gel permeation chromatography (GPC) 46
3.6.7. Optical microscope (OM) 46
3.6.8. Field emission scanning electron microscope (FESEM) 47
4. Results and Discussion 48
4.1. Purity of ILs 48
4.2. Activation of cellulose chemical reactivity by IL pre-treatment 51
4.2.1. Crystallinity reduction of cellulose with [P_{4444}][OAc] 51
4.2.2. Enhanced reactivity of [P_{4444}][OAc] pre-treated cellulose 53
4.3. Cellulosic sample analyses by liquid state NMR 58
4.3.1. Regioselectivity studies in acetylation reactions 58
4.3.2. Analyses of oxidised nanocelluloses 62
4.4. Reactivity of ILs – Their non-innocent nature 70
4.4.1. C2 Chemistry of IMILs 70
4.4.2. [TMG][OAc]; a mild acylation reagent 72
4.4.3. Design and synthesis of RILs and their application 76
4.4.4. Can there be benefits from the non-innocent nature of ILs? 81
5. Conclusions 82
6. References 83

LIST OF ORIGINAL PUBLICATIONS

This thesis is based on the following publications:

I. **D. Rico del Cerro**,* R. Mera-Adasme,* A. W. T. King, J. E. Perea-Buceta, S. Heikkinen, T. Hase, D. Sundholm,* K. Wähälä. *On the mechanism of the reactivity of 1,3-dialkylimidazolium salts under basic to acidic conditions: a combined kinetic and computational study. Angew. Chem. Int. Ed.*, **2018**, *57*, 11613-11617. doi:10.1002/anie.201805016.

II. **D. Rico del Cerro**, T. V. Koso. T. Kakko, A. W. T. King,* I. Kilpeläinen.* *Crystallinity reduction and enhancement in the chemical reactivity of cellulose by non-dissolving pre-treatment with tetrabutylphosphonium acetate. Cellulose,* **2020**, *27*, 5545–5562. https://doi.org/10.1007/s10570-020-03044-6.

III. T. Koso*, **D. Rico del Cerro**, S. Heikkinen, T. Nypelö, J. Buffiere, J. E. Perea-Buceta, A. Potthast, T. Rosenau, H. Heikkinen, H. Maaheimo, A. Isogai, I. Kilpeläinen, A. W. T. King.* *2D assignment and quantitative analysis of cellulose and oxidised celluloses using solution-state NMR spectroscopy. Cellulose*, **2020**, *27*, 7929–7953. https://doi.org/10.1007/s10570-020-03317-0.

IV. **D. Rico del Cerro**, A. W. T. King, M. Kemell, I. Kilpeläinen.* *Reactive Ionic Liquids (RILs) from 1,1,3,3-tetramethylguadine and their applications*. Manuscript.

The publications are referred to in the text by Roman numerals.

Other related publications:

1. T. Laksonen, J. K. J. Helminen, L. Lemetti, J. Långbacka, **D. Rico del Cerro**, M. Hummel, I. Filpponen,* A. H. Rantamälo, T. Kakko, M. L. Kemell, S. K. Wiedmer, S. Heikkinen, I. Kilpeläinen, A. W. T. King.* WtF-Nano: One-Pot dewatering and water-free topochemical modification of nanocellulose in ionic liquids or γ-valerolactone. *Chem Sus Chem*, **2017**, *10*, 4879-4890. https://doi.org/10.1002/cssc.201701344.
2. J.E. Perea-Buceta, **D. Rico del Cerro**, I. Kilpeläinen, S. Heikkinen.* Incorporated diffusion ordered heteronuclear multiple bond correlation spectroscopy, 3D iDOSY-HMBC. Merging of diffusion delay with long polarisation transfer delay of HMBC. *Journal of Magnetic Resonance*, **2020**, 106892. https://doi.org/10.1016/j.jmr.2020.106892.

AUTHOR CONTRIBUTIONS

For **publication I**, D. Rico del Cerro provided the conceptual idea of the investigation, carried out the experimental designs, conducted all of the experimental work, as well as the kinetic result analyses, and wrote the main text of the manuscript and supporting information, including the creation and editing of figures. In this publication, professors R. Mera-Adasme and D. Sundholm conducted all of the computational work and contributed to the writing process of the manuscript. Professors K. Wähälä and T. Hase contributed to the scientific discussion of the original idea and the preliminary results of the investigation. Dr A. King contributed to the experimental designs and results analyses. Additionally, Dr A. King, together with Dr J. E. Perea-Buceta helped with the editing of figures and the final manuscript. NMR Chief Engineer, PhD. S. Heikkinen was a huge help with the setup of the NMR experiments.

In **publications II and IV**, in all cases, D. Rico del Cerro contributed to the joint conception of the research ideas, performed the experimental designs, experimental work and analyses of the results, wrote the main text of the manuscripts and the corresponding supporting information, and created all of the figures. Supervisor professor I. Kilpeläien and co-supervisor Dr A. King were responsible for the joint conception of the investigations, as well as providing input and advice for the structure and content of the publications and experimental designs, editing and contributing to the final manuscripts and supervision of the research projects. In **publication II**, T. Kakko trained D. Rico del Cerro in the use of the GPC instrument and together with T. V. Koso, helped in the preparation of GPC samples, running the samples and analysing the results. They also contributed to the manuscript preparation. **In publication IV**, Dr M. Kemell helped to run the imaging of the nanostructured materials by field emission scanning electron microscopy (FESEM) and contributed to this part of the manuscript.

For **publication III**, D. Rico del Cerro performed the syntheses of the tetrabutylphosphonium acetate ($[P_{4444}][OAc]$) ionic liquid and the preparation of its electrolyte solution in deuterated dimethylsulphoxide (DMSO-d_6) for NMR analyses. He also contributed to the sample preparation and analyses of wide-angle X-ray scattering (WAXS), helped with the analysis of results and contributed to the manuscript preparation. T. V. Koso performed the experimental designs, experimental work, and wrote the main text of the manuscript. Supervisor professor I. Kilpeläien and co-supervisor Dr A. King were responsible for the joint conception of the investigations, as well as input into and advice on the structure and content of the publications and experimental designs, as well as editing and contributing to the final manuscripts and supervising the research projects. In this publication, NMR Chief Engineer, PhD. S. Heikkinen helped with the setup of the NMR experiments. The rest of the co-authors contributed to the oxidation studies.

ABBREVIATIONS

[bmim][OAc]	1-butyl-3-methylimidazolium acetate
[bmim]Cl	1-butyl-3-methylimidazolium chloride
[P_{4444}][OAc]	Tetrabutylphosphonium acetate
[TMG][OAc]	1,1,3,3-tetramethylguanidinium acetate
'TMG$_2$SA'	1,1,3,3-tetramethylguanidinium succinate
Å	Angstrom
AA	Acetic anhydride
AcNH-TEMPO	4-acetamido-2,2,6,6-tetramethylpiperidine-1-oxyl
AGA	Anhydroglucopyranosiduronic acid
AGU	Anhydroglucose unit
ATR-FTIR	Attenuated total reflexion-Fourier transform infrared spectroscopy
BNC	Bacterial nanocellulose
CC	Carboxylic content
CF_{diff}	Correction factor for diffusion-edited ^{1}H NMR
CI	Crystallinity index
cm	Centimetres
CMA	Cellulose monoacetate
CNCs	Cellulose nanocrystals
CNFs	Cellulose nanofibrils
CTA	Cellulose triacetate
D_2O	Deuterated water
DBN	1,5-diazabicyclo[4.3.0]non-5-ene
DBU	1,8-diazabicyclo[5.4.0]undec-7-ene
DCl	Deuterated acid chloride
DESs	Deep eutectic solvents
DILS	Distillable ionic liquids
DMF	Dimethylformamide
DMSO	Dimethylsulphoxide
DMSO-d_6	Deuterated dimethylsulphoxide

DO	Degree of oxidation
DP	Degree of polymerisation
DS	Degree of substitution
DS_{diff}	Degree of substitution for diffusion-edited ^{1}H NMR
E_a	Activation energy
Eq.	Equation
FESEM	Field emission scanning electron microscope
GPC	Gel permeation chromatography
GVL	Gamma-valerolactone
HMBC	Heteronuclear multiple bond correlation (spectroscopy)
HPLC	High performance liquid chromatography
HSQC	Heteronuclear single-quantum correlation (spectroscopy)
HSQC-TOCSY	Heteronuclear single quantum coherence-total correlation spectroscopy
I_A	NMR integral for acetate signal region
I_C	NMR integral for cellulose backbone signal region
IL-PT-NW	Ionic liquid pre-treated pulp non-washed
IL-PT-W	Ionic liquid pre-treated pulp washed
ILs	Ionic liquids
IMILs	Imidazolium ionic liquids
INEPT	Insensitive nuclei enhanced by polarization transfer (spectroscopy)
IPA	Isopropenyl acetate
KBr	Potassium bromide
LCOF	Linear combination of functions
LDP-CNC	Low degree of polymerisation-cellulose nanocrystals
LiCL/DMA	Lithium chlorite in dimethylacetamide
MCC	Microcrystalline cellulose
NaClO	Sodium hypochlorite
$NaClO_2$	Sodium chlorite
NFC	Nanofibrillated cellulose
nm	Nanometres

NMR	Nuclear magnetic resonance (spectroscopy)
NRE	Non-reducing end
ns	Number of scans
OM	Optical microscope
PSILs	Phase separable ionic liquids
Q-CAHSQC	Quantitative CPMG-type sequences adjusted HSQC
RE	Reducing end
RILs	Reactive ionic liquids
RTILs	Room temperature ionic liquids
SBILs	Super-base ionic liquids
sc-H_2O	Supercritical water
SILs	Switchable ionic liquids
TBBA	Tetrabutylammonium acetate
TBD	1, 5, 7-triazabicyclo[4.4.0]dec-5-ene
td	Time domain
TEMPO	2,2,6,6-tetramethylpiperidine-1-oxyl
THF	Tetrahydrofuran
TMG	1,1,3,3-tetramethylguanidine
Tox-LDP-CNC	TEMPO oxidised low degree of polymerisation-cellulose nanocrystals
TSILs	Task specific ionic liquids
VinAc	Vinyl acetate
WAXS	Wide-angle X-ray scattering
W_{LC}	Dry weight of loaded nanocellulose
W_{RN}	Dry weight of recovered nanocellulose
XRD	X-ray diffraction

More the knowledge lesser the ego, lesser the knowledge more the ego.

Albert Einstein (1879-1955)

1. Background

1.1. Components of lignocellulosic biomass

The most important sources of renewable feedstock are hardwoods, softwoods or agricultural residues (e.g., white straw). All of them belong to lignocellulosic biomass, which consists of a complex matrix including 1) pectins, 2) light molecular weight chemicals, known as extractives, 3) lignin, a polyphenolic biopolymer, and 4) cellulose and hemicellulose, which are carbohydrate polymers. The plant biomass is based on 40–45 wt% of cellulose, 25–35 wt% of hemicellulose, 15–30 wt% of lignin and up to 10 wt% other compounds.[1] This thesis mainly focuses on cellulose, due to its greater availability in the biomass. The three main polymeric components of biomass are briefly described below.

1.1.1. Lignin

Lignin fills the spaces between plant cells and strengthens cell walls by covering cellulose microfibrils. It provides compressive strength to conductive tissues, gives structural support to the plant, facilitates water transport and also acts as a barrier against the attack of insects and microbes.[2]

Chemically, lignin is an amorphous highly branched biomacromolecule, the detailed structure of which is still open to research due to its complexity. This heterogeneous polyphenolic biopolymer is formed by the radical polymerisation of three *p*-hydroxycinnamyl alcohol precursors known as monolignols,[3] which are *p*-coumaryl (4-hydroxycinnamyl) alcohol, coniferyl (4-hydroxy-3-methoxycinnamyl) alcohol, and sinapyl (3,5-dimethoxy-4-hydroxycinnamyl) alcohol (**Figure 1a**). In lignin, these monolignols are linked by different types of carbon-carbon or ether bonds forming *p*-hydroxylphenyl-, guaiacyl-, and syringyl lignin units, also known as H-, G-, and S units, respectively (**Figure 1b**). The abundance of these units, which form the structure of lignin, depends on several factors such as the plant species, location, growth duration and extraction process to separate it from cellulose and hemicellulose. For instance, guaiacyl units are predominant in softwood lignin, while hardwood lignin presents two major components: guaiacyl and syringyl units. In contrast, grass lignin has three units, but guaiacyl units predominate.

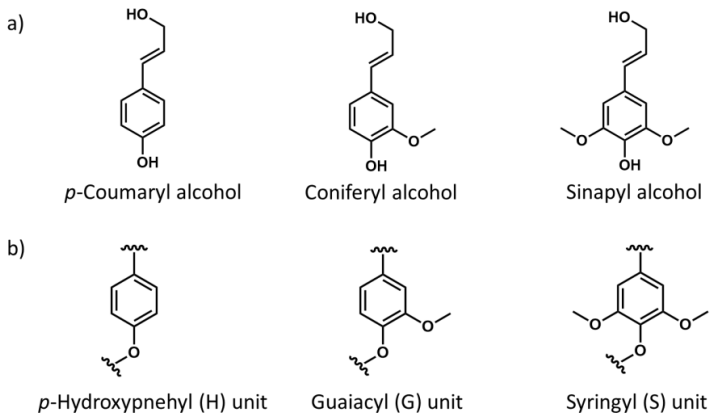

Figure 1. Main components of lignin adapted from Ralph et al. (2004). a) Monolignols. b) Typical linkages of monolignols in lignin; lignin units.

1.1.2. Hemicellulose

Hemicellulose is a branched polymer formed of glucose, galactose, mannose, xylose, arabinose and glucuronic acid.[4] The variety of substituents in the branches prevents an ordered crystal structure, thus enhancing its reactivity.[5] The composition and structure of hemicellulose depends on the wood species. Thus, there are various types of hemicelluloses, which are defined as a group of polysaccharides in the cell wall that are neither cellulose nor pectin and have a β-(1→4)-linked backbone of glucose, mannose or xylose moieties in equatorial configuration;[6] this also includes β-(1→4) glucans, β-(1→4) xylans, β-(1→4) mannans and β-(1→4) glucomannans (**Figure 2**). Hemicellulose is a relatively short polymer, with a degree of polymerisation (DP) between ~50 and 200.

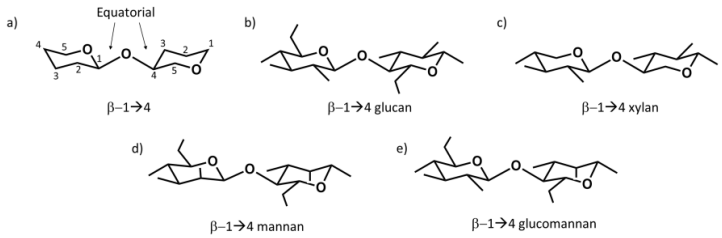

Figure 2. β-(1→4)-linked backbone of hemicelluloses. a) General hemicellulose backbone with equatorial configuration at C1 and C4, characteristic of all biomass hemicelluloses. b) β-(1→4) glucan. c) □-(1→4) xylan. d) β-(1→4) mannan. e) β-(1→4) glucomannan.

1.1.3. Cellulose

The word "cellulose" was first introduced by a French chemist, Anselme Payen in 1838.[7] Payen reported that ligneous matter, then considered a single substance, contained two chemically distinct materials. One of these, the French chemist declared, had the same chemical composition as starch, but differed in its structure and properties. Later, many other researches (*i.e.* Hermann Staudinger or Bernhard Tollens, among others) contributed to determine and characterise the biopolymer's structure.[8]

Cellulose is the most abundant natural polymer produced by living organisms and is the most important skeletal component in plants, due to its rigid structure.[9] As the main component of biomass, cellulose has a major role in the natural circulation of carbon, with plants acting as a huge sink for excess atmospheric CO_2.[10] Thus, cellulose is a vast source of environmentally friendly, sustainable and biocompatible raw material.[11] In Sections 1.1.3.1 and 1.1.3.2, cellulose is defined according to its structure and crystallinity, respectively.

1.1.3.1. Structure

In contrast with lignin and hemicellulose, cellulose is a partially crystalline polymer. Its primary structure consists of D-anhydroglucopyranose (AGU) units (cellulose monomer)[12]linked by β-(1→4) glycosidic bonds. These repeating units are bonded together through an acetal linkage between the first carbon of one glucose ring and the fourth carbon of the adjacent ring[11] (**Figure 3a**). The polymer present two different ends: 1) the reducing end (RE), which is an open ring structured AGU with a hemi-acetal group in the C_1 carbon with reductive properties, and 2) the non-reducing end (NRE), which lacks such reducing qualities (**Figure 3a**).

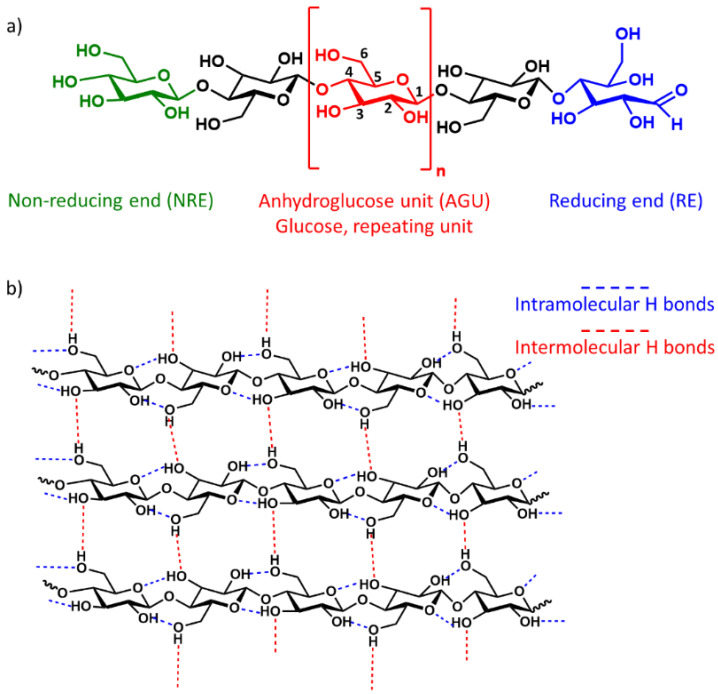

Figure 3. Molecular structure of cellulose. a) Linear representation of the polymer showing the non-reducing end (NRE), the repeating unit and the reducing end (RE). b) Hydrogen bonding network of cellulose with intermolecular H bonds in red and intramolecular H bonds in blue.

The AGU units are in $^{4}C_{1}$ chair conformation with the hydroxyl groups and the hydrogen atoms in equatorial and axial positions, respectively. The conformation and orientation of these units form the network of cellulose, which is based on intermolecular (between cellulose chains) and intramolecular (within a cellulose chain) hydrogen bonds[13] (**Figure 3b**). In this figure, a general hydrogen bonding network is pictured. However, the hydrogen bonding network of naturally occurring structures might contain anomalies in the H-bonding network.[14] These changes are associated with the different cellulose allomorphs (see Section 1.1.3.2 Cellulose Crystallinity).

Other important features used to distinguish between different types of celluloses are the length and molecular weight of the polymer, which depend on the source of the cellulose as well as on the processing methods.[15] These are measured by the degree of polymerisation (DP), describing the amount of anhydroglucose units per cellulose chain. In contrast to hemicelluloses, natural (non-treated) sources of cellulose present high DP values (DP_{w} ~10000),[11] whereas

processed celluloses show lower DP values (DP_w between 1000-8000).[15] In this study (**publications II-IV**), the DP_w of the used celluloses is approximately 1333, 1765, 1956 and 372 for Enocell pulp (mainly from birch) birch kraft pulp, eucalyptus kraft pulp and microcrystalline cellulose (MCC ~ 50 μm particle size, cotton linters, Avicel® PH-101), respectively.

Polydispersity is one more factor to consider, especially when there is a mixture of different length cellulose chains in the system (most of the cellulose samples). When the molecular weight distribution is broad, the sample is polydisperse, yet when the molecular weight is narrower, the sample is less polydisperse.[11]

Morphologically, cellulose is based on a complex system of fibrils, as shown in **Figure 4**, starting with cellulose macrofibrils (cellulose fibres observed under optical microscope (OM)), followed by microfibrils and elementary fibrils, which contain bunches of cellulose molecules.[11, 16]

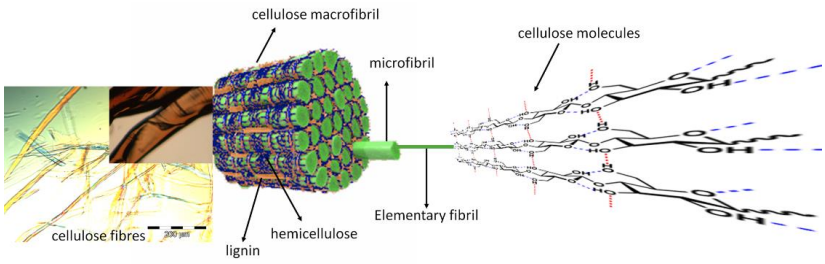

Figure 4. Morphological structure of cellulose. The complex system of fibrils, lignin and hemicellulose, shown in green, brown and blue, respectively.

1.1.3.2. Crystallinity

The mentioned anomalies in the H-bonding pattern of cellulose suggest that cellulose has two different regions: 1) high ordered, and 2) lower ordered parts. In other words, cellulose is a partially crystalline polymer with both crystalline and amorphous regions, as described by the fringed fibrillar model.[17]

Four different crystalline polymorphs of cellulose are known (cellulose I-IV), with different unit-cells for each of them. Cellulose I is native cellulose, with cellulose chains organised in a parallel sheet-like structure. The intermolecular H-bonds are between the C_3 hydroxyl oxygen (C_3-OH) and the C_6 hydroxyl hydrogen (C_6-OH) parallel to the pyranose

ring.[13a] Cellulose I can also be distinguished into two polymorphs,[18] depending on how the glucose units are staggered: 1) the anomeric hydroxyl group (C_1 carbon) of the reducing end is in the axial conformation, **cellulose I_α**, or in the equatorial conformation, **cellulose I_β** (**Figure 5**). Cellulose I_α is typically produced by algae and bacteria and cellulose I_β is from plants.

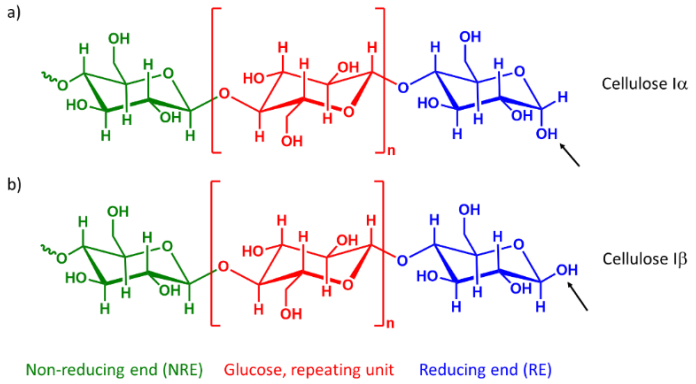

Figure 5. Polymorphs of cellulose I, depending on the conformation of the anomeric hydroxyl group of the reducing end (marked with a black arrow). a) Cellulose Iα. b) Cellulose Iβ.

Regenerated cellulose usually consists of Cellulose II crystal polymorphs, which cannot be converted back to cellulose I. Regenerated cellulose is obtained by dissolution and precipitation in an anti-solvent of cellulose I.[11] Cellulose II intermolecular hydrogen bonds are between the C_6 hydroxyl hydrogen (C_6-OH) and the C_2 hydroxyl oxygen (C_2-OH).[13b] Cellulose III and cellulose IV are manufactured polymorphs of lower importance. Cellulose III is produced by treatment with ammonia or amines, while cellulose IV is produced by treating cellulose II with hot water.[11]

Cellulose crystallinity can be measured by X-ray methods, including XRD (X-Ray Diffraction) or WAXS (Wide Angle X-ray Scattering). In this study (**publication II**), WAXS was used to quantify the relative amount of crystalline versus amorphous regions (crystallinity index, *CI*) in cellulose samples, as well as the identity of the crystalline regions.

1.2. Cellulose solvents

Certain cellulose applications require the prior dissolution of cellulose, for instance the production of textile fibres from wood.[19] Additionally, the solution state is the most efficient way to conduct chemical modification in cellulose, due to the higher accessibility of the polymer.[20] However, cellulose present a rigid highly ordered structure due to the polymer chain length and its hydrogen bonding network, which confers crystallinity to the biopolymer. This makes cellulose dissolution difficult, being insoluble in water and in most organic solvents. The requirement to dissolve cellulose is believed to be the elimination of the H-bonding network[21] (see Section 1.4.2).

Generally, cellulose in solution could be involved in many processes. For instance, acting as a) an acid if mixed with a base, such as sodium hydroxide, b) as a base, when mixed with an acid such as sulphuric acid or trifluoracetic acid, c) with a strong acid such as trifluoroacetic acid, when cellulose behaves as a reactive compound turning into a soluble derivative, and d) also acting as a ligand when mixed with a complexing agent like cuprammonium hydroxide.[22] The different roles that cellulose can adopt depend on the chemical or reagent it is confronted with, leading to a broad range of possible cellulose solvents and dissolution mechanisms. Therefore, a different cellulose solvent categorisation was established, where the cellulose solvents were classified into two main groups depending on whether 1) the solvent chemically modifies the polymer, so called 'derivatising solvents', or 2) the polymer is not chemically modified, 'non-derivatising solvents'.[21a] Ionic liquids (ILs, see Section 1.4 in this thesis) have been considered as non-derivatising solvents.[21b, 23] However, there are both types of ILs. For instance, certain ILs are known to react towards certain substrates, such as cellulose[24] or benzyl alcohol (**publication IV**). Thus, in this work, those ILs reacting with cellulose are so-called *reactive ionic liquids (RILs)*, corresponding to the 'derivatising' solvent classification. The term RILs is used independently of the IL category (see Section 1.4.1 in this thesis), including certain IMILs, such as 1,3-dialkylimidazolium acetates,[24] 1,1,3,3-tetramethylguanidinium acetate ([TMG][OAc]) and 1,1,3,3-tetramethylguanidinium succinate (TMG_2SA'), as shown in **Figure 6**.

To date, a broad list of the most typical derivatising and non-derivatising solvents, as well as the use of deep eutectic solvents (DESs) can be found in previous doctoral theses.[25] Thus, this work continues with its focus on the dissolution of cellulose (Section 1.3) and the cellulose solvents used, and ionic liquids (**publication I-IV**) in biomass processing (Section 1.4.2). Despite ionic liquids having also been reported in the above-mentioned theses,[25a-c] this topic has been extended here towards 1) understanding the reactivity of imidazolium ionic liquids (IMILs, **Figure 6a**) (**publication I**), 2) the use of the already known

tetrabutylphosphonium acetate[26] ([P_{4444}][OAc], **Figure 6b**) on cellulose activation and analyses of cellulosic samples via liquid state nuclear magnetic resonance spectroscopy (NMR, **publications II** & **III**), and 3) the design and synthesis of reactive ionic liquids (RILs, **Figure 6c**) and their applications (**publication IV**).

In summary, an ideal cellulose solvent needs to be chemically inert, preferably dissolving cellulose directly without sweeling stage and then the cellulose could be easily regenerated. However, 'non-innocent nature' solvents, such as RILs, might be attractive if the process could be optimised in a sustainable approach (i.e., reagent/solvent recyclability, low environmental impact and added value of the product.) In this study, RILs (**publication IV**, **Figure 6c**) are shown to have solvent/reagent duality. In other words, RILs acts as both the solvent and reagent, producing cellulose derivatives of interest in a single, relatively low cost and simple step. However, further research is still needed for its optimisation into, perhaps, a future alternative for the production of nanocellulose-type materials.

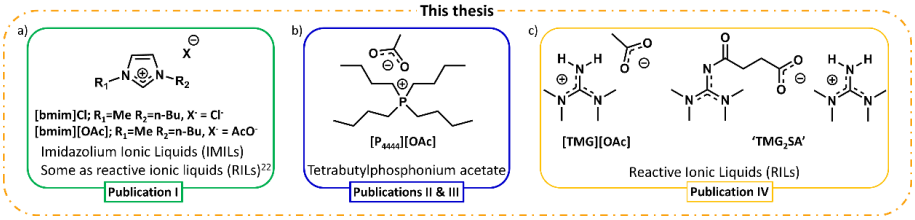

Figure 6. Ionic liquids studied in this thesis. a) Imidazolium ionic liquids (IMILs) in **publication I**, 1-methyl-3-butylimidazolium chloride ([bmim]Cl) and 1-butyl-3-methylimidazolium acetate ([bmim][OAc]). b) tetrabutylphosphonium acetate ([P_{4444}][OAc]), in **publications II** & **III**. c) Reactive Ionic Liquids (RILs), 1, 1, 3, 3-tetramethylguanidinium acetate ([TMG][OAc]) and 1,1,3,3-tetramethylguanidinium succinate ('TMG_2SA'), in **publication IV**.

1.3. Cellulose swelling and dissolution

Cellulose swelling correlates to relatively bad solvents, which are 'on the limit' for dissolution. With effective solvents there is no swelling, meaning that fibres go directly into solution. However, if a non-solvent is added to an efficient solvent, ballooning is observed. It is based on the competition of H-bonding between the cellulose chains and the swelling solvent. This solvent can be an organic liquid,[27] water,[28] or an ionic liquid.[29] The cellulose complex structure means that the mechanism of swelling and dissolution is heterogeneous. The swelling occurs by the diffusion of the solvent through the cellulosic material, breaking some of the hydrogen bonds in selected zones along the fibres (accessible regions of cellulose, i.e., amorphous regions). This localised swelling resembles "balloons" and it is known as swelling by ballooning.[30] In the swelling process of a wood fibre, four different zones are identified (**Figure 7**): 1) non-swollen fibres, 2) inside the balloon, 3) membrane surrounding the balloon, and 4) non-swollen sections between two balloons.[28, 29]

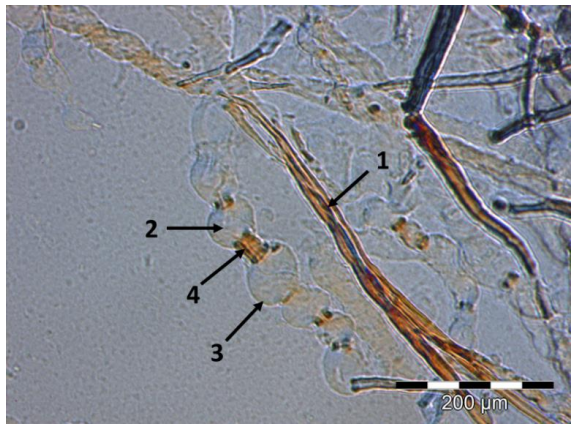

Figure 7. Enocell pulp in ´TMG_2SA´:DMSO-d_6 (20:80 wt%) electrolyte system at room temperature over weekend in absence of mechanical stirring (**publication IV**). 1) Non-swollen fibre, 2) inside of the balloon, 3) membrane surrounding the balloon, and 4) the non-swollen section between two balloons.

Based on the previous study of cellulose dissolution in NMMO and water mixtures, Cuissinat and Navard performed observations by optical microscopy for a wide range of solvent qualities, identifying four main modes of dissolution for wood and cotton fibres depending on the quality of the solvent.[28] **Figure 8** shows similar observations for the solvent systems used in this thesis.

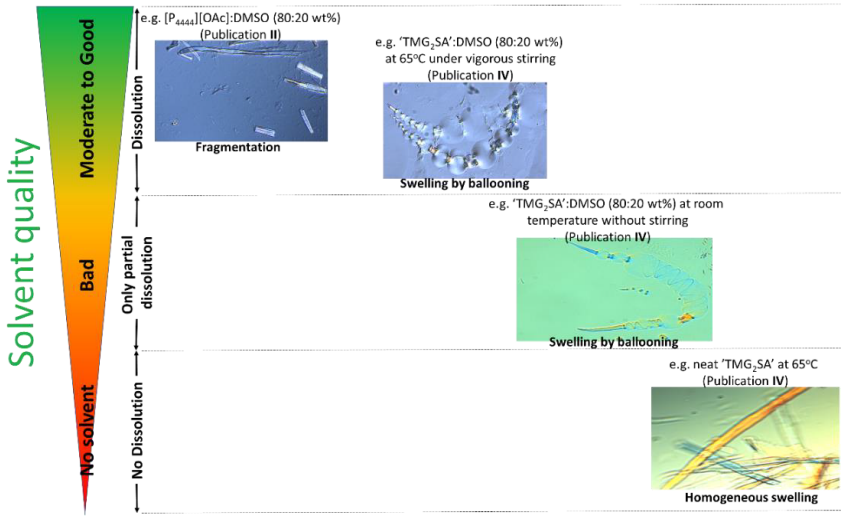

Figure 8. Swelling and dissolution mechanism of wood fibre as a function of solvent quality.

1.4. Ionic liquids (ILs)

Ionic liquids (ILs) can be considered an evolution from the traditional high melting temperature molten salts. The investigations for useful molten salts with lower melting points led to the discovery of diverse ionic liquids, as shown in **Figure 9**.

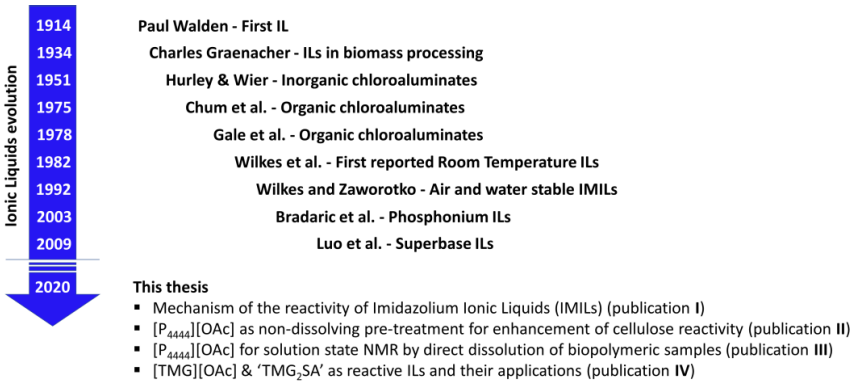

Figure 9. Historical evolution of ILs. [P_{4444}][OAc] = phosphonium ILs, more specifically in tetrabutylphosphonium acetate. [TMG][OAc] = 1, 1, 3, 3-tetramethylguanidinium acetate. 'TMG_2SA' = 1, 1, 3, 3-tetramethylguanidinium succinate.

The research into ILs was considered to have begun in 1914, with the conductivity investigations of molten salts by Paul Walden.[31] However, the neutralisation of ethylamine with concentrated nitric acid carried out by Walden was not yet termed IL and this discovery did not cause significant interest at the time. Nevertheless, today it is considered a remarkable legacy for the field of ILs, stabilising the current ionic liquid definition as 'a material composed of a cation and an anion with a melting point at or below 100°C'.[31] There were not many reports of ILs until 1934, when Charles Graenacher referred to ILs as "liquefied quaternary ammonium salts" for cellulose dissolution.[32] This patent could be considered as the milestone of the current research into ILs in biomass processing.

Just after World War II, ILs reappeared as inorganic chloroaluminates in a publication by Hurley & Wier[33] and later as organic chloroaluminates by Chum et al.,[34] both with a clear goal: the development of IL battery electrolytes. However, the very narrow compositional range and the easy reduction of the cations used limited their use and opened up the research into ILs with 1,3-dialkylimidazolium cations as an alternative, which were shown to be much less viscous and presented a wider electrochemical window.[35] This was the very first known report regarding room temperature ionic liquids (RTILs). However, these ILs were still moisture sensitive, which was their major drawback (chloride ILs are well-known

for their hygroscopic character). This led to the development of "air and water stable 1-ethyl-3-methylimidazolium based ionic liquids" in 1992 by Wilkes and Zaworotko, with alternative counter anions.[36] Since then, a wide range of ionic liquids has been developed, with many different counter anions and cations. Thus, the work of Wilkes and Zaworotko can be considered as the second milestone of ILs. Over the years to date, new classes of ionic liquids have been developed, such as phosphonium-based ILs[37] (**publication II**), and superbase ILs[38] (**publication IV**) with different applications. This thesis focuses on three different IL types: 1) imidazolium ionic liquids (IMILs, **publication I**), 2) phosphonium ILs, more specifically in tetrabutylphosphonium acetate[26] ([P_{4444}][OAc], **publications II** & **III**), and 3) superbase ILs, with two in particular: the well-known 1,1,3,3-tetramethylguanidinium acetate ([TMG][OAc])[39] and 1,1,3,3-tetramethylguanidinium succinate ('TMG_2SA'), a novel superbase IL designed and synthesised in this work (**publication IV**).

1.4.1. Classification of ILs based on their physical properties

The research into ILs has been growing exponentially in the past years, and most traditional and 'new' ILs to date can be classified in different groups, as shown in **Figure 10**.

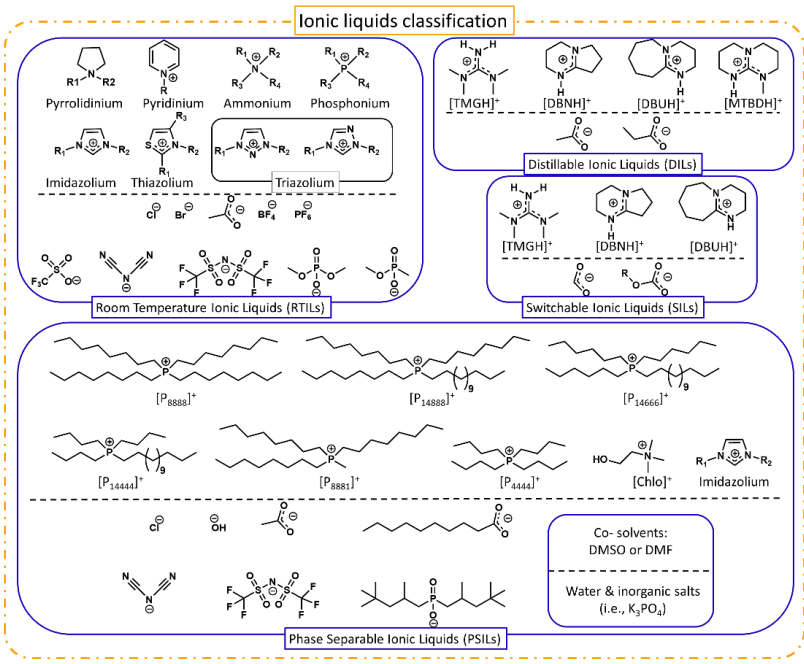

Figure 10. Classification of ILs into RTILs,[35-36, 40-41] DILs,[38-39, 42] SILs[43-44] and PSILs.[9, 26, 45-47]

In first place are the so-called **room temperature ionic liquids** (**RTILs**), whose melting point is at or below room temperature. This class of ILs started with the work of Wilkes and co-workers.[35, 36] From the original imidazolium cations, the RTILs had an explosive growth, with many other different heteroaromatic rings including pyrrolidinium, pyridinium, ammonium, phosphonium, thiazolium and triazolium cations.[40] The most commonly found anions are chlorides, bromides, acetates, tetrafluoroborates, hexafluorophosphates, triflates, dicyanamides, bis(trifluoromethylsulphonyl)imide, phosphates and phosphonates. The tetrafluoroborate and hexafluorophosphate ILs must be treated extremely carefully as they are readily hydrolysed to boric acid and phosphate, respectively.[41]

The significantly low melting points of these ILs allows lower processing temperatures in their applications, which is a great advantage, for instance in biomass processing (see Section 1.4.2), avoiding the thermal degradation of cellulose. In the last decade, some of these RTILs, such as 1-ethyl-3-methylimidazolium acetate ([emim][OAc]), among others, have been scaled up to industrial production by chemical companies like BASF.

In second place are the **distillable ionic liquids** (**DILs**), characterised by their ability to dissociate back to the original components which form the ionic liquid, by simple distillation. These ILs are normally formed by a superbase such as 1,1,3,3-tetramethylguanidine (TMG), 1,5-diazabicyclo[4.3.0]non-5-ene (DBN) or 1,8-diazabicyclo[5.4.0]undec-7-ene (DBU) and an organic acid, for instance acetic acid or propionic acid.[38-39] However, in some other cases, the distillable IL can also be composed of a base like dimethylamine and CO_2.[42] Ideally, these type of ILs would overcome the purification and recyclability issues in the industrial processes, but not the high cost, due to the current price of ILs.

Switchable ionic liquids (**SILs**) are in third place. These types of ionic liquids are typically formed by the mixture of an alcohol and organic superbase, such as 1,8-diazabicyclo[5.4.0]undec-7-ene (DBU) while bubbling CO_2 gas at room temperature, producing the corresponding IL [DBUH][RCO_3]. The IL reverts to the original components by simple inert gas (nitrogen or argon) bubbling. [43a] This principle is based on CO_2 capture by the superbase and the resulting IL has been reported in cellulose dissolution[43b-c] as a method for cellulose derivatisation.[44]

Finally, in fourth place are **phase separable ionic liquids** (**PSILs**), which are either 1) two combined ionic liquids,[45] or more commonly 2) an IL together with a co-solvent. The co-solvent is an aprotic organic solvent such as dimethyl sulphoxide (DMSO) or dimethylformamide (DMF).[26a, 46] These ILs are mainly

phosphonium or imidazolium ILs, and IL-water mixtures with added inorganic salts have also been reported in this category.[47]

In summary, the first IL category (RTILs) is formed by a wide range of IL families, including pyrrolidinium, pyridinium, ammonium, phosphonium, imidazolium, thiazolium, and triazolium ionic liquids (IMILs), while the second (DILs) and third (SILs) categories are mainly formed of superbase ionic liquids (SBILs), and the fourth category (PSILs) is formed primarily by phosphonium ionic liquids (**Figure 10**).

Additionally, the non-innocent nature of certain ILs need to be considered (see Section 4.1 in this thesis), which is highly important, especially in biomass processing. In some cases, the unexpected reactivity of ILs is not desirable at all; however, certain reactivity in the ionic liquid might be required for others . Thus, this is where the design and synthesis of RILs is needed (**publication IV**). The reactivity of ILs is not limited to their category. For instance, [emim][OAc] and [TMG][OAc] are RILs, but they belong to different IL categories: RTIL and DIL, respectively. Therefore, the term RILs is used independent of the IL category.

1.4.2. ILs in biomass processing

This thesis focuses mainly on the utilisation of ILs in cellulose. Thus, lignin or hemicelluloses will be discussed in this section.

The history of ILs in biomass processing dates from 1934 in Graenacher's patent using "liquefied quaternary ammonium salts" for cellulose dissolution.[31] In more recent times, Swatloski and co-workers demonstrated the solubility of cellulose by a series of IMILs, with 1-butyl-3-methylimidazolium chloride being the most effective solvent.[23] In the last decade, the first RTILs for cellulose dissolution were reported by Fukaya et al.[49] This was a huge improvement, due to the lower melting point of the IL allowing for lower operating temperatures, thereby avoiding the thermal degradation of cellulose. Furthermore, the ILs introduced by Fukaya and co-workers show very low viscosity, allowing for rapid cellulose dissolution at high concentrations.[49] Apart from this, a well-known IL for cellulose dissolution is [emim][OAc], which was one of the first ILs to be industrially produced. The very first ILs for cellulose dissolution were mainly IMILs. However, their high toxicity and low biodegradability,[50] as well as the non-innocent nature of some of them,[24] forced the researchers to look for other alternatives, such as distillable (DILs),[38-39, 42] switchable (SILs)[43-44] and phase separable ionic liquids (PSILs).[9, 26, 45-47]

Regarding the cellulose dissolution mechanism, researchers agree that the dissolution in ionic liquids is based on the role of the hydrogen bond interaction of the basic anion, which breaks the cellulose hydrogen bonding network.[51] However the role of the IL cation is more controversial, with some authors suggesting 1) a negligible role,[51a-b, 52] 2) a minor role by van der Waals interactions or electrostatic interactions,[53] and 3) hydrogen bonding between the cation and cellulose.[51d, 54]

Finding ideal IL candidates for biomass processing is a challenge. For instance, an essential factor to be considered when working with ILs in biomass processing is their purity. Impurities can cause solubility issues[55] or may introduce degradation problems (acid or base residues), colour formation, etc. (see Section 4.1). In **publication I**, the presence of different impurities in IMILs have been demonstrated to drastically influence their thermodynamics. Furthermore, PSILs are usually expensive and often toxic. SILs are not good solvents for cellulose (poor solubility), unless they are combined with a co-solvent. Additionally, the super bases on SILs and DILs are usually prone to hydrolysis.

However, certain ILs have been shown to be more attractive than others. For example, in **publication II**, tetrabutylphosphonium acetate ([P_{4444}][OAc]) is shown to enhance cellulose reactivity due to the reduction in crystallinity. Additionally, in **publication III**, analyses of oxidised celluloses by 2D NMR techniques are performed in [P_{4444}][OAc]:d_6-DMSO (20:80 wt.%) electrolytes. Furthermore, in **publication IV**, the design and synthesis of ILs targeting specific cellulose chemical modifications in a single step is demonstrated. Thus, the general assumption of ILs as non-derivatising solvents[21b, 23] is wrong, as it depends on the type of IL.

Finally, major concerns to be considered in biomass processing are cost and toxicity, as in any process using complex solvents. Regarding ILs, the cost is dictated by the starting materials needed for their production. In general, the IL cost is rather high, which will certainly limit its applicability. With respect to the toxicity, it is well-known that certain IMILs and phosphonium ILs are highly toxic. However, there are not many in-depth studies about the toxicity of the huge variety of ILs. However, some preliminary toxicity studies have been performed,[56] where phosphonium ILs with short chains in the cation (*e.g.* P_{4441}) seem to be preferred over IMILs. In addition, tetraalkylphosphonium-based ionic liquids are much more stable than other cation classes, such as imidazolium or choline-based structures.

1.5. Chemical modification of cellulose

To date, the only commercial product with thermoplastic properties derived from the chemical modification of cellulose is cellulose acetate. However, the cellulose acetate market tends towards an asymptotic behaviour. Thus, other alternatives are currently under investigation at an industrial level with focus on two main targets: end products with thermoplastic properties (other than cellulose acetate) and textile fibres from wood feedstock.

The chemical modification of cellulose enables the introduction of functional groups in the cellulose backbone. Cellulose presents two main reaction sites: primary or secondary hydroxyl groups. In general, primary hydroxyls are more prone to react. Additionally, cellulose, as well as hemicelluloses, contain glycosidic bonds, which are susceptible of hydrolytic cleavage reactions, especially under acidic conditions, leading to chain degradation and lowering the degree of polymerisation (DP).[11]Certain desired cellulose products, such as thermoplastic cellulose derivatives require keeping cellulose integrity. In an appropriate solvent selection system, reagents and reaction conditions avoid the degradation of the biopolymer. Nevertheless, degradation of the biopolymer can be also a desired property. For instance, production of bioethanol requires hydrolysis of cellulose.

The degree of substitution (DS) quantifies the chemical modification of cellulose. It is a measure of the average amount of substituted hydroxyl groups which have been replaced by a functional group in an anhydroglucose unit. The DS value varies from 0 to 3, meaning that there are 3 hydroxyl groups in one anhydroglucose unit. There are two main types of cellulose chemical modification: homogeneous (cellulose is dissolved, and cellulose chains are modified in a homogenous solution) and heterogeneous (fibres, microfibrils, nanofibres or nanocrystals, etc. are modified in a heterogeneous suspension).

The chemical modification of cellulose covers an extended research area, including esterified, etherified and oxidised celluloses.[11] This thesis mainly focuses on the acetylation, oxidation and succinylation of cellulose. These were chosen as model reactions, as they have been commonly studied in other cellulose solvents.[57]

1.5.1. Acetylation

The acetylation of cellulose has been widely studied in common non-derivatising cellulose solvents.[58] This reaction is commonly performed in the presence of catalysts[58b, 59] with different acetylating agents, such as AA[60] and recently with vinyl acetate (VinAc) or isopropenyl acetate (IPA).[61, 62] The manufacturing of cellulose acetate is done by activation or pre-treatment, involving mixing the raw material with water and acetic acid. The pre-activation mixture might contain small amounts of sulphuric acid. The activated raw material is then reacted with a mixture of pre-chilled acetic anhydride, acetic acid and sulphuric acid to produce primary cellulose triacetate, which may be subjected to hydrolysis to produce cellulose acetate of any desired degree of acetyl content.[63] In this work (**publication II**), cellulose acetylation is performed by acetic anhydride (AA) and IPA assisted by non-dissolving IL pre-treatment (see Section 4.2 in this thesis).

1.5.2. Oxidation

The selective oxidation of cellulose at C6 has been heavily studied using the popular 2,2,6,6-tetramethylpiperidine-1-oxyl (TEMPO)[64] nitroxyl radical catalyst or the more water soluble 4-acetamido-2,2,6,6-tetramethylpiperidine-1-oxyl (AcNH-TEMPO) catalyst.[65] The latter is used in this study (**publication II**) due to its higher activity.

1.5.3. Succinylation

Succinic anhydride-modified celluloses have been previously used in several different reaction conditions, such as tetrabutylammonium acetate (TBAA)/DMSO solvent mixtures without catalysts,[66] organic solvents[57d] with high shear mixers,[57e] and also with IL as a solvent[57f] and by ball milling.[67] However, in this thesis (**publication IV**) the succinylation of cellulose is studied by IL-cellulose modification. A novel IL designed with a succinic anhydride lateral chain is used to react with cellulose. This results in the production of a nanocellulose-type material, with the succinic anhydride chain attached.

1.6. Nanocellulose

Nanocellulose (**Figure 11**) is described as the product or extract from native cellulose and can be classified into three main types: 1) **cellulose nanocrystals (CNCs)**, also known as nanocrystalline cellulose, cellulose nanowhiskers or rod-like cellulose microcrystals, 2) **cellulose nanofibrils (CNFs)**, also called nanofibrillated cellulose (NFC), and 3) **bacterial nanocellulose (BNC)**, also referred to as microbial cellulose.

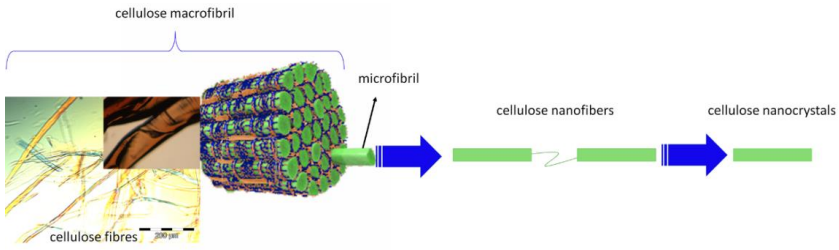

Figure 11. Illustration of cellulose macrofibril to cellulose nanocrystals.

The development of nanotechnology has attracted great attention on nanocellulose as an advanced material. Nanocellulose has small dimensions and a high surface-to-volume ratio. Nanocelluloses in general have excellent structural, physicochemical, mechanical, and biological properties.[68] For instance, bacterial cellulose has high mechanical strength, improved crystallinity, high biocompatibility, biodegradability, polyfunctionality, hydrophilicity and moldability into 3D structures.[68a, 68c-d] CNFs also have good mechanical strength and optical transparency. All of these properties make nanocellulose, both alone and as composite form with other materials, considered a prime candidate for a myriad of applications such as wound dressing, textiles and clothing, food, cosmetics, regenerative medicines, tissue engineering, energy optoelectronics, bioprinting, etc.[9, 68-69] Additionally, the great number of hydroxyl groups in nanocellulose make it highly hydrophilic and it can be modified via different chemical and physical strategies.[70]

1.6.1. Classification of nanocelluloses

According to the production strategies, nanocelluloses are classified as follows:

1.6.1.1. Cellulose nanocrystals (CNCs)

CNCs are typically prepared in two steps: the pre-treatment of the raw material followed by its hydrolysis into CNCs. The pre-treatment, usually alkaline or bleaching, removes impurities from the raw material such as waxes,

hemicelluloses and lignin. Then, the purified raw material is heated in an acidic environment to hydrolyse the fibers,[71] resulting in a suspension which, after centrifugation, leads to CNCs. The size of the obtained CNCs varies depending on several factors like cellulose source, acid type, operating temperature and time.[72]

In the hydrolysis step, sulphuric acid[73] is preferred over hydrochloric acid due to the stability of the whiskers solution.[74] However, phosphoric acid has been reported as an alternative resulting in the higher thermal stability of the nanocrystals when compared to nanocrystals produced with sulphuric acid or hydrochloric acid.[75] Alternatively, CNCs can be produced by enzymatic-mediation,[76] or by oxidants such as 2,2,6,6-tetramethylpiperidine-1-oxyl (TEMPO).[77]

1.6.1.2. Cellulose nanofibres (CNFs)

CNFs are prepared by the physical separation of cellulose fibres, for instance by grinding, homogenisation and ultrasonication.[78] Additionally, chemical methods such as TEMPO oxidation[79] are also utilised to help the homogenisation. Furthermore, both mechanical (high-pressure homogenisation) and chemical (carboxymethylation) methods can be combined for the production of CNFs.[80] Similarly to CNCs, the size of the produced CNFs can vary.[81]

In both CNCs and CNFs, the production procedures consist of cutting off the large unit (cm) from the small unit (nm).

In the present work, the lack of mechanistical understanding on how the nanocellulose type material is formed, makes challenging yet to categorize it as CNC or CNFs.

1.6.1.3. Bacterial nanocellulose (BNC)

BNC is naturally produced by different microorganisms such as *Acetobacter, Rhizobium, Agrobacter, Achromobacter, Azotobacter, Salmonella, Escherichia and Sarrcina*.[82] In contrast with CNCs and CNFs, BNC production is a non-destructive process, consisting of a construction process from tiny units (Å) to small units (nm). The structural characteristics and physico-mechanical properties of BNC

depends on the microbe type, synthesis method and culture conditions, including carbon and nitrogen sources.[83]

1.6.2. Nanocellulose outlook

The methodologies to produce nanocelluloses exhibit several drawbacks, such as the use of high concentrations of acids,[71, 84] several purification steps,[85] or the use of mechanical approaches.[86] All of these go along with an expensive technology which requires high energy consumption and, in some cases, leads to environmental issues, such as the generation of effluents or sulphur containing by-products.[87] In addition, the reported yields among all the different methods are relatively low,[88] with the exception of carboxylated cellulose nanocrystals produced via oxidising agents.[89] Recently, Kontturi et al. reported a high yield methodology for the preparation of CNCs, which was based on acid hydrolysis by hydrogen chloride vapour,[90] meaning that chlorinated products were expected as side effects.

On the other hand, nanocellulose surface chemistry has been intensively researched during the last decades, aiming for specific physical properties, which can be easily achieved by different strategies.[91] However, the production of nanostructured cellulose avoiding the use of corrosive acids or expensive technologies seems to be a challenge. Thus, in this study (**publication IV**) a novel RIL has been designed and synthesised to produce high yield chemically modified nanocellulose-type materials in a single low demanding energy step in the absence of acids or mechanical treatments other than simple mechanical stirring. However, further research is still needed for its optimisation.

2. Aims of the study

This work presents a double aim. The **first aim** is based on already known ILs, where the work focuses on;

> 1) The mechanistic study of the C_2-chemsitry of the imidazolium ionic liquids, such as 1-butyl-3-methylimidazolium chloride ([bmim]Cl), 1-butyl-3-methylimidazolium acetate ([bmim][OAc]).
>
> 2) The utilisation of tetrabutylphosphonium acetate ($[P_{4444}][OAc]$) in both, the activation of cellulose by non-dissolving pre-treatment and in the quantitative analysis of oxidised celluloses by 2D NMR techniques.

The **second aim** of this work is the investigation of novel task-specific ionic liquids towards cellulose derivatization and nanocellulose-type material production, which yet could not be classified as CNCs or CNFs, due to the lack of understanding on its mechanism formation. However, it is for sure not BNC, due to the formation of nanocellulose-type material is obtained via destructive, rather than constructing approach.

Although imidazolium ionic liquids (IMILs) have been broadly investigated, a variation in the deuteration speed of the C-2 position of the imidazolium ring was observed. Typically, the C-2 chemistry of imidazolium rings has been explained via carbene formation. However, the speed of the reaction in some of the experiments was too slow to have carbene species involved. The reaction mechanism, as well as the role of the basicity of the anion and impurities, were investigated (**publication I**). This firs publication in the present work is highly important to understand better the mechanism of C2-chemistry of IMILS. This C2-chemistry is known to be related with the reactivity of IMILs at the reducing ends of cellulose.

The high toxicity and low thermal stability of the IMILs, together with their 'unexpected' reactivity, motivate these studies to be continued with $[P_{4444}][OAc]$, a less reactive alternative. This IL has been widely used in biomass processing. Thus, its use in cellulose activation by a non-dissolving pre-treatment was investigated, resulting in the enhancement of cellulose reactivity, due to the reduction of cellulose crystallinity (**publication II**). Additionally, this IL in combination with a polar co-solvent, such as DMSO or DMF, is known to dissolve cellulose. Therefore, the $[P_{4444}][OAc]$:DMSO-d_6 (20:80 wt%) electrolyte system was investigated for NMR solution state analyses of cellulosic samples, where a general quantitative NMR spectroscopic method for the structural determination of crystalline cellulose samples was rigorously demonstrated (**publication III**).

The trend in recent years towards the utilisation of superbase-based ILs together with the controversial role of CO_2 in cellulose dissolution with switchable solvents, motivated the work to continue towards the study of superbase ILs, with a clear goal: the design and synthesis of task-specific ionic liquids for cellulose modification, which also resulted in the production of chemically-modified nanocellulose-type materials by a readily available, low cost and simple method

(**publication IV**). However, further research is still needed for its optimisation to, perhaps, a future alternative for the production of nanocellulose-type materials.

3. Experimental & Methods

Cellulosic materials, ILs syntheses, IL pre-treatment of cellulose pulps, reactions with cellulose and analytical methods in this thesis are briefly reported in this section. More experimental details are to be found in the attached publications or in their supporting information.

3.1. Cellulosic materials

The cellulosic materials used in this work are microcrystalline cellulose (MCC, Avicell® PH-101), which was purchased from Sigma-Aldrich, Enocell (bleached hardwood pre-hydrolysis kraft pulp containing ~6.8 % xylan), which was obtained from the Enocell Mill of Stora Enso company, located in Uimaharju (Finland), and birch (bleached birch kraft pulp, 87.7% α-cellulose) and eucalyptus (eucalyptus kraft pulp, 87.4% α-cellulose), obtained from UPM Kaukas Mill (Finland) and UPM Fray Bentos Mill (Uruguay), respectively.

3.2. Synthesis of ILs

All of the ILs used in this thesis have been synthesised in the laboratory and characterised by NMR. The synthesis of ILs have been performed by 1) Menshutkin reaction, 2) metathesis reaction, or 3) simple acid-base chemistry reaction by the addition of an acid to a superbase.

3.2.1. Menshutkin reaction

The conversion of a tertiary amine into a quaternary ammonium salt by its reaction with an alkyl halide is known as a quaternisation reaction or Menshutkin reaction. A similar reaction also occurs with phosphines. The most common examples are the synthesis of 1,3-dialkylimidazolium ILs (**publication I**) and tetrabutylphosphonium acetate (**publications II** & **III**)

3.2.1.1. Synthesis of 1-butyl-3-methylimidazolium chloride

1-methylimidazole was charged into a two necked round bottomed flask with a calcium chloride tube capped reflux condenser. The system is flushed with argon. Then, *n*-butyl chloride, 1.5 molar equivalents, was added dropwise under vigorous stirring and refluxed for 48 hours. The excess of butyl chloride was removed under reduced pressure resulting in a pale-white solid, which was recrystallised obtaining white crystalline 1-butyl-3-methylimidazolium chloride. It was needed to be sealed under argon due to its high hygroscopicity.

3.2.1.2. Synthesis of tetrabutylphosphonium chloride

Tri-*n*-butylphosphine and *n*-butyl chloride were added sequentially and in one portion to a Teflon-lined Parr acid digestion vessel under argon atmosphere. The vessel was sealed, and the reaction is conducted at 120°C under vigorous stirring overnight. The light excess of *n*-butyl chloride was removed under reduced pressure resulting in a wet white solid, which is further dried in a high-vacuum rotary evaporator at 60°C to produce the desired tetrabutylphosphonium chloride and stored under argon.

3.2.2. Metathesis reaction

The metathesis reaction was a commonly used technique for exchanging counter-anions of ILs.[26] In this work we utilised it to change the chloride to acetate anion by 1) silver acetate and 2) potassium acetate to obtain 1-butyl-3-methylimidazolium acetate and tetrabutylphosphonium acetate, respectively.

3.2.2.1. Synthesis of 1-butyl-3-methylimidazolium acetate

1-butyl-3-methylimidazolium chloride was charged into 100 ml round bottomed flasks and dissolved in methanol (HPLC grade). Silver acetate, 1 molar equivalent, was added under light protection. The reaction mixture was continuously

mixed at room temperature overnight. Silver particles were filtered out of the crude product and methanol was evaporated to obtain a light yellow highly viscous 1-butyl-4-methylimidazolium acetate, which was also stored under argon.

3.2.2.2. Synthesis of tetrabutylphosphonium acetate

Tetrabutylphosphonium chloride was dissolved in Isopropanol (IPA 10 x v/w) and 1.05 mol equivalents of potassium acetate were added. The solution was stirred under reflux for two hours and continuously stirred at room temperature overnight. The solution was cooled down in a fridge (~4-6°C), filtered through celite, and then the filtrate was evaporated to dryness. Acetone was added and left to settle in the fridge overnight to precipitate the excess of potassium salts. Finally, the solution was filtered through celite once more and the acetone was eliminated by reduced pressure yielding white-light yellow tetrabutylphosphonium acetate.

3.2.3. Acid-base chemistry reaction

Superbase ILs utilised in this work have been synthesised by a simple acid-base chemistry reaction, consisting of the mixture of a superbase and an organic acid. Generally, this reaction is highly exothermic. Thus, an ice bath was used for cooling the reaction during the addition of the base over the acid (or vice versa). This work (**publication IV**) focuses mainly on two superbase ILs: 1,1,3,3-tetramethylguanidinium acetate ([TMG][OAc]) and 1,1,3,3-tetramethylguanidinium succinate (TMG_2SA').

3.2.3.1. Synthesis of [TMG][OAc]

1,1,3,3-tetramethylguanidine (TMG) was loaded into a 250 ml round bottomed flask equipped with an addition funnel. TMG was cooled down to 0°C and acetic acid, 1 molar equivalent, was added dropwise under ice-bath and vigorous stirring, rapidly producing a white solid. The remaining acidic vapours were removed by reduced pressure.

3.2.3.2. Synthesis of 'TMG$_2$SA'

1,1,3,3-tetramethylguanidine (TMG) was mixed with tetrahydrofuran (THF) in a 250 ml round bottomed flask equipped with an addition funnel. Two molar equivalents of succinic anhydride, dissolved in tetrahydrofuran, were added dropwise into the TMG-THF solution. This was a highly exothermic mixture. Thus, slow addition was of high importance for the thermal stability of the product. Tetrahydrofuran was eliminated under vacuum and the white powdery product was dried in the Schleck line for 4 hours. The product, which was highly hygroscopic was stored under argon.

3.3. IL pre-treatment of cellulose pulps

The selected IL for cellulose pulp pre-treatment, [P_{4444}][OAc], was charged into a glass pressure tube and melted at 80°C. Then, 10 wt% of the desired dry pulp was soaked into the IL and the mixture was homogenised using a vortex and heated at 120°C for 5 hr. The non-dissolved pre-treated pulp was stored in a sealed flask under argon atmosphere for further homogeneous experiments. Additionally, a portion of this material was thoroughly washed with distilled water to remove the IL, filtered, dried under vacuum and stored in a sealed flask prior to further heterogeneous reactions and crystallinity analyses.

3.4. Cellulose acetylation

Reactivity studies of pre-treated and non-treated cellulose pulps were performed by reacting ~1wt% of pulp at 165°C for 18 hr in either of two different acetylating agents: acetic anhydride (AA) and the less reactive isopropenyl acetate (IPA).

Three different approaches for each type of pulp were conducted in parallel. These include the reaction of 1) the raw pulp as a reference, 2) the pre-treated pulp, with the consecutive aqueous IL removal step (heterogeneous reaction, IL-PT-W), and 3) the pre-treated pulp without the consecutive IL removal step (IL-PT-NW). This is termed as a 'homogeneous reaction' by virtue of the fact that when acetylating agent is added, the cellulose rapidly swells and mostly dissolves during the reaction. The full procedures are reported in **publication II**.

The acetylated products were analysed by ^{1}H NMR and diffusion-edited ^{1}H NMR for the quantification of DS values (see sections 3.6.2.2 & 4.2), and

by HSQC (Heteronuclear Single-Quantum Correlation) and HSQC-TOCSY (Total Correlation Spectroscopy) for regioselectivity determination (See section 4.3 in this thesis).

3.5. Cellulose oxidation

Oxidation of the raw and pre-treated materials in **publication II** was achieved using the AcNH-TEMPO/NaClO/$NaClO_2$ system at pH 5.8, as described in previous publications.[65] Acidic oxidation conditions, in the presence of $NaClO_2$, were applied, to allow for the conversion of intermediate aldehydes/acetals to carboxylates. A further acidification protocol was applied to all of the samples in preparation for gel permeation chromatography (GPC) analyses, as polymeric sodium salts typically do not dissolve in LiCl/DMA. Full procedures are found in **publication II**.

The main hypothesis for choosing acidic oxidation conditions was to avoid the formation of aldehyde/acetals, which have the potential to halt the reaction at the acetal stage and cross-link the material, thus preventing complete oxidation and accurate analyses. $NaClO_2$ under mildly acidic conditions is known to oxidise aldehydes to carboxylic acids and acidic conditions are known to break acetals. Thus, acidic conditions (pH 5.8) were chosen, in combination with $NaClO_2$ as a co-oxidant, to allow for the complete conversion to carboxylate.

3.6. Analytical methods

3.6.1. Attenuated total reflection fourier transform infrared (ATR-FTIR) spectroscopy

FTIR spectra were collected (400-4000 cm^{-1}) from cellulosic samples with a Bruker alpha-P FTIR spectrometer with a diamond ATR. The ATR-IR spectra were baseline corrected and normalised to the cellulose backbone signal (1010 cm^{-1}) intensity. This is a rapid and non-destructive characterisation technique, which allows qualitative analyses of the expected products by identification of the functional groups.

This technique is used for the cellulose acetylation and oxidation studies in this work (**publication II**). The relative degrees of substitution (DS) for each acetylated sample are determined by the deconvolution of the carbonyl (1500-1800 cm^{-1}) and cellulose backbone bands (700-1200 cm^{-1}) of the ATR-IR data. The ATR-IR results are also compared with the DS values obtained from ^1H

NMR integration over the entire DS range. The combination of the ATR-IR deconvolution and NMR methods is applied to give more confidence to the general trends.

On the other hand, the degree of oxidation (DO) in AcNH-TEMPO oxidations are also determined by the deconvolution of the ATR-IR data of both the acidified and sodium salt forms from the ratio of the C=O vs. C-O total peak areas, for the acidified fractions. To determine the relative degrees of oxidation for these samples, a correlation of the peak ratios was drawn for those samples with ATR-IR analysis on both the acidified and sodium salt forms (see Section 4.2.2.2 in this thesis). The relative degree of oxidation, by IR, could then be determined from this correlation.

The data are regarded as semi-quantitative, as a correlation between the IR data and conductometric titration (directly yielding the carboxylate content in mmol/g), which is performed for key samples.

3.6.2. Nuclear magnetic resonance (NMR) spectroscopy

The NMR technique allow local magnetic fields around atomic nuclei to be observed, and is a very useful characterisation technique in many different disciplines such as medicine, organic synthesis or polymer chemistry, among others. NMR spectroscopy gives crucial information regarding the chemical environment in a molecule, leading to a better understanding of its structural identification. Additionally, NMR can be used for many other purposes such as kinetic studies or imaging. In organic synthesis, NMR is a tool of almost daily use.

In this thesis, NMR has been used for the kinetics studies enabling understanding of the reaction mechanism of IMILs (**publication I**) and for both structural analyses of cellulosic samples and the DS quantification of the chemical modification of cellulose (**publications II** & **III**). The kinetics studies were monitored by ^{1}H NMR and ^{13}C NMR spectroscopy on a Varian Unity Inova 600 (600 MHz ^{1}H-frequency) and Varian Mercury Plus 300 (300 MHz ^{1}H frequency) spectrometers, respectively. However, the rest of the NMR analyses in this thesis were performed on a Bruker AVANCE *NEO* (400 MHz and 600 MHz ^{1}H-frequency) spectrometer. For some of the oxidised cellulose samples, an inverse triple resonance probe-head (^{1}H/^{19}F, ^{13}C, ^{31}P) and a cryogenically cooled quadruple resonance (^{1}H, ^{13}C, ^{31}P, ^{14}N) probe-head were used.

3.6.2.1. Kinetics

The NMR technique is used for investigation of the H/D exchange of IMILs in the temperature range from 300.25 K to 339.45 K (**publication I**). Two different IMILs ([bmim]Cl and [bmim][OAc] are studied in different chemical environments. The activation energy (E_a) is calculated from the Arrhenius plots in each of the different studied scenarios. This study allows for a better understanding on the mechanism of the reactivity of 1,3-dialkylimidazolium salts (see Section 4.4.1 in this thesis).

3.6.2.2. Cellulose analyses

As mentioned above, NMR is also used in cellulose analyses. The acetylated cellulosic products are analysed by ^{1}H NMR and diffusion-edited ^{1}H for the quantification of DS values. In these analyses, the soluble cellulosic samples (high DS) are dissolved directly in an organic deuterated solvent at a concentration of 3-5 wt%. The DS values are obtained by integration of the ^{1}H cellulose backbone spectral region (I_C, 5.82 – 2.80 ppm) and the acetate spectral region (I_A, 2.40 – 1.60 ppm). The DS values are calculated according to equation 1 **[Eq.(1)]**.

$$DS = \left({}^{I_A}/_{3} \Big/ {}^{I_C}/_{7} \right) \qquad (1)$$

On the other hand, the non-soluble cellulosic samples (low DS) are dissolved in the $[P_{4444}][OAc]$:d_6-DMSO (20:80 wt.%) electrolyte with a similar load of cellulose. This electrolyte allows their dissolution and therefore their analysis by liquid state NMR. In this case, due to the presence of different molecular weight molecules (cellulose and electrolyte), diffusion-edited ^{1}H spectra are required for their analysis. However, the diffusion-edited ^{1}H NMR experiments tends to overestimate I_A because the different types of nuclei have quite different relaxation rates (T_1 and T_2). This allows for a disproportionate loss of signal for I_C relative to I_A during the pulse sequence, before the acquisition period. Thus, a correction factor (CF_{diff}) must be applied while maintaining the same analysis conditions

(most importantly the sample concentration & probe temperature) for the diffusion-edited experiments.

CF_{diff} values using standard acetylated cellulose samples of known DS are needed for the accurate calculation of DS values from the diffusion-edited experiments. The samples had to be homogeneously acetylated as they needed to be soluble in both the electrolyte and DMSO-d_6 to yield DS values from both solvents/methods. For this purpose, three reference samples of known DS (0.7, 1.30, and 1.92) were used. CF_{diff} is determined by the linear correlation of the DS values, through the diffusion-edited experiments (in electrolyte) vs. standard ^1H experiment (in DMSO-d_6) of the reference samples.

An average of the 3 CF_{diff} values (for 3 different DS values) is applied for estimation of the DS values directly from the diffusion-edited degrees of substitution (DS_{diff}), according to equation 2 **[Eq.(2)]**.

$$CF_{diff} = \frac{DS}{DS_{diff}} \qquad (2)$$

The DS is then determined from the product of the average CF_{diff} and DS_{diff}. For deeper understanding of these calculations, see **publication II**.

The results regarding the DS determination together with the regioselectivity studies in acetylation reactions by HSQC (Heteronuclear Single-Quantum Correlation) and HSQC-TOCSY (Total Correlation Spectroscopy) are found in Sections 4.2.2.1 and 4.3.1 of this thesis, respectively. Additionally, HSQC is also used for quantitative analyses of oxidised celluloses (**publication III**), whose results are found in Section 4.3.2 of this work.

3.6.3. Conductometric titration

In AcNH-TEMPO oxidations, for separate insoluble samples with lower degrees of oxidation, conductometric titrations were performed, giving a correction factor to the ATR-IR data and extend the estimate of degree of oxidation to the full series of reaction products.

AcNH-TEMPO-oxidised material in freeze-dried sodium formed from the insoluble fractions was suspended in distilled water (100

mg in 20 mL) and diluted with 0.01 M NaCl, to raise the conductivity of the slurry to significant levels. Then, 0.1 M HCl was added to the suspension to set the values to 2.4–2.7 pH (2–3 mL). The mixtures were titrated with 0.04 M NaOH at the rate of 0.2–0.3 mL/min, with efficient stirring, to pH 11.

The carboxylic content (CC) in mmol/g of the fractions is calculated by equation 3 **[Eq.(3)].**

$$CC = \frac{C \times (V_2 - V_1)}{w} \qquad (3)$$

Where C is the concentration of the NaOH in mol/L, V_1 *and* V_2 stand for the volumes of the NaOH in mL, w is the weight of the sample in g.

3.6.4. Computational studies

Computational studies in this thesis were investigated by DFT transition-state modelling, which were carried out by professors Dage Sundholm (University of Helsinki, Finland) and Raúl Mera-Adasme (Santiago de Chile University, Chile).

3.6.5. Wide angle x-ray scattering (WAXS)

The crystallinity of the cellulosic samples was analysed by wide-angle X-ray scattering (WAXS). These measurements were performed on a PANalytical X'Pert Pro MPD system. The diffracted intensity of Cu Kα radiation (λ = 1.54Å, under a condition of 45 kV and 40 mÅ) was measured in a 2θ range between 5° and 50°. Samples for WAXS were initially prepared by loading 50 mg of freeze-dried samples into a KBr press (typically used for preparation of KBr discs for transmittance FT-IR analysis) and pressed for 45 s at 9 psi. The samples were placed on a glass stage and the height calibrated for surface reflection.

In this work (**publication II**), the crystallinity index (CI) is calculated by deconvolution (pseudoVoigt fitting) of the 1D X-ray diffractograms, over 2θ values of 5-50°. A suitable amorphous standard is critical, as is the glass background support. This method requires a curve fitting software, such as '*Fityk*',[92] to separate the background, amorphous and crystalline contributions to the diffractograms. This is achieved by defining an equation for a linear

combination of functions (LCOF), required to fit the background and amorphous diffractograms. When fitting these LCOFs to the actual experimental data, the LCOF can be represented by a single variable (in this case height, corresponding to a specific total area of the LCOF), which can then be used to calculate the CI values during the final deconvolution-fitting procedure. Thus, we are able to fit the crystalline phases, glass background and a pre-defined 'amorphous' phase.

CI values are calculated according to equation 4 **[Eq.(4)]**, as the % ratio of the area of the crystalline signals ($A_{Cel\text{-}I}$) to the total area (A_{Tot}).

$$CI = 100\ x\ \left({}^{A_{Cel-I}}/_{A_{Tot}}\right) \qquad (4)$$

For a deeper explanation and graphical understanding of the whole process, see **publication II** and its corresponding supporting information.

3.6.6. Gel permeation chromatography (GPC)

Molar mass determination was performed by GPC with an Agilent Infinity 1260, using LiCl/DMA as mobile phase, according to previous studies.[61, 62] Cellulosic material (17.5 mg) was weighed in a glass vial, DMA (1.25 ml) was added and the suspension was stirred at 130°C for 2 h. Then, the sample was cool down to 90°C and anhydrous LiCl (87.5 mg) was added. The sample was further stirred overnight at ambient temperature. On the next day, the sample was diluted with DMA (16.25 ml) so that the final concentration of LiCl in the solution is 0.5 w/v % and allowed to stir for 1 h more. All of the samples were additionally filtered through Pall Acrodisc GHP 0.45µm filters, prior to injection. Pullulan standards (6100, 9600, 22000, 47100, 107000, 194000, 337000 and 642000 g/mol) from Shodex™ STANDARD (Japan) were used to calibrate the GPC system.

3.6.7. Optical microscope (OM)

The morphology of certain cellulosic samples of this study (**publications II** & **IV**) was analysed by an Olympus BX51TF microscope, equipped with a DP70 colour camera and adjustable polarised lenses. The cross-polariser angle was optimised for better image contrast, producing differences in colour.

3.6.8. Field emission scanning electron microscope (FESEM)

Nanostructured materials were imaged by a Hitachi S-4800 field emission scanning electron microscope (FESEM). The samples were coated with 5 nm Au-Pd alloy prior to imaging to make their surface conductive.

4. Results and Discussion

4.1. Purity of ILs

The primary factor to be considered when working with ILs is their purity, especially in biomass processing, where the impurities can cause solubility issues[55] or may introduce degradation problems (acid or base residues), colour formation, etc. In **publication I**, the presence of impurities in IMILs has been demonstrated to drastically influence the thermodynamics of the IMILs. In this study a notable difference in the H/D exchange ratios of [bmim]Cl and [bmim][OAc] was observed, which was assumed to be related to the basicity of the counter anions.[93] Thus, the study continued focus on the influence of different environments (acidic, neutral and basic) in the IL with slower H/D exchange ratio, [bmim]Cl. **Table 1** shows the different environments of study.

Table 1. *Kinetic data for the H/D conversion of [bmim][OAc] and [bmim][Cl] in different environments: neutral environments (experiments 1-2), basic environments (experiments 3-9) and acidic environments (experiments 10-14).*

Experiment	Conditions[a]	Ionic Liquid (IL)	mol% with respect to the IL	Temperature / K	Time / h	D incorporation / %		
						C2	C4	C5
1	Pure D_2O	**[bmim][OAc]**	82	311.90	4.8	97	20	26
2	Pure D_2O		82	339.45	27	53	7	7
3	1-MeIm		0.38	311.90	3.3[b]	99	15	20
4	1-MeIm		0.75	311.90	0.85[b]	99	15	20
5	1-MeIm		1	311.90	0.57[b]	99	15	20
6	1-MeIm		1.5	311.90	0.29[b]	99	15	20
7	1-MeIm	**[bmim]Cl**	3	311.90	0.16[b]	99	16	21
8	Et_3N		3	300.25	0.16[b]	99	19	24
9	NaOD (40 wt. %)		3	300.25	0.16[b]	99	31	37
10	DCl (35 wt. %)		1	300.25	192	10	13	16
11	DCl (35 wt. %)		10	300.25	192	7	10	12
12	DCl (35 wt. %)		50	300.25	192	11	14	19
13	DCl (35 wt. %)		100	300.25	192	6	9	13
14	DCl (35 wt. %)		200	300.25	192	0	2	4

[a] ionic liquid (0.370 – 0.424 mmol) in D_2O (34.4 mmol), [b] these time increments, corresponding to 99% conversion at C2, were selected from the arrayed kinetic data.

The primary finding was that the H/D exchange under neutral conditions mainly occurred at C2, while the deuteration was more effective under basic conditions for all positions of the ring. However, in acidic environments, the D incorporation slowed down considerably and H/D exchange was even slightly preferential at C4 and C5, over C2. At elevated acid concentrations, the H/D exchange was rather much slower. This finding clearly shows the catalytic effect of the basic impurities in the H/D conversion of IMILs, as demonstrated in **Figure 12**.

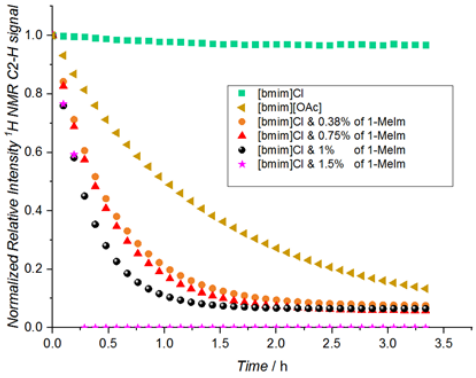

Figure 12. Effect on the H/D conversion by the counter anion (chloride or acetate under neutral conditions) versus the inclusion of an explicit neutral base such as 1-methylimidazole (1-MeIm) at 311.90 K.

By comparison of the H/D exchange of the synthesised IL to a commercial sample of [bmim]Cl, more rapid kinetics were observed for the commercial sample, without the addition of any base (**Figure 13**). This indicates that the presence of impurities in commercial ionic liquids may have a huge impact on the validity of any chemistry performed within. This investigation gave an interesting insight towards the reactivity of IMILs, which is discussed in Section 4.4.1 of this thesis.

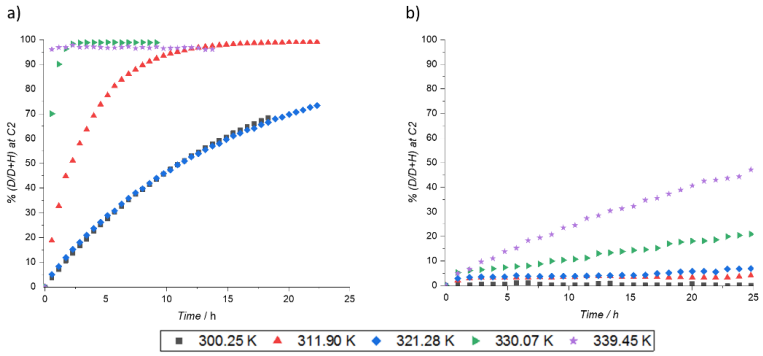

Figure 13. Deuterium incorporation at C2 with the time in a temperature range from 300.25 K to 339.45 K. a) Commercial [bmim]Cl (Strem chemicals, 98%). b) Synthesised [bmim]Cl. The commercial sample (Strem Chemicals) showed a more rapid exchange kinetics than the freshly synthesised sample, without the addition of any base.

Therefore, the purity of commercial ILs needs to be known before making assumptions about the reactivity of the IL itself when it is considered pure. However, commercial suppliers do not describe their synthetic approaches, making it difficult to figure out the origin of these impurities. Furthermore, purchased ILs present different properties (melting points or coloration) to those synthesised in the laboratory (**Figure 14**). Nevertheless, synthesising the IL *in situ* might not ensure that the IL is totally free of impurities, but provides an opportunity to minimise the known impurities. The most common impurities found in ILs are basic or acidic impurities remaining from synthetic approaches or water.

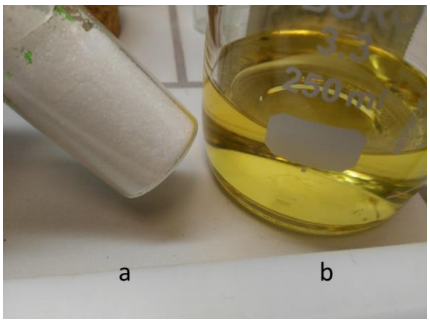

Figure 14. 1-butyl-3-methylimidazolium chloride ([bmim]Cl) at room temperature. a) White crystalline solid synthesised in the laboratory. Melting point 69°C. b) Yellow viscous liquid purchased from commercial supplier (BASF).

Certain ILs, such as chloride IMILs, are extremely hygroscopic. Therefore, work under inert gas atmosphere is required. Furthermore, IMILs such as [bmim]Cl and [bmim][OAc] are toxic and have relatively low thermal stability. However, some phosphonium homologues, such as $[P_{4444}][OAc]$ are much more thermally stable and reasonably less reactive than [bmim][OAc], which is prone to reacting with cellulose via imidazolium-C2 carbon[24] (see Section 4.4.1 in this thesis).

Therefore, due to the above-mentioned advantages of phosphonium homologues over IMILs, these studies continued to focus on the tetraalkylphosphonium ILs, more specifically on the tetrabutylphosphonium acetate ($[P_{4444}][OAc]$) for its use in the activation of cellulose chemical reactivity (Section 4.2) and for its efficient cellulose dissolution capabilities in presence of co-solvent, such as DMSO, which is very useful for instance in the NMR analyses of celluloses (Section 4.3).

4.2. Activation of cellulose chemical reactivity by IL pre-treatment

While $[P_{4444}][OAc]$ is not able to dissolve cellulose in the absence of a polar co-solvent, it has been observed that the treatment of cellulose with pure $[P_{4444}][OAc]$ introduces a crystallinity reduction, thus enhancing cellulose chemical reactivity, as proven in **publication II**. In this work, high molecular weight technical kraft pulps, such as Enocell, birch and eucalyptus, were utilised. The pulps were homogenously mixed with the melted IL at 120°C for 5h for reactivity assessments and crystallinity analyses. During this pre-treatment, the cellulosic materials become partially swollen. Then, the IL was either directly washed away yielding IL-free material or retained in the matrix during reaction. This pre-treatment clearly reduced the crystallinity of pulps significantly, enhancing their accessibility, and thus their reactivity.

4.2.1. Crystallinity reduction of cellulose with $[P_{4444}][OAc]$

The decrease in crystallinity of the pulps was followed by the X-ray diffraction patterns of the raw materials and IL pre-treated samples as shown in **Figure 15**. The main diffraction peak regions for cellulose I are $1\bar{1}0$ at ~14.5°, 110 at ~16.5°, 012 at ~20.5°, 200 at ~23.0° and 004 at ~34.5°.[94]

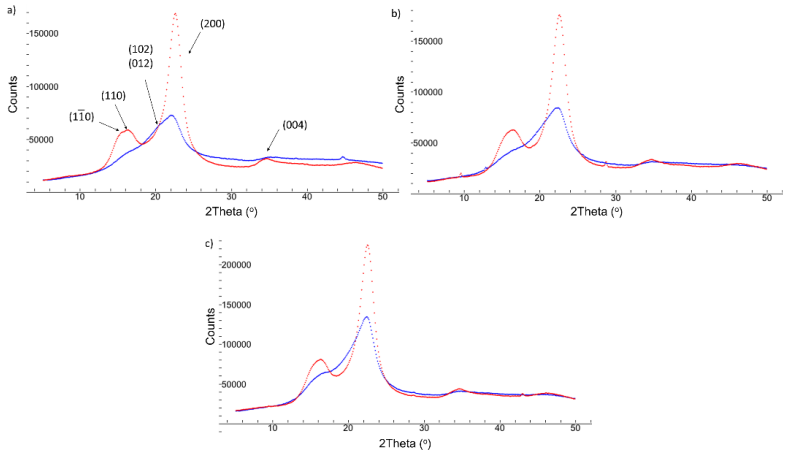

Figure 15. WAXS diffractograms for untreated pulps (red) and non-dissolved pre-treated pulps (blue): a) Enocell B-H-PHK-P. b) Birch B-H-K-P pulp. c) Eucalyptus B-H-K-P pulp.

The IL non-dissolving pre-treated Enocell pulp (**Figure 15a**) mainly exhibits a single broad asymmetric diffraction peak, denoting a considerable decrease in crystallinity. However, small shoulders, corresponding to the (110) and ($1\bar{1}0$) diffraction planes in cellulose I, are still present but are more obvious in the IL non-dissolving pre-treated birch and eucalyptus pulps (**Figures 15b** and **15c**, respectively). None of the samples show the characteristic diffraction planes for cellulose II, the most obvious of which would be the ($1\bar{1}0$) plane at ~12.5°. However, a slight splitting or shoulders on the (200) peak can be observed indicating a small amount of cellulose II phase formation. These results indicate the significantly removal of crystallinity, being most efficiently removed from the higher purity Enocell pulp (**Figure 16**). In the case of the kraft pulps (not pre-hydrolysed), surface adsorbed hemicelluloses or increased molecular weight may be a restricting factor for decrystallisation.

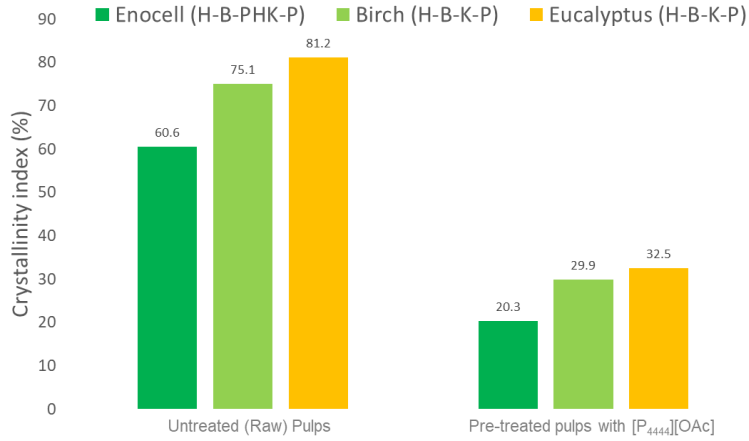

Figure 16. Crystallinity index (CI) values of the untreated and pre-treated pulps.

Additionally, crystallinity reduction was also observed under dissolving conditions (dissolution and regeneration). This procedure produced a more porous material, which may be beneficial for chemical conversion. In all of these crystallinity studies, several factors such as, crystallite sizes, porosity and the effect due to hemicellulose content were considered, as shown in **publication II**.

The observed minimisation in crystallinity is directly related to the accessibility of the cellulose, and thus its reactivity. In other words, the greater the reduction of crystallinity, the more reactive cellulose is expected to be.

4.2.2. Enhanced reactivity of [P_{4444}][OAc] pre-treated cellulose

To assess the reactivity of the pre-treated pulps, acetylation reaction under organic swelling conditions and nitroxyl radical-mediated oxidation of cellulose were chosen as model reactions.

4.2.2.1. Acetylation of [P_{4444}][OAc] pre-treated cellulose

The above-mentioned non-dissolving IL pre-treated and raw pulps were acetylated using both acetic anhydride (AA) and isopropenyl acetate (IPA) as acetylation reagents.

Two different routes were performed in these reactivity studies: 1) a 'heterogeneous route', where the samples were IL pre-treated and washed free of IL (IL-PT-W), and 2) a 'homogeneous route' where the samples were IL pre-treated but not washed (IL-PT-NW), to retain the swollen state of the molecules and observe the difference in reactivity that this allows. This second route is not technically a homogeneous reaction, as it starts off in the solid state and then progresses into solution over a period of time. These pathways led to DS values ranging from 0-2.99, as shown in **Table 2**. The DS value are calculated as explained in Section 3.6.2.2.

Table 2. *DS values depending on the acetylating reagent, pulp type and pre-treatment of the pulp.*

Acetic anhydride (AA) as acetylating reagent									
Pulp	Enocell			Birch			Eucalyptus		
Treatment	Raw pulp	IL PT W[a]	IL PT NW[b]	Raw pulp	IL PT W[a]	IL PT NW[b]	Raw pulp	IL PT W[a]	IL PT NW[b]
DS	0.32	1.90	2.68	0.18	1.61	2.81	0.42	0.19	2.59
Isopropenyl acetate (IPA) as acetylating reagent									
Pulp	Enocell			Birch			Eucalyptus		
Treatment	Raw pulp	IL PT W[a]	IL PT NW[b]	Raw pulp	IL PT W[a]	IL PT NW[b]	Raw pulp	IL PT W[a]	IL PT NW[b]
DS	0	0.33	2.92	0	0.35	2.81	0	-	2.71

[a] IL-PT-W is the IL pre-treated pulp with a further washing step to remove the IL before the addition of the acetylating reagent (heterogeneous route). [b] IL-PT-NW is the IL non-washed pre-treated pulp, which still contains the IL upon the addition of acetylation reagents (homogeneous route).

In general, the pre-treated samples clearly show increased reactivity over the untreated samples. For instance, under the heterogeneous route, the DS values were shown to be 1.61 and 1.90 for pre-treated birch and Enocell, but 0.18 and 0.32 for untreated birch and Enocell pulps, respectively. IL-PT-W eucalyptus acetylated with AA only gave a DS value of 0.19, due to an error in the experimental set-up. However, the IPA reactions did not show a significant enhancement in reactivity under the heterogeneous route. This shows that an increase in reactivity is possible with the IL pre-treatment, specifically with the more reactive reagent, AA, where some autocatalysis may occur.

On the other hand, the homogeneous route, where the cellulose samples were dissolved (IL-PT-NW) clearly shows higher reactivity than the heterogeneous pathway (IL-PT-W). These differences in reactivity depending on the reaction pathway were somehow expected, since cellulose in the heavily swollen state should give much easier access to all hydroxyls, whereas typical heterogeneous acetylation reactions, in the absence of an activating acid catalyst, should give very limited reactivity.

The differences in reactivity of the two used acetylating reagents, especially under heterogeneous conditions, were also expected. AA is known as a more reactive reagent than IPA or other vinylic esters.[61] However, under homogeneous conditions, IPA also allowed for conversion to high DS for all pulp samples.

In this reactivity study, two other important factors were also considered: 1) possible hornification of the pulps after IL removal and drying, which seems to have a significant effect on the pulp reactivity. This also contributes to the observed lower reactivity in IL-PT-W compared to IL-PT-NW samples. 2) Reduction in the molecular weight. However, the crystallinity removal did not introduce a major decrease in MW during acetylation, but only minor reduction in the number-average molecular weights (DP_N), as shown in **Figure 17** and **Table 3**.

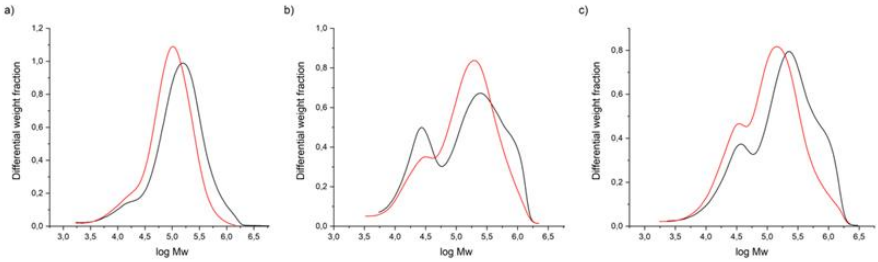

Figure 17. GPC traces for the raw (black) and pre-treated (red) pulps: a) Enocell B-H-PHK-P, b) Birch B-H-K-P, c) Eucalyptus B-H-K-P.

Table 3. *Number-average molecular weight of the pulp before (raw) and after the pre-treatment under heterogeneous route.*

Pulp	Enocell B-H-PHK-P		Birch B-H-K-P		Eucalyptus B-H-K-P	
	Raw pulp	IL PT W[a]	Raw pulp	IL PT W[a]	Raw pulp	IL PT W[a]
DP_N (g/mol)	330.4	272.5	330.9	320.3	365.7	273.5

[a] IL-PT-W is the IL pre-treated pulp with a further washing step to remove the IL before the addition of the acetylating reagent (heterogeneous route).

These changes are not enough to be especially implicated in the increased reactivity, although there may be some effect.

4.2.2.2. Nitroxyl radical-mediated oxidation of $[P_{4444}][OAc]$ pre-treated cellulose

To evaluate the enhanced reactivity of $[P_{4444}][OAc]$ pre-treated cellulose, birch and dissolving quality (enocell) pulps were chosen as representative samples. After the oxidation, water-insoluble fractions with low carboxylate contents were separated by centrifugation from the reaction mixture, while water-dispersible fractions with higher carboxylate contents were regenerated from the combined water supernatant by ethanol precipitation and centrifugation, as described in the experimental procedure of **publication II**. Raw pulps in the oxidation process were not solubilised in the reaction media, thus, the amount of regenerated water-dispersible fractions was very low. The freeze-dried samples were analysed by ATR-IR, comparing the peak areas of the carbonyl stretches (Gaussian fitting between 1800-1600 cm^{-1}) vs. the normalised C-O backbone stretch (Gaussian fitting between 1200 and 850 cm^{-1}). In addition, three samples of insoluble fractions, in the Na salt form, were titrated to determine the carboxylate content, which was then compared with the ATR-IR results. A linear correlation was drawn (**Figure 18**)

to allow for the comparison of all samples using IR which was then used for estimation of the remaining carboxylate contents, in mmol/g (**Figure 19** and **Table 4**).

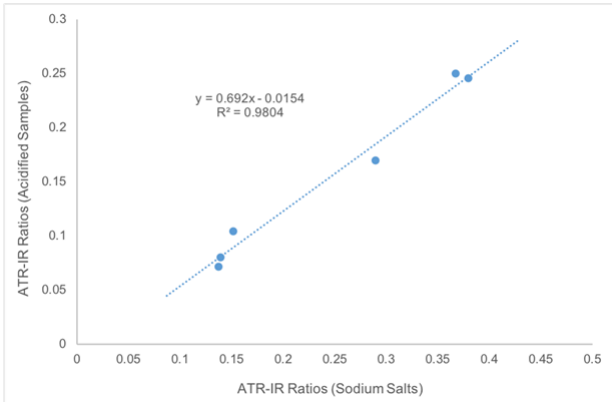

Figure 18. Correlation between IR ratios from acidified and sodium salt forms of AcNH-TEMPO-oxidised samples

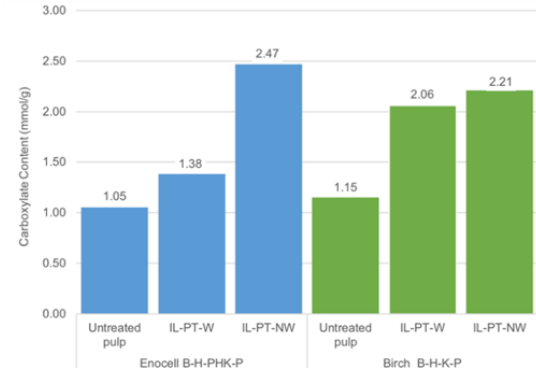

Figure 19. Total carboxylate content for different pulps and pre-treatment types based on ATR-IR peak volume data.

Table 4. *$\%_{DO}$ and carboxylate content for different pulp types and their fractional mass distributions, obtained by semi-quantitative ATR-IR analyses, based on peak volume data.*

Pulp	Enocell B-H-PHK-P						Birch B-H-K-P					
Treatment	Untreated pulp		IL PT W[a]		IL PT NW[b]		Untreated pulp		IL PT W[a]		IL PT NW[b]	
$\%_{DO}$[c] (%)	Insol.[e]	Sol.[e]	Insol.	Sol.	Insol.	Sol.	Insol.	Sol.	Insol.	Sol.	Insol.	Sol.
	22.0	34.4	18.5	37.1	47.0	63.9	23.5	36.2	38.5	61.5	36.5	62.4
Carboxylate content (mmol/g)	1.02	1.47	0.87	1.61	2.01	2.69	1.07	1.61	1.67	2.61	1.61	2.61
m[d] (%)	96	4	40	60	66	34	91	9	76	24	58	42

[a] IL-PT-W is the IL pre-treated pulp with a further washing step to remove the IL before the addition of the acetylating reagent (heterogeneous route). [b] IL-PT-NW is the IL non-washed pre-treated pulp, which still contains the IL upon addition of the acetylation reagents (homogeneous route). [c] $\%_{DO}$ = Degree of oxidation. [d] *m* = mass of the fraction in percentage. [e] Insol. and Sol. are the insoluble and soluble fractions, respectively.

The primary finding in the oxidation studies was that the [P_{4444}][OAc] pre-treatment significantly increased the reactivity of the cellulose samples. Remarkable differences in the carboxylate content between untreated pulps and IL pre-treated samples were found. The carboxylate contents for both pulps are clearly decreasing in the following order: IL-PT-NW > IL-PT-W > Untreated pulp.

Increased reactivity towards aqueous nitroxyl radical oxidation was demonstrated by the [P_{4444}][OAc] pre-treatments. The samples retained in the swollen state, with IL (IL-PT-NW), were even more accessible than the washed samples (IL-PT-W), indicating the benefits of retaining the IL in the cellulose towards oxidation.

The carboxylate contents are also represented by the degrees of oxidation ($\%_{DO}$), the percentage of C6 converted to carboxylate, to better understand how effective the oxidations are (**Table 4**). While the $\%_{DO}$ for the IL pre-treated samples was clearly increased compared to those of the untreated pulps, they are still quite far from the theoretical maximum $\%_{DO}$ (a carboxylate content of 4.67 mmol/g for pure cellulose conversion to the sodium polyglucuronate). However, some studies of regenerated cellulose samples (cellulose II) have shown even higher carboxylate contents. The carboxylate contents are somewhat lower (0.87–2.69 mmol/g in the present study vs. 3.7–4.0 mmol/g in Hirota et al.).[65b]

The non-dissolving IL pre-treatment showed an increase in reactivity in both non-aqueous (organic swelling) acetylation and the aqueous nitroxyl radical-catalysed oxidation of cellulose studied model reactions. This proved the enhancement of reactivity caused by removal of the crystallinity after IL pre-treatment.

4.3. Cellulosic sample analyses by liquid state NMR

The poor solubility of cellulosic materials in common molecular solvents makes the analysis of polymers where dissolution is a requirement challenging, such as the NMR liquid-state technique. Usually, low-resolution solid-state techniques (*e.g.* solid-state NMR[95]) or indirect methods for the characterisation of biopolymers are used. However, the resolution of the above-mentioned commonly used techniques is limited and compromises the accurate characterisation of different chemical species. Recently, solution-state NMR techniques have been applied for the characterisation of cellulose and reaction products in the $[P_{4444}][OAc]$:DMSO-d_6 (20:80 wt%) electrolyte[26] as an NMR solvent.

In this thesis, ^{1}H, ^{13}C and diffusion-edited ^{1}H NMR have been applied in the investigation of the H/D exchange kinetics of IMILs towards understanding the reaction mechanism (**publication I**) and in the DS determination of acetylated cellulose products (**publication II**) as shown in Sections 4.1 and 4.2.2.1, respectively. Additionally, 2D NMR spectroscopy techniques for cellulose analyses are also shown in **publication II & III**.

4.3.1. Regioselectivity studies in acetylation reactions

As previously mentioned in Section 4.2.1, the removal of crystallinity also moderates the relative reactivity of hydroxyl units throughout the sample, as certain restrictions caused by crystallinity are removed during the pre-treatment with $[P_{4444}][OAc]$. To assess this, the regioselectivity of the reaction under heterogeneous conditions was studied by multiplicity-edited HSQC spectroscopic analyses (**Figure 20**). Two examples of **Table 2**, one low DS (Enocell raw material in acetic anhydride (Enocell-raw-AA)) and one high DS (Enocell IL pre-treated pulp after removal of IL in acetic anhydride (Enocell-IL-PT-W- AA)) were chosen for this study.

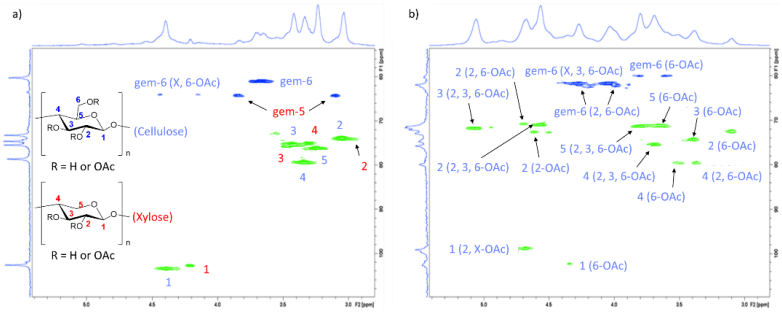

Figure 20. Multiplicity-edited ^{1}H-^{13}C HSQC spectra of acetylated Enocell samples: a) low DS sample (Enocell-raw-AA) in $[P_{4444}][OAc]$:DMSO-d_6 electrolyte, and b) high DS sample (Enocell-IL-PT-W-AA), in DMSO-d_6, at 65°C. Correlation assignment numbers represent the positions in either cellulose (blue) or xylan (red). The numbers in parentheses show which hydroxyls in that spin-system are acetylated for that resonance, with 'X' representing uncertainty as to whether additional hydroxyls are acetylated or not. Assignments are aided by, and consistent with, Kono et al.[96]

The low DS sample (DS 0.32, **Figure 20a**, **Table 2**) shows characteristic correlations for unmodified cellulose, with no acetylated correlations visible, except for close to the baseline noise (Ac-*gem*-6 is clearly visible). However, analysis of the diffusion-edited ^{1}H spectra plainly show acetylated $^{1}H2$, $^{1}H3$ and *gem*-$^{1}H6$ positions on cellulose (**Figure 21**).

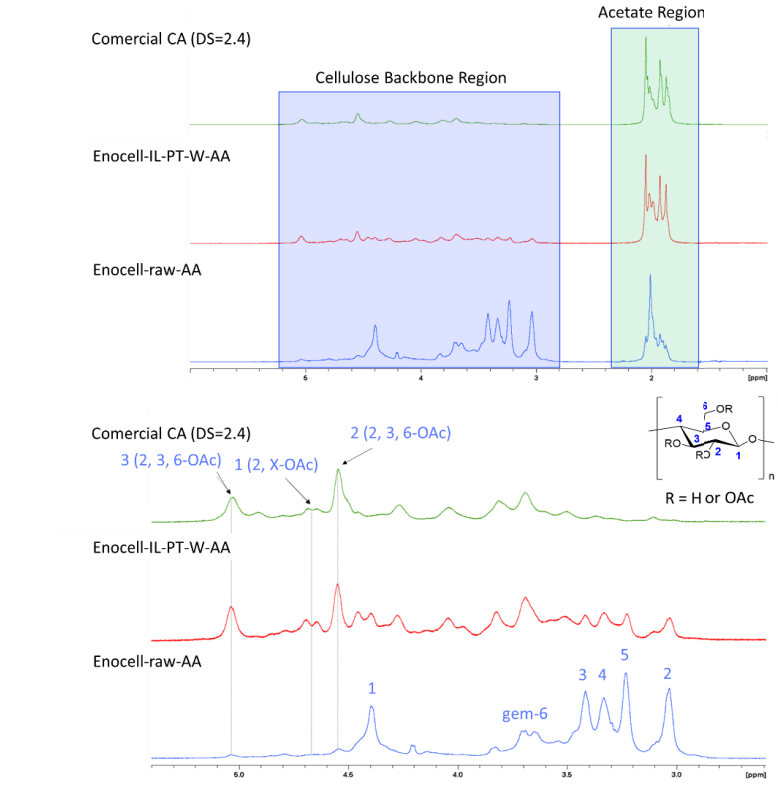

Figure 21. Diffusion-edited ^{1}H spectra of low DS sample (Enocell-raw-AA), high DS sample (Enocell-IL-PT-W-AA) and commercial sample (DS = 2.4) for comparison. Full spectrum (top), H2-H6 region (bottom).

This is a strong indication of cellulose triacetate (CTA) formation, as expected from acid-catalysed acetylation with AA.[97] A small proportion of correlations corresponding to xylan are quite clear. This is not unexpected as Enocell B-H-PHK-P contains ~5% xylan. The higher DS sample (DS 1.90, **Figure 20b**, **Table 2**) clearly shows correlations for acetylated hydroxyls. Most of the *gem*-6 positions are acetylated. In the 2,3-OAc region, most of the acetylated 2 and 3 CH resonance pairs are of the form where 2 & 3 hydroxyls are both acetylated at the same time.

For the high DS sample (Enocell-IL-PT-W-AA), additional resonances are also present, which may correspond to alternately non-acetylated-acetylated 2 or 3 positions, in cellulose or xylan. Other correlations also remain, corresponding to completely unacetylated cellulose. The visible 4 and 5 CH correlations seem to be split into at least two separate regions each. This splitting is also apparent for the acetylated *gem*-6 CH resonances. By combining the cellulose acetate assignments published by Kono et al.[96] and 2D HSQC-TOCSY spectroscopy, it was possible to trace the separate

spin-systems to CTA and cellulose monoacetate (CMA), where only C6-OH is acetylated (**Figure 22**). Additional spin-systems were not abundant enough to be identified using this experiment.

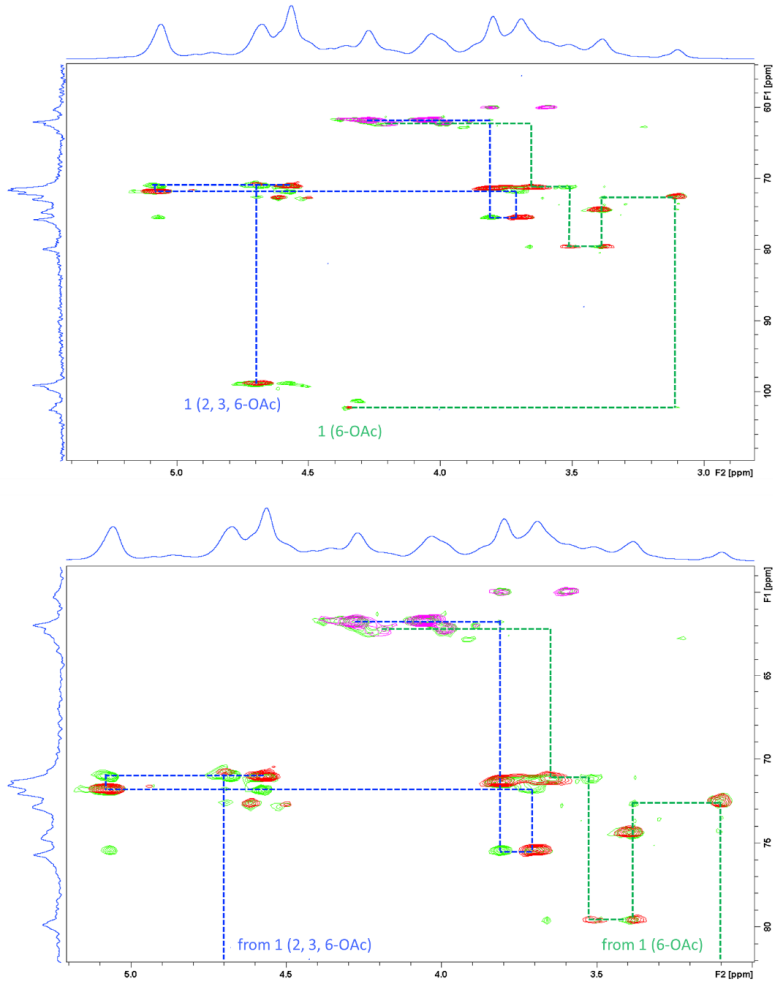

Figure 22. HSQC-TOCSY (short-range, 15 ms mixing time) for Enocell-IL-PT-W-AA: full spectrum (top), CH2-CH6 (bottom). The HSQC spectrum is overlaid.

Therefore, the enhancement of reactivity in the heterogeneous system after IL pre-treatment seems to offer a little more 'control' over regioselectivity, leading to increased monoacetylation at C6-OH. However, the main acetylation product is CTA, consistent with heterogeneous acetylation.

The [P_{4444}][OAc] cellulose pre-treatment is not only shown to be beneficial for the enhancement of cellulose reactivity, but also provides direct insight into the outcome of a chemical process in cellulosic materials. Furthermore, the [P_{4444}][OAc]:d_6-DMSO (20:80 wt.%) electrolyte is a

suitable system for cellulose NMR analyses, since its NMR signals do not overlap with the cellulosic NMR signals. However, the mentioned NMR solvent system is still presenting certain limitations: 1) the need for a polar co-solvent for cellulose dissolution, 2) a non-fully deuterated system is not yet possible, 3) the high cost and toxicity of ILs, and 4) solvent recovery. Thus, further research is still needed to find an 'ideal' solvent system which overcomes these four drawbacks.

4.3.2. Analyses of oxidised nanocelluloses

In **publication III**, characterisation of common cellulose oxidation reaction products was investigated, by comparison with the cellulosic material prior to reaction, utilising $[P_{4444}][OAc]$:DMSO-d_6 electrolyte by HSQC and HSQC-TOCSY.[26] Low degree of polymerisation-cellulose nanocrystals (LDP-CNC), isolated by super-critical water (sc-H_2O) extraction of microcrystalline cellulose (MCC),[98] were selected as substrates for these studies. The spin-systems were assigned using a range of common NMR methods and with the help of the monomeric (glucose, gluconic acid and glucuronic acid) and dimeric model compounds (cellobiose and cellobionic acid).

The full 2D NMR assignment for the dimers, polymeric units and terminal units (**Figure 23**) were thoroughly studied.

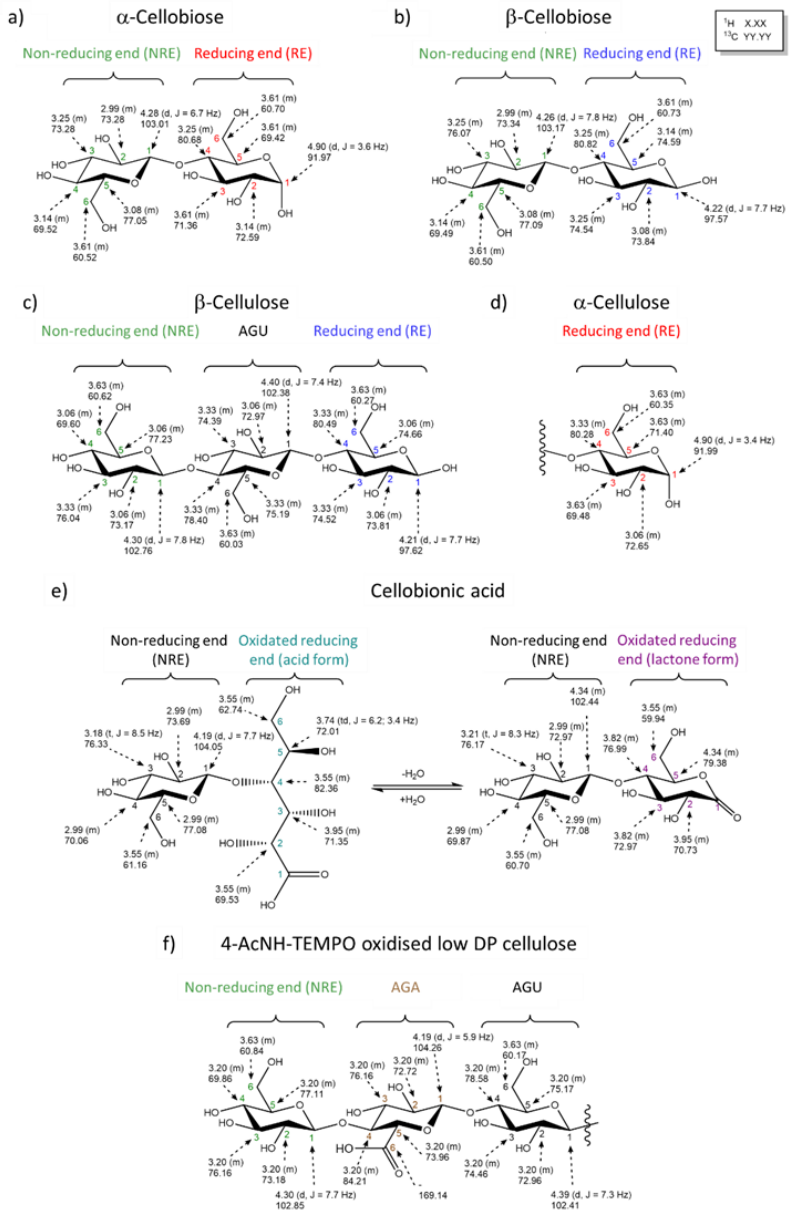

Figure 23. Representative structures, atom numerations and resonance assignments for ^{1}H and ^{13}C NMR sets of: a) α-anomer of cellobiose; b) β-anomer of cellobiose; c) LDP-CNC β-anomer of cellulose (DP_N 37); d) LDP-CNC α-anomer of cellulose (DP_N 37); e) equilibrium between cellobionic acid (turquoise) and cellobionolactone (purple); f) 4-AcNH-TEMPO oxidised LDP-CNCs. AGU and AGA stand for anhydrous glucose unit and anhydroglucuronic acid unit, respectively.

4.3.2.1. Low-DP CNCs

Low degree of polymerisation-cellulose nanocrystals (Low-DP CNCs), isolated by super-critical water (sc-H_2O) extraction of microcrystalline cellulose (MCC) were selected as substrates for this study. Low-DP CNCs consist of chains of β-(1,4)-linked glucopyranose units terminated by RE and NRE groups (**Figure 23c-d**). These are true nanocrystals, formed by the partial depolymerisation and recrystallisation of MCC using sc-H_2O.[98]

The CH-1 region in the HSQC spectrum (**Figure 24**) was characterised by four clear signals; the signal with the highest intensity was assigned as the anhydroglucose unit (AGU)-1 that belongs to the bulk polymeric CH-1 (δ_H = 4.40 ppm (d); δ_C = 102.38 ppm), while the remaining signals correspond to NRE-1, RE-α-1 and RE-β-1. This region is characteristic of (hemi)acetals and such close grouping is caused by the rigid conformation adopted by the sugar unit, with the α-anomer showing a characteristic down-field shift (to >4.5 ppm) in the ^1H dimension and up-field shift in the ^{13}C domain. Further detailed assignments are found in the supplementary information of **publication III**.

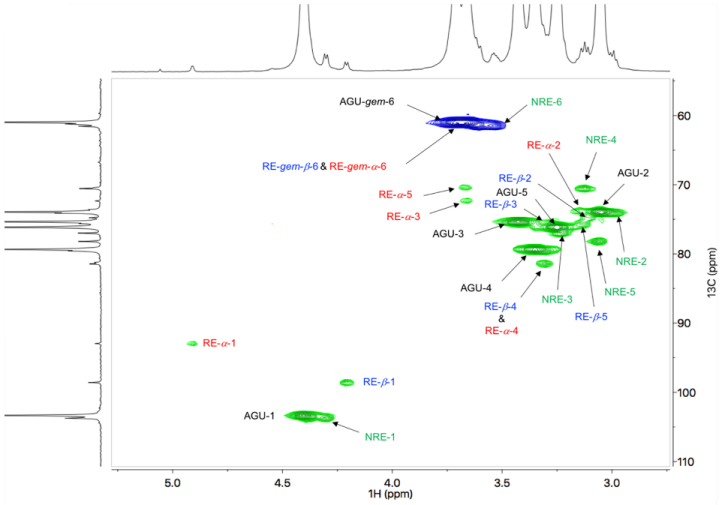

Figure 24. Multiplicity-edited 2D HSQC spectra of LDP-CNCs at 65°C in [P_{4444}][OAc]:DMSO-d_6 (5 wt %). Non-reducing end (NRE) resonances are shown in green, reducing end resonances α and β (RE-α and RE-β) are shown in red and blue, respectively, and internal (middle chain) anhydrous glucose unit resonances (AGU) are shown in black.

4.3.2.2. Nitroxyl-radical oxidation of Low-DP CNCs

Nitroxyl-radical oxidation of the Low-DP CNCs (**Figure 25a**) was carried out in the $NaClO/NaClO_2$ system in the presence of 4-acetamido-2,2,6,6-tetramethylpiperidine 1-oxyl (4-AcNH-TEMPO), under acidic conditions, according to Hirota et al.[65b] This yielded 4-AcNH-TEMPO-oxidised LDP-CNCs (TOx-LDPCNCs). The prepared sodium polyglucuronic acid salt form (AGA unit in **Figure 23f**) of the TOx-LDP-CNCs was acidified to pH 1.0 and separated by centrifugation with subsequent water washing and freeze-drying. Pinnick oxidation of the reducing ends of LDP-CNCs (**Figure 25b**) was carried out under acidic conditions in the presence of one weight equivalent of $NaClO_2$, to yield Pinnick oxidised LDP-CNCs (POx-LDP-CNCs).

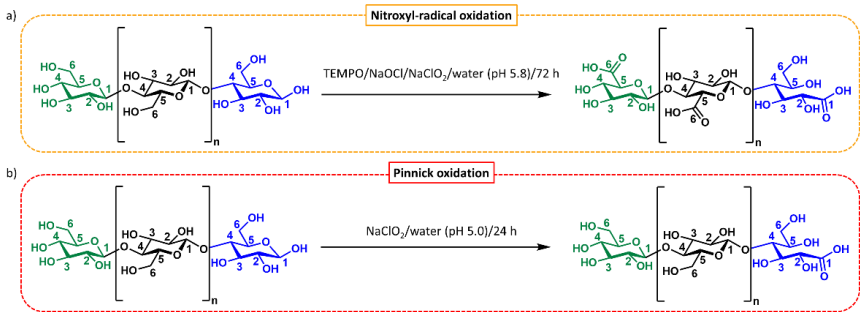

Figure 25. Oxidation of cellulose under a) acidic nitroxyl-radical (e.g. TEMPO or AcNH-TEMPO) or b) Pinnick ($NaClO_2$) oxidation conditions.

Pinnick oxidation at the reducing ends of CNCs is commonly used as the first step in reducing end functionalization, typically via amide formation leading to nanostructures with self-assembly potential.[99]

The insoluble fraction expectedly consisted of minimally oxidised cellulose, whereas the soluble TOx-LDP-CNC fraction had clearly identifiable correlations in the HSQC, not corresponding to polymeric glucose resonances (**Figure 26**). HSQC-TOCSY and HMBC spectral data for AGA resonances assignments are found in supplementary information of **publication III**.

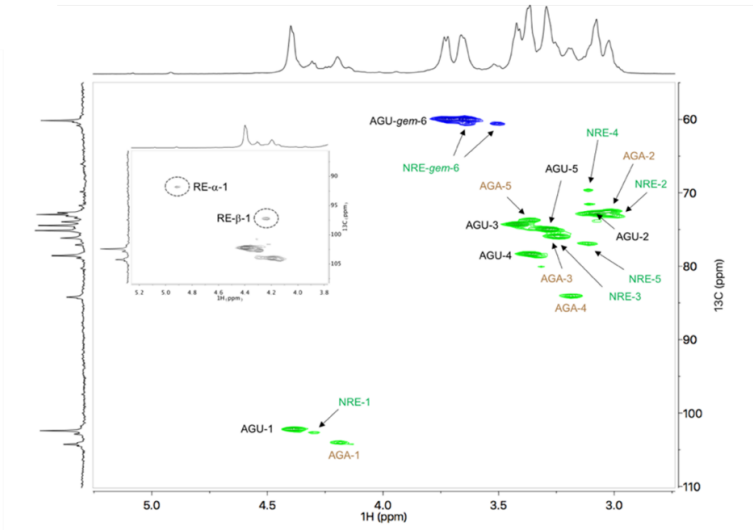

Figure 26. Multiplicity-edited 2D HSQC spectra of TOx-LDP-CNCs at 65°C in $[P_{4444}][OAc]$:DMSO-d_6 (5 wt %). Non-reducing end (NRE) of cellooligomeric resonances and anhydroglucopyranosiduronic acid (AGA) unit resonances are marked in green and brown, respectively. The internal (middle chain) non-oxidised anhydroglucose unit resonances (AGU) are shown in black.

The RE and NRE peaks corresponding to glucose terminated chains were also assignable. One might assume that the NRE C6-OHs should be more accessible to oxidation than any other C6-OH. However, they were clearly present with the NRE more abundant than the RE signals, requiring scaling of the spectra close to the background to visualise the RE signals (**Figure 26-inset**).

4.3.2.3. Overview of oxidised nanocelluloses analyses

The chemical shifts of polymeric units in cellulose (**Figure 23**, p. 51), including NRE and RE units, were unambiguously assigned using solution-state NMR in the $[P_{4444}][OAc]$:DMSO-d_6 electrolyte. The main monomeric units in Low-DP CNCs and 4-AcNH-TEMPO oxidised Low-DP CNCs (polyglucuronic acid) were also assigned (**Figures 24 & 26**, p. 52 & 54), as were the terminal units for the non-oxidised and oxidised materials. The latter led to the identification of the terminal open-chain gluconate moiety after both the acidic 4-AcNH-TEMPO protocol and Pinnick

oxidation conditions were used. However, in both instances, RE groups remained in the oxidised products, indicating a further need for optimisation of this reaction for different substrates or the more defined structural characterisation of substrates for surface oxidation sites, which may undergo β-elimination, yielding new reducing ends.

NMR analysis in the electrolyte medium seems to be a useful probe of the stability of these compounds, in addition to providing the necessary chemical species resolution that other techniques cannot. This is a direct method to follow the progress of oxidation reactions. Nitroxyl-radical-type oxidations (to 6 position carboxylates), under mild acidic conditions, were quite robust in terms of the resulting product stability in the electrolyte and under aqueous alkaline conditions. Thus, avoiding aldehyde formation under alkaline oxidation conditions was clearly important for improving the quality of the oxidised products, by preventing losses and molecular weight reduction due to the fragmentation of surface chains.

Additionally, in **publication III**, quantitative CPMG adjusted HSQC[100] (Q-CAHSQC, **Figure 27**) was investigated towards the quantitation of the oxidised products from the low molecular weight LDP-CNC and Tox-LDP-CNC samples, resulting in a suitable experiment to yield quantitative data from HSQC, without the need for calibration against internal standards. Overall, the CH1 signals for the low molecular weight samples were easily separable with 512 f1 increments (td1), due to their slower T_2 relaxation (**Figure 27a-b**). With the higher molecular weight MCC, separation of the CH1 resonances was improved with the higher number of increments (**Figure 27c-d**). There was sufficient separation of the RE-1 and AGU-1 signals, so that f1 resolution could be lowered further (to allow for increased collection times), whereas the poor S/N is still an issue for the RE-1 signal in both spectra (**Figure 27c-d**). This situation was improved somewhat with the use of the cryoprobe-head, where S/N is approximately doubled. However, if the quantitation of DS values is all that is required, lower resolutions are acceptable to reduce collection times. If resolution eventually becomes an issue in the quantitation of the DS of some substituent, for higher molecular weight samples, then ball milling will likely have to be applied to reduce molecular weights,[101] preventing disproportionate T_2 losses.

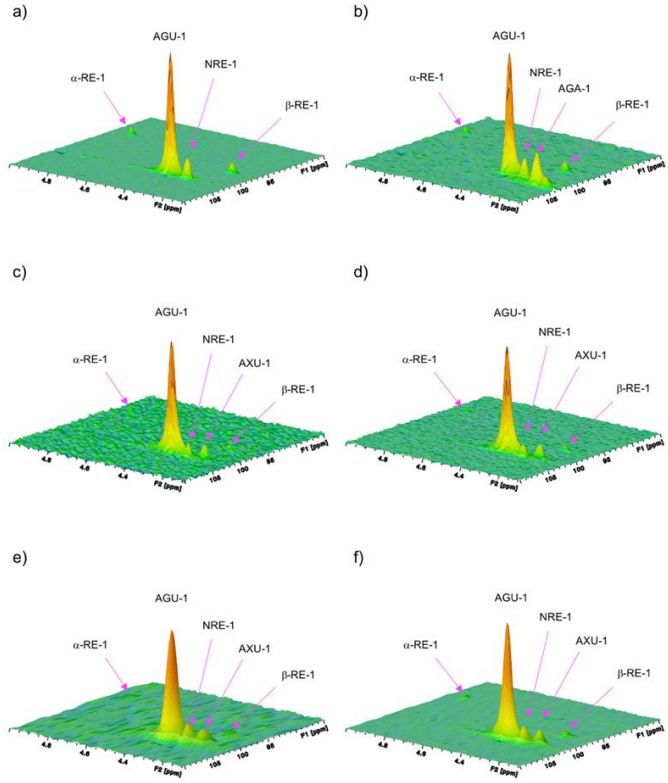

Figure 27. 2D Q-CAHSQC (quantitative HSQC) 3D projections of the CH1 region for a) LDP-CNCs, b) TOx-LDP-CNCs, c) MCC (ns=8, td1=640) with a room temperature probe-head, d) MCC (ns=8, td1=640) with a cryoprobe-head, e) MCC (ns=40, td1=128) with a room temperature probe-head, and f) MCC (ns=40, td1=128) with a cryoprobe-head. F1 is the ^{13}C dimension and F2 is the ^{1}H dimension. No forward linear prediction was used to improve resolution.

Despite this technique still not being suitable for the accurate determination of DP_N for higher molecular weight and low polydispersity samples, accurate DS and regioselectivity determination will be possible for certain chemical modifications, even at reducing ends in lower molecular weight samples, such as model CNCs. However, it should be stressed that this solvent system and processing strategy are not only applicable to nanocelluloses but offer the chance to significantly improve the opportunities for the quantitative analysis of whole biomass samples, which contain a significant crystalline cellulose phase composition.

Therefore, all of these results illustrated the potential of this method for cellulose analyses. Furthermore, currently

undergoing research might produce novel electrolyte systems in the short-term, similar to the $[P_{4444}][OAc]$:DMSO-d_6 for NMR analyses of celluloses.

4.4. Reactivity of ILs – Their non-innocent nature

ILs have gained much attraction in biomass processing due to their ability to dissolve cellulose.[23, 31, 49] A desirable cellulose solvent needs to be chemically inert, where the cellulose could be easily regenerated for example by the addition of a non-solvent, like water. However, certain ILs have been considered not suitable for biomass processing due to their non-innocent nature, behaving as RILs with cellulose.[24] Most of these ILs belong to the IMIL family, which opened up a different perspective of the C-2 chemistry of these ILs (Section 4.4.1). Thus, different options such as phosphonium ionic liquids[26a] or SBILs, like 1,1,3,3-tetramethylguanidinium acetate ([TMG][OAc]),[39] among others[38c-d] have been chosen for cellulose dissolution and processing. However, in **publication IV**, this non-innocent nature was also found in [TMG][OAc], which seems to be a mild acylation reagent not only in cellulose modification (Section 4.4.2).

The finding of the reactive character of [TMG][OAc] encouraged me to continue these studies towards the design of reactive ILs with a dual character, such as cellulose solvents and simultaneous mild acylation reagents to obtain cellulose derivatives (Section 4.4.3).

4.4.1. C2 Chemistry of IMILs

There are numerous reported investigations on the liability and acidity of the proton at the C2 position of the imidazolium ring in IMILs and its implication in carbene chemistry.[102] However, the findings on the relatively slow H/D conversion rates (see Section 4.1) make us consider a complementary alternative for the C2 chemistry of IMILs under neutral (D_2O) or acidic conditions (DCl). While the H/D exchange in neutral conditions has been previously reported, none of these reports provided a solid mechanistic insight into the reactivity.[103]

In **publication I**, the computational studies give solid support to the experimental observations on the H/D exchange at C2 under neutral and acidic conditions. Thus, the deuterium conversion is demonstrated to undergo via concerted 'carbene-free' mechanisms, as shown in **Figure 28**, which complement the initially proposed mechanistic scenario.[104] The transition-state geometry is shown, where a concerted proton exchange occurs, mediated by H-bound water molecules.

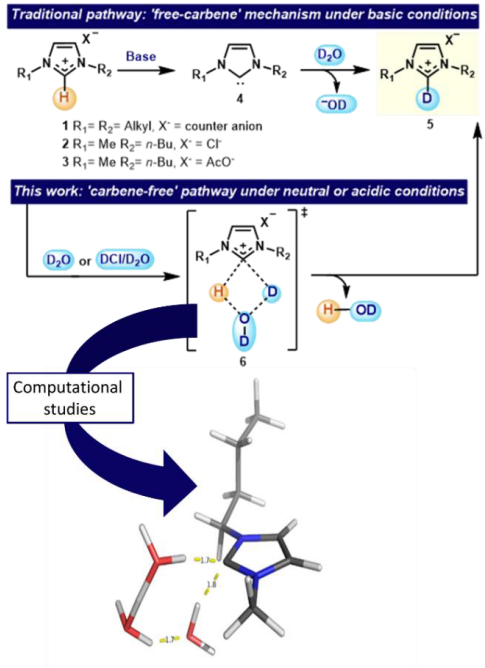

Figure 28. Reported mechanism under basic conditions, alternative mechanism proposed under neutral and acidic conditions in **publication I** and geometry of the optimised transition state **6**, modelled as proton exchange. Dotted lines in **6**, denote bonds which are broken and formed simultaneously. H-bond distances are shown in Å.

The proposed mechanism is proved by the kinetics studies on the H/D conversion (section 4.1), where the obtained Arrhenius parameters, according to equation 5 **[Eq.(5)]**, allowed for the experimental activation energy (E_a) determination (**Figure 29**), which gave very close results to the calculated E_a (31.1 and 31.3 kcal/mol, respectively).

$$K = Ae^{-E_a/RT} \qquad (5)$$

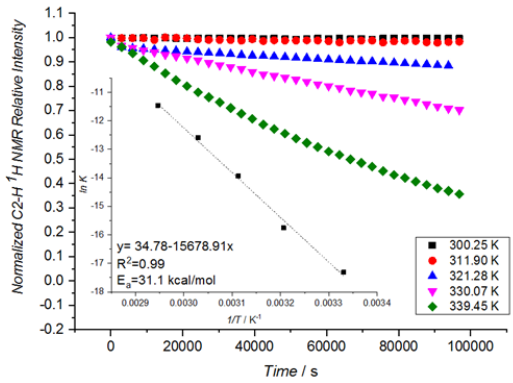

Figure 29. Initial 1st order kinetics, as a function of temperature for C2-H deuteration, in excess of D_2O, leading to an Arrhenius plot (inset).

Activation energies from computational and experimental results are of the same magnitude, which gives very strong support for the suggested alternative mechanism. Furthermore, these findings agree with the computational observations by Gehrke and Hollóczki.[13] In addition, no experimental evidence has yet been produced which has clearly identified free carbene in ionic liquid solutions.

IMILs were demonstrated to be reactive, not only under strong or mild basic conditions, but also under neutral or acidic conditions. Thus, their use in biomass processing or as electrolyte systems for cellulose NMR analyses would not be recommended.

4.4.2. [TMG][OAc]; a mild acylation reagent

In previous literature, the use of dimethyl sulphoxide (DMSO) as a co-solvent was reported with 1,8-diazabicyclo[5.4.0]undec-7-ene (DBU) for cellulose chemical modification.[105] DMSO helps to reduce the viscosity and allows proper mixing. However, dimethyl sulphoxide has a very high boiling point and its removal from the final cellulosic product is challenging. Thus, in **publication IV** the utilisation of [TMG][OAc] as a cellulose solvent was aimed for replacement of the DMSO:DBU solvent system. These studies were performed in the absence of co-solvent and utilising gamma-valerolactone (GVL, a more environmentally friendly alternative than DMSO) as a co-solvent alternative, as shown in **Figure 30**. Parallel experiments with and without CO_2 were also investigated (**Table 5**).

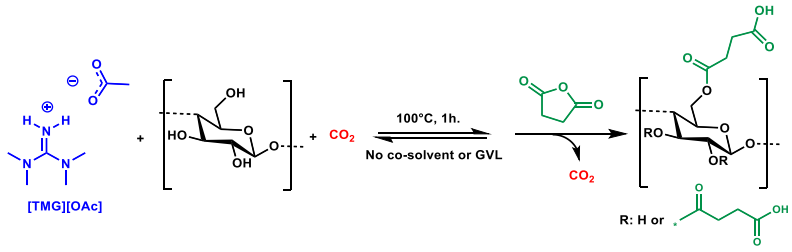

Figure 30. Reaction conditions for the studies of [TMG][OAc] as alternative to previous reports.[105]

Table 5. *Studies on the activation of the biopolymer and the effect of CO_2. Comparison of DBU:DMSO solvent system[105c] (experiment 1) and experiments utilising [TMG][OAc] as replacement. All the experiments were run with succinic anhydride as esterifying reagent and birch as pulp source at 107°C for 1 hour.*

Experiments	Reaction conditions				Yield (%)
	Superbase	IL	Co-solvent	CO_2 pressure (bar)	
1	DBU[a]	None	DMSO	5	86
2	None	[TMG][OAc]	None	5	86
3			GVL	5	92
4			None	0	89
5			GVL	0	88

[a]1,8-diazabicyclo[5.4.0]undec-7-ene.

The replacement of DBU:DMSO solvent system by [TMG][OAc] led to similar results, as shown in **Table 5**. These results showed that CO_2 does not really play a role when utilising [TMG][OAc] as a solvent. This is not totally unexpected, since CO_2 forms an adduct with the superbase (DBU), but not with the ionic liquid ([TMG][OAc]). The use of GVL as a co-solvent slightly increased the reaction yield and helped to reduce the viscosity, ensuring a proper mixing.

Interestingly, additional NMR signals (2.043 and 2.796 ppm) to the typical succinylated cellulose (2.29-2.62 ppm) were found in diffusion-edited ^{1}H NMR (**Figure 31**) of the reaction products. The signal at 2.043 ppm corresponds to acetylated cellulose $-CH_3$ and the signal at 2.796 ppm corresponds to the TMG moiety linked to the cellulose chain.

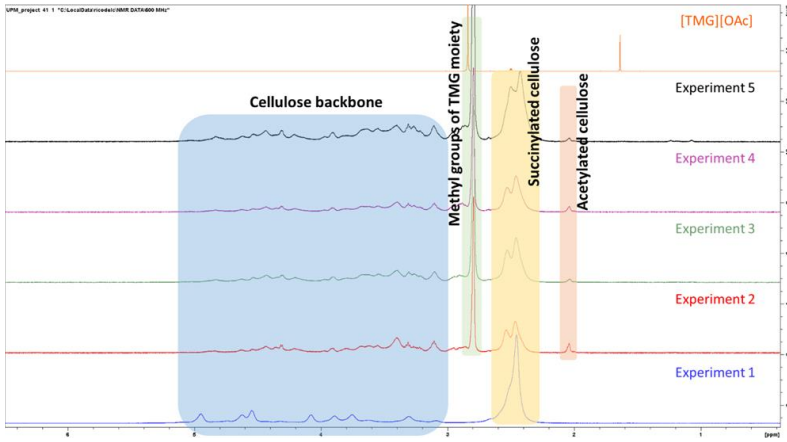

Figure 31. Comparison of diffusion-edited ^{1}H NMR spectra of experiments 1-5 in **Table 5** and ^{1}H NMR spectrum of [TMG][OAc].

The initial observation of the NMR signals at 2.043 and 2.796 ppm suggests that [TMG][OAc] may act as a mild acetylation reagent for cellulose. To demonstrate this, an experiment was run with only [TMG][OAc] and enocell pulp at 107°C for 1 hour. The cellulosic material after the work-up procedure was not fully soluble in DMSO-d_6 indicating low DS, thus the sample was solubilised in the [P_{4444}][OAc]:DMSO-d_6 (20:80 wt%) electrolyte.[26] Diffusion-edited ^{1}H NMR and ^{13}C NMR qualitatively analyses proved the acetylation of cellulose by [TMG][OAc] (**Figure 32**).

The acetylation of cellulose using acetate ionic liquids, such as [bmim][OAc], is known in the chemical literature,[24] but this reactivity was somewhat unexpected for [TMG][OAc], whose use as a cellulose solvent has been previously reported.[39]

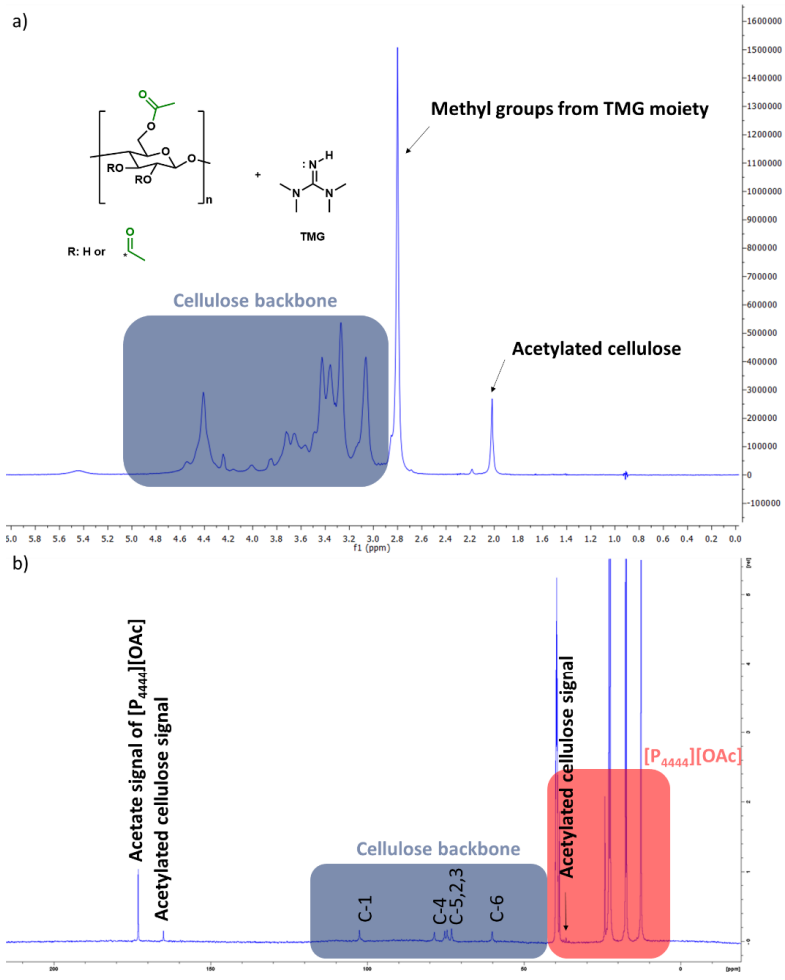

Figure 32. Acetylated Enocell in melted [TMG][OAc] after work-up procedure. a) Diffusion-edited ^{1}H NMR. b) ^{13}C NMR spectra of acetylated Enocell.

The current findings of the unexpected reactivity of [TMG][OAc] encouraged me to continue the investigation towards benzyl alcohol as a model primary alcohol. As expected, the treatment of benzyl alcohol with [TMG][OAc] resulted in the formation of benzyl acetate, which confirms the reactive nature of this IL (**Figure 33**). The detailed synthesis of the IL, reaction set up, work up and the purification procedure are found in **publication IV**.

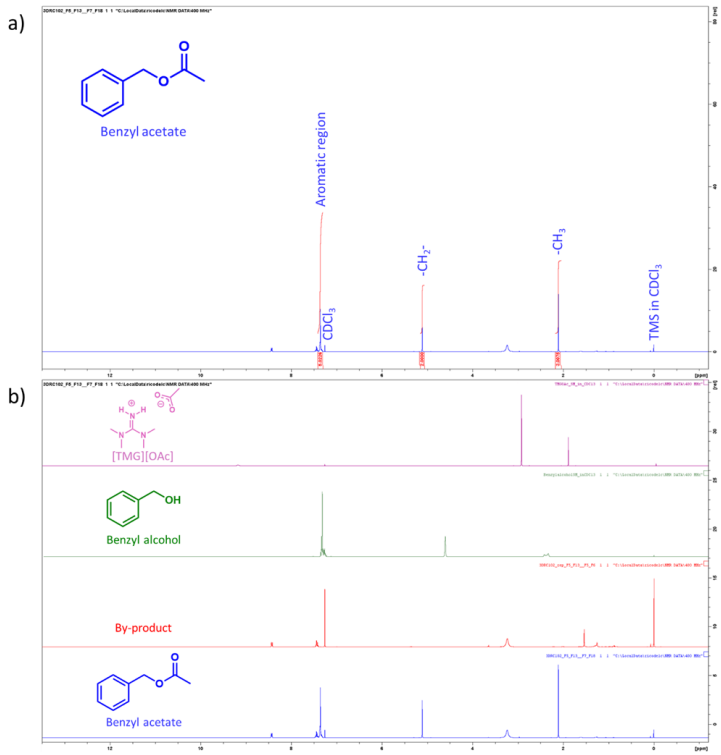

Figure 33. ^{1}H NMR spectra of the reaction products and starting materials. a) ^{1}H NMR spectrum of the reaction product after work up and purification procedures. Benzyl acetate is identified as major product. b) Comparison of ^{1}H NMR spectral data of the obtained fractions during the purification procedure and utilised starting materials: benzyl acetate (blue), unknown by-product (red), benzyl alcohol (green) and [TMG][OAc] (purple).

4.4.3. Design and synthesis of RILs and their application

The continuation of this work towards the design and synthesis of novel task specific ionic liquids (TSILs, **publication IV**) was inspired by the unexpected reactivity of [TMG][OAc] and the interesting research into the formation of strong succinic anhydride-modified cellulose nanofibres by Sehaqui et al.[106] and the proposed TMG-promoted ring-opening polymerisation initiation mechanism II by Chan and co-workers.[107]

Publication IV focuses on the design and synthesis of an ionic liquid with a succinate functional group. This investigation aimed at cellulose dissolution or succinylation by its reactivity with the above-mentioned ionic liquid. Succinic anhydride and TMG were selected as precursors for the synthesis of ionic liquids, which consisted of the succinic anhydride ring opening by the nucleophilic attack of the lone pair of electrons in the nitrogen atom of TMG, in

a similar manner as in the TMG-promoted ring opening polymerisation of *N*-carboxyanhydride.[107] The obtained product is a new ionic liquid, so-called 'TMG$_2$SA', due to the stoichiometry of the synthetic approach, as shown in **Figure 34**. Two molar equivalents of superbase were needed to stabilise the carboxylate formed by the ring opening of succinic anhydride, avoiding further crosslinking. In other words, the second molar equivalent of super base acts as an acid scavenger. Detailed procedures are found in **publication IV**.

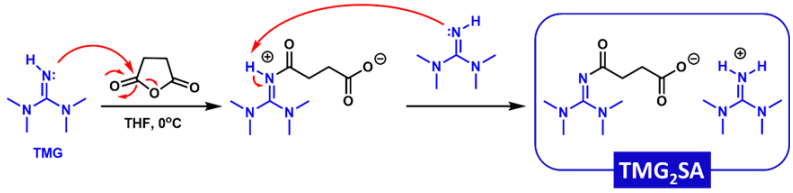

Figure 34. Synthesis of the new ionic liquid 'TMG$_2$SA'.

According to the above-mentioned aim of the investigation, the studies continued towards 'TMG$_2$SA' utilisation in cellulose dissolution and reactivity. The first attempt to dissolve cellulose in neat melted 'TMG$_2$SA' failed due to the high viscosity of the solution. Thus, experiments with the 'TMG$_2$SA':DMSO (20:80 wt.%) electrolyte were evaluated. The fibrillation of cellulose eventually yielded nanocellulose-type materials with one low-demanding energy step in the absence of acids or other mechanical treatments than simple mechanical stirring (**Figure 35)**. Detailed experimental descriptions are found in **publication IV**.

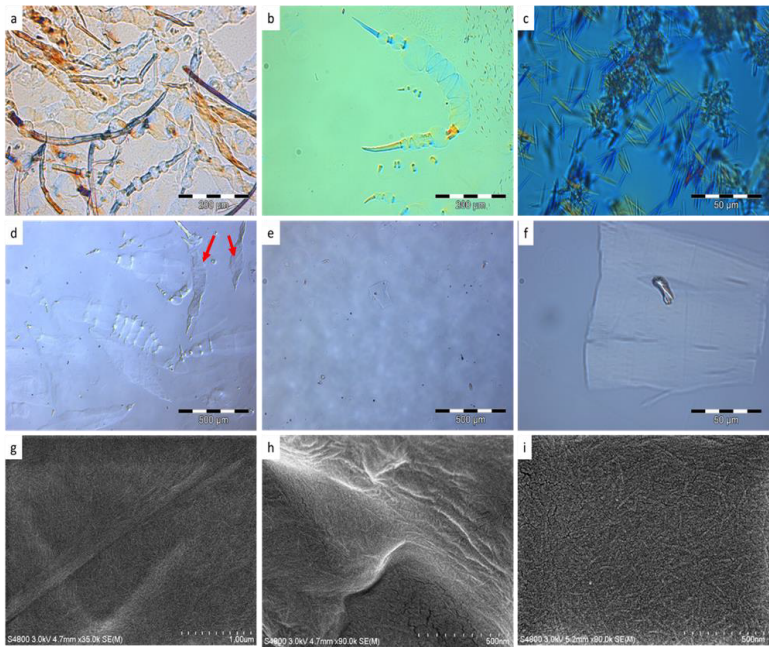

Figure 35. Evidences of pulp fibrillation by OM (a-f) and SEM (g-i) images. Enocell pulp soaked into the '*TMG₂SA*':DMSO (80:20 wt%) electrolyte. OM images were taken directly from the crude reaction mixture, whereas SEM images were taken after the work up in distilled water. a) Swelling by ballooning. Sample standing at room temperature over the weekend without stirring. b-c) Helical unwinding and small needle-like particles. d-f) All of the balloons burst, but secondary cell walls still present together with very small particles. Winding of the secondary cell walls is highlighted with red arrows in image d. g-i) SEM images showing both fibrillar-like structure and nano-sized particles.

It is shown in **Figure 35** that pulp soaked into the 'TMG₂SA':DMSO (20:80 wt.%) electrolyte leads to fibrillation under gentle mechanical stirring. The fibrillation was observed to start at room temperature by swelling (ballooning, **Figure 35a**), and slowly progressed to helical unwinding, reducing the size of the fibres to small needle-like particles (**Figures 35b-c**). Fibrillation occurred more rapidly at 65°C, yielding nano-sized particles (**Figures 35d-i**). The same results were also observed with birch pulp and MCC. The nano-sized particles were recovered in a high yield (**Table 6**). The yields were calculated according to **[Eq.(5)]**, where W_{RN} stands for the dry weight of the recovered nanocellulose-type material and W_{LC} stands for the dry weight of the loaded cellulose.

$$Yield\ (\%) = (W_{RN}/W_{LC}) \cdot 100 \qquad \textbf{(5)}$$

Table 6. *Recovery of nanocellulose-type materials after work-up procedure.*

Pulp	Loaded pulp (g)	Recovered nanocellulose-type material (g)	Yield (%)
Enocell	0.177	0.166	94
MCC	0.169	0.152	90
Birch	0.172	0.151	88

The diffusion-edited ^{1}H NMR of enocell after work-up procedure suggests that the IL reacted with the cellulose chain (**Figure 36a**), which is also visible in the multiplicity-edited ^{1}H-^{13}C HSQC NMR, showing the esterification of cellulose at C6, C3 and C2 (**Figure 36b**).

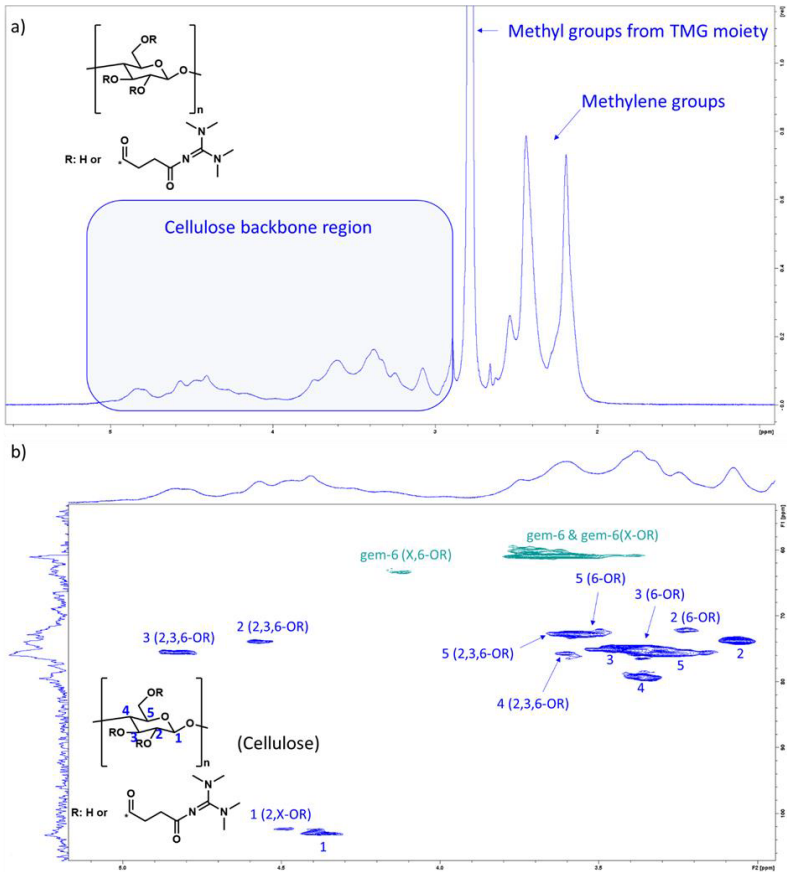

Figure 36. NMR data of Enocell pulp in IL electrolyte after the work-up procedure. a) Diffusion-edited ^{1}H spectrum. b) Multiplicity-edited ^{1}H-^{13}C HSQC spectrum. Correlation assignment numbers represent the positions in cellulose. The numbers in parentheses show which hydroxyls are esterified for that resonance, with 'X' representing uncertainty around whether additional hydroxyls are esterified or not.

β-cyclodextrin was selected as an additional model compound to demonstrate the reactive character of 'TMG$_2$SA' IL. β-cyclodextrin was chosen due to its simpler NMR spectrum, making the NMR analyses less tedious. These experiments resulted in the esterification of β-cyclodextrin at C2 (4.45 ppm) and C3 (5.14 ppm), but not at C-6 (**Figure 37**). The inert nature of hydroxyl groups at C6 is possibly caused by their orientation toward the narrower opening of the β-cyclodextrin conical cylinder shape.[108]

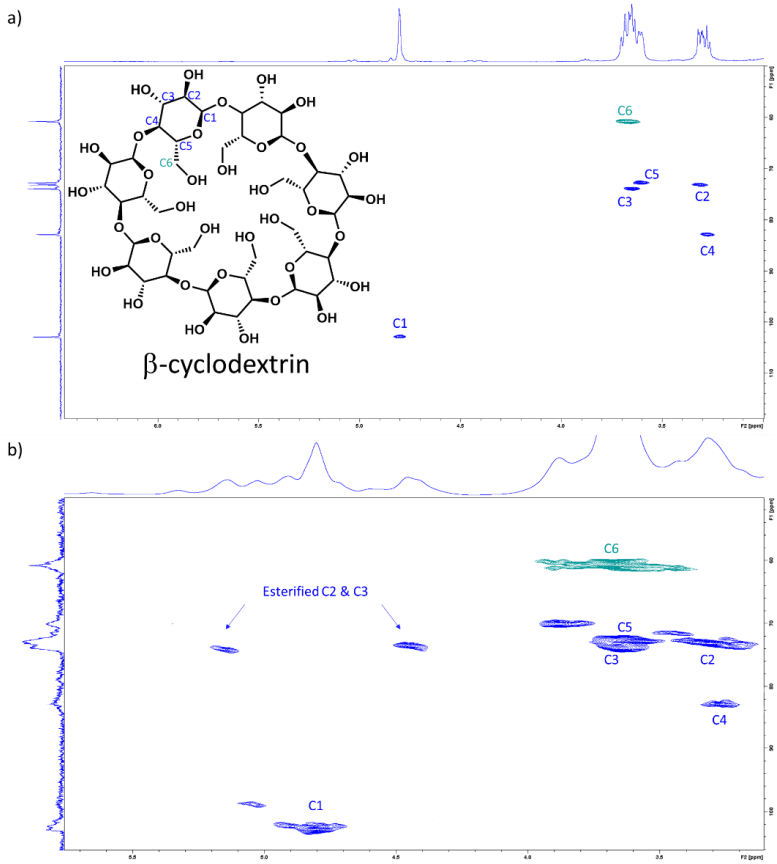

Figure 37. ^{1}H-^{13}C HSQC of β-cyclodextrin. a) Starting material. b) Esterified β-cyclodextrin in IL electrolyte after work-up procedure.

The observed results confirm the success of the investigation, addressing the desired reactivity of the designed novel IL ('TMG$_2$SA') towards cellulose chemical modification. The relatively easy fibrillation of cellulose without involving acids or expensive mechanical treatments might be explained due to the repulsion of negative charges at the succinic anhydride-modified fibril surfaces,

leading to the 'easy' isolation of nanofibres.[106] Similar nanofibrillation phenomena by succinic anhydride have been recently published by Kim and co-workers.[109] In addition, DMSO seems to be a suitable solvent for nanocrystal growth according to the recent work by Meng et al.[110]

Overall, 'TMG_2SA' might offer some possibility as a specific ionic liquid for the esterification of cellulose towards the production of nanocellulose-type materials. Due to its reactive character, 'TMG_2SA' is considered a reactive ionic liquid (RIL). This investigation opened up a broad window to future possibilities combining different superbases (TMG, 1, 5, 7-triazabicyclo[4.4.0]dec-5-ene (TBD), TBD derivatives, etc.) and other anhydrides.

4.4.4. Can there be benefits from the non-innocent nature of ILs?

In general, the reactivity of ionic liquids is undesirable, especially when utilising the IL for dissolution purposes or as a reaction media. This is the case for some IMILs, such as [bmim][OAc][24] or [TMG][OAc], as recently demonstrated in this work. Nevertheless, 'reverse' scientific learning could be adopted from those 'undesired' or 'unexpected' reactions towards the design and synthesis of future reactive ionic liquids (RILs) with a specific application. In this thesis, 'TMG2SA' is a good example, leading to the high yield production of nanocellulose-type materials by a different approach than previously reported.

There are endless possibilities to produce ILs combining different acids and bases. Thus, the future discovery of novel systems with similar synthetic approaches for cellulose chemical modification is just a matter of time and research.

5. Conclusions

Overall, this thesis provides an understanding of the chemistry of different types of ILs and their application in cellulose processing, as well as in the chemical analysis of pulps. The ILs are applied either on their own or as electrolytes with DMSO or GVL as co-solvents.

The results and discussion presented in this thesis show the successful approach towards the mechanistic understanding of the C2 chemistry of IMILs under neutral and acidic conditions, which completes the understanding of the mechanistic scenario of the C2 chemistry of IMILs. This work highlights that the quality of ILs is of great importance.

This work continued the focus on phosphonium ionic liquids, $[P_{4444}][OAc]$ more specifically, mainly due to its better thermal stability. The activation of cellulose chemical reactivity by $[P_{4444}][OAc]$ non-dissolving pre-treatment is demonstrated, where crystallinity removal is proven to be the driving force in the enhancement of the chemical reactivity of the studied pulps. Additionally, the electrolyte $[P_{4444}][OAc]$:d_6-DMSO (20:80 wt.%) is demonstrated to be extremely useful in both the regioselectivity studies of acetylation reactions and the oxidised nanocellulose NMR analyses. This work showed quantitative HSQC as a suitable method for the quantification of the oxidised products from the low molecular weight LDP-CNC and Tox-LDP-CNC samples, demonstrating the potential of this method for cellulose analyses.

On the other hand, the side reactions of IMILs together with the findings of the unexpected reactivity of [TMG][OAc] motivated the author to investigate the design and synthesis of a new, task-specific ionic liquid, 'TMG_2SA'. This novel IL has been shown to be capable of cellulose chemical modification and cellulose fibrillation in an innovative approach. The work performed highlights the potential application of this new type of IL in cellulose chemical modification, the so-called RILs.

The huge range of plausible combinations of cations and anions to form ionic liquid-like compounds opens a very broad range of future plausible candidates for biomass processing. This huge potential of combinations together with deeper understanding in biomass topics such as cellulose dissolution or delignification mechanisms, could bring very interesting future perspectives on the research field. Additionally, more detailed data in the toxicity and recyclability, as well as, reasonable feasibility (e.g., production cost) of new ionic liquids species currently utilized in biomass processing are needed for ILs potential expansion at industrial level in certain areas, such as production of textiles fibers from wood.

6. References

1. K. H. Wahyudiono, M. Sasaki, M. Goto, *Chemical Engineering and Processing,* **2008**, *47*, 1609-1619.
2. A.-M. Boudet, *Phytochemistry* **2007,** *68,* 2722-2735.
3. a) A. T. Martínez, J. Rencoret, G. Marques, A. Gutierrez, D. Ibarra, J. Jiménez-Barbero, J. C. del Río. *Phytochemistry,* **2008**, *69*, 2831-2843. b) Y. Pu, S. Cao, A. J. Ragauskas, *Energy Environ. Sci.,* **2011**, *4*, 3154-3166. c) J. Ralph, K. Lundquist, G. Brunow, F. Lu, H. Kim, P. F. Schatz, J. M. Marita, R. D. Hatfield, S. A. Ralph, J. H. Christensen, W. Boerjan, *Phytochemistry reviews,* **2004**, *3*, 29-60.
4. J. Puls, *Macromol. Symp.* **1997**, *120*, 183-196.
5. E. Sjöström, *Wood chemistry fundamentals and applications.* Academic Press Inc.: Orlando, **1981**, p 223.
6. H. V. Scheller, P. Ulvskov, *Annu. Rev. Plant Biol.*, **2010**, *61*, 263-289.
7. A. Payen, *Comptes Rendus* **1838**, *7*, 1052-1056.
8. P. Zugenmaier, *History of cellulose research. In: Crystalline Cellulose and Derivatives*. Springer series in wood sciences. Springer, Berlin, Heidelberg, **2008**, *chapter 2*, p 7.
9. D. Klemm, B. Heublein, H. P. Fink, A. Bohn, *Angew. Chem. Int. Ed.*, **2005**, *44,* 3358-3393.
10. Y. Pan, R. A. Birdsey, J. Fang, R. Houghton, P. E. Kauppi, W. A. Kurz, O. L. Phillips, A. Shvidenko, SL. Lewis, J. G. Canadell, P. Ciais, R. B. Jackson, S. W. Pacala, A. D. McGuire, S. Pia, A. Rautiainen, S. Sitch, D. Hayes, *Science* **2011**, *333*, 988-993.
11. D. Klemm, B. Philipp, T. Heinze, U. Heinze, W. Wagenknecht, *Comprehensive Cellulose Chemistry. Fundamentals and Analytical Methods*. Wiley-VCH, Chichester, **1998**.
12. A. D. French, *Cellulose*, **2017**, *24*, 4605-4609.
13. a) K.H. Gardner, J. Blackwell, *Biopolymers*, **1974**, *13*, 1975-2001. b) F. J. Kolpak, J. Blackwell, *Macromolecules*, **1976**, *9*, 273-278.
14. F. Horii, A. Hirai, R. kitamura, *ACS symp. Ser.*, **1987**, *340*, 119-134.
15. A. Potthast, S. Radosta, B. Saake, S. Lebioda, T. Heinze, U. Henniges, A. Isogai, A. Koschella, P. Kosma, T. Rosenau, S. Schiehser, H. Sixta, M. Strlič, G. Strobin, W. Vorwerg, H. Wetzel, *Cellulose*, **2015**, *22*, 1591-1613.
16. E. Sjöström, *Wood Chemistry,* Elsevier, **1993**.
17. J. W. S. Hearle, *J. Polym. Sci.*, **1958**, *28*, 432-435.
18. a) Y. Nishiyama, P. Langan, H. Chanzy, *J. Am. Chem. Soc.*, **2002**, *124*, 9074-9082. b) Y. Nishiyama, J. Sugiyama, H. Chanzy, P. Langan, *J. Am. Chem. Soc.*, **2003**, *125*, 14300-14306.
19. a) A. Michud, M. Tanttu, S. Asaadi, Y. Ma, E. Netti, P. Kääriainen, A. Persson, A. Berntsson, M. Hummel, H. Sixta, *Textile Research Journal*, **2016**, *86*, 543-552. b) R. Aitken, *Journal of the Society of Dyers and Colourists*, **1983**, *99*, 150-153. c) J. Chen, S*ynthetic Textile Fibres: Regenerated Cellulose Fibres. In: Woodhead Publishing Series in Textiles*. Textiles and Fashion, Woodhead Publishing, **2015**, Chapter 4,

79-95. d) S. Zhang, C. Chen, C. Duan, H. Hu, H. Li, J. Li, Y. Liu, X. Ma, J. Stavik, Y. Ni, *Bioresources*, **2018**, *13*, 4577-4592.
20. H. A. Krässig, *Cellulose: structure, accessibility and reactivity*. Gordon and Breach Science Publishers, New York. **1993.**
21. a) B. Lindman, G. Karlström, L. Stigsson, *Journal of Molecular Liquids*, **2010**, *156*, 76-81. b) B. Medronho, B. Lindman, *Advances in Colloid and Interface Science*, **2015**, *222*, 502-508.
22. A. F. Turbak, R. B.Hammer, R. E. Davies, H. L. Hergert, *Chemtech*, **1980**, *10*, 51-57.
23. R. P. Swatloski, S. K. Spear, J. D. Holbrey, R. D. Rogers, *J. Am. Chem. Soc.*, **2002**, *124*, 4974-4975.
24. a) G. Ebner, S. Schiehser, A. Potthast, T. Rosenau, *Tetrahedron Letters*, **2008**, *49*, 7322-7324. b) M. T. Clough, K. Geyer, P. A. Hunt, S. Son, U. Vagt, T. Welton, *Green Chem.*, **2015**, *17*, 231-243. c) T. Zweckmair, H. Hettegger, H. Abushammala, M. Bacher, A. Potthast, M.-P. Laborie, T. Rosenau, *Cellulose* **2015**, *22*, 3583; d) H. Abushammala, H. Hettegger, M. Bacher, P. Korntner, A. Potthast, T. Rosenau, M.-P. Laborie, *Cellulose*, **2017**, *24*, 2767. e) S. Gehrke, K. Schmitz, O. Hollóczki, *J. Phys. Chem. B* **2017**, *121*, 4521-4529.
25. a) A. P. Parviainen, *Acid-base conjugate ionic liquids in lignocellulose processing: synthesis, properties and* applications. **2016**. Doctoral dissertation, University of Helsinki, Helsinki, Finland. Retrieved from digital repository of the University of Helsinki (HELDA). http://urn.fi/URN:ISBN:978-951-51-2519-4. b) A. J. Holding, *Ionic liquids and electrolytes for cellulose dissolution*. **2016**. Doctoral dissertation, University of Helsinki, Helsinki, Finland. Retrieved from digital repository of the University of Helsinki (HELDA). http://urn.fi/URN:ISBN:978-951-51-2642-9. c) T. A. Kakko, *Modification and characterization of wood components*. **2019**. Doctoral dissertation, University of Helsinki, Helsinki, Finland. Retrieved from digital repository of the University of Helsinki (HELDA). http://urn.fi/URN:ISBN:978-951-51-4837-7. d) R. Häkkinen, *Carbohydrates in deep eutectic solvents*. **2020**. Doctoral dissertation, University of Helsinki, Helsinki, Finland. Retrieved from digital repository of the University of Helsinki (HELDA). http://urn.fi/URN:ISBN:978-951-51-5813-0.
26. a) A. J. Holding, M. Heikkilä, I. Kilpeläinen, A. W. T. King, *ChemSusChem*, **2014**, *7*, 1422-1434. b) A. J. Holding, V. Mäkelä, L. Tolonen, H. Sixta, I. Kilpeläinen, A. W. T. King, *ChemSusChem*, **2016**, *9*, 880-892. c) A. W. T. King, V. Mäkelä, S. A. Kedzior, T. Laaksonen, G. J. Partl, S. Heikkinen, H. Koskela, H. A. Heikkinen, A. J. Holding, E. D. Cranston, I. Kilpeläinen, *Biomacromolecules*, **2018**, *19*, 2708-2720. d) C. A. Pena, A. Soto, A. W. T. King, H. Rodríguez, *ACS Sustainable Chem. Eng.*, **2019**, *7*, 9164-9171.
27. G.I. Mantanis, R. A. Young, R. M. Rowell, *Cellulose*, **1995**, *2*, 1-22.
28. C. Cuissinat, P. Navard, *Macromol. Symp.*, **2006**, *244*, 1-18; *Macromol. Symp.*, **2006**, *244*, 19-30; *Cellulose*, **2008**, *15*, 67-74.
29. C. Cuissinat, P. Navard, T. Heinze, *Carbohydr. Polym.*, **2008**, *72*, 590-596.

30. a) N. Fleming, A. C. Thaysen, *Biochem J.*, **1920**, *1*, 25-28.1; *Biochem J.*, **1921**, *15*, 407-414.1. b) C. W. Hock, *Text. Res. J.*, **1950**, *20*, 141-151. c) V. W. Tripp, M. L. Rollins, *Anal. Chem.*, **1952**, *24*, 1721-1728. d) M. L. Rollins, V. W. Tripp, *Text. Res. J.*, **1954**, *24*, 345-357.
31. P. Walden, *Bull. Acad. Impér. Sci. St. Pétersbourg*, **1914**, *8*, 405-422.
32. C. Graenacher, *Cellulose solution*, **1934**, *US patent*, 1943176.
33. F. H. Hurley, T. P. Wier, *J.Electrochem. Soc.*, **1951**, *98*, 203-206; *J. Electrochem. Soc.*, **1951**, *98*, 207-212.
34. a) H. L. Chum, V. R. Koch, L. L. Miller, R. A. Osteryoung, *J. Am.Chem. Soc.*, **1975**, *97*, 3264-3265. b) R. J. Gale, B. Gilbert, R. A. Osteryoung, *Inorg. Chem.*, **1978**, *17*, 2728-2729.
35. J. S. Wilkes, J. A. Levisky, R. A. Wilson, C. L. Hussey, *Inorg. Chem.*, **1982**, *21*, 1263-1264.
36. J. S. Wilkes, M. J. Zaworotko, *J. Chem. Soc., Chem. Commun.*, **1992**, 965–967.
37. C. J. Bradaric, A. Downard, C. Kennedy, A. J. Robertson, Y. Zhou, *Industrial preparation of phosphonium ionic liquids. In: Ionic liquids as green solvents*. ACS symposium series. American Chemical Society, Washington, DC, **2003**, chapter 4, p 41. doi: 10.1021/bk-2003-0856.ch004.
38. a) H. Luo, G. A. Baker, J.S. Lee, R. M. Pagni, S. Dai, *J. Phys. Chem. B.*, **2009**, *113*, 4181-4183. b) A. Parviainen, A. W. T. King, I. Mutikainen, M. Hummel, C. Selg, L. K. J. Hauru, H. Sixta, I. Kilpeläinen, *ChemSusChem*, **2013**, *6*, 2161-2169. c) A. Parviainen, R. Wahlström, U. Liimatainen, T. Liitiä, S. Rovio, J. K. J. Helminen, U. Hyväkkö, A. W. T. King, A. Suurnäkki, I. Kilpeläinen, *RSC Adv.*, **2015**, *5*, 69728-69737. d) H. Sixta, A. Michud, L. Hauru, S. Assadi, Y. Ma, A. W. T. King, I. Kilpeläinen, M. Hummel, *Nord. Pulp Pap. Res. J.*, **2015**, *30*, 43-57.
39. a) A. W. T. King, J. Asikkala, I. Mutikainen, P. Järvi, I. Kilpeläinen, *Angew. Chem. Int. Ed.* **2011**, *50*, 6301-6305. b) L. K. J. Hauru, M. Hummel, A. W. T. King, I. Kilpeläinen, H. Sixta, *Biomacromolecules*, **2012**, *13*, 2896-2905. c) A. Parviainen, A. W. T. King, I. Mutikainen, M. Hummel, C. Selg, L. K. J. Hauru, H. Sixta, I. Kilpeläinen, *ChemSusChem*, **2013**, *6*, 2161-2169. d) L. K. J. Hauru, M. Hummel, K. Nieminen, A. Michud, H. Sixta, *Soft Matter*, **2016**, *12*, 1487-1495.
40. S. T. Handy, *Current Organic Chemistry*, **2005**, *9*, 959-988.
41. M. G. Freire, C. M. S. S. Neves, I. M. Marrucho, J. A. P. Countinho, A. M. Fernandes, *J. Phys. Chem. A.*, **2010**, *114*, 3744-3749.
42. S. A. Chowdhury, R. Vijayaraghavan, D. R. MacFarlane, *Green Chem.*, **2010**, *12*, 1023-1028.
43. a) P. G. Jessop, D. J. Heldebrandt, X. Li, C. A. Eckert, C. L. Liotta, *Nature*, **2005**, *436*, 1102. b) H. Xie, X. Yu, Y. Yang, Z. K. Zhao, *Green Chem.*, **2014**, *16*, 2422-2427. c) L. F. B. Wilm et al., *Green Chem.*, **2019**, *21*, 640–648.
44. a) Q. Zhang, N. S. Oztekin, J. Barrault, K. O. Vigier, F. Jérôme, *ChemSusChem*, **2013**, 6, 593-596. b) Y. Yang, L. Song, C. Peng, E. Liu, H. Xie, *Green Chem.*, **2015**, 17, 2758-2763. c) Z. Söyler, K. N. Onwukamike,

S. Grelier, E. Grau, H. Cramail, M. A. R. Meier. *Green Chem.*, **2018**, 20, 214–224.
45. C. M. S. S. Neves, A. M. S. Silva, A. M. Fernandes, J. A. P. Coutinho, *J. Phys. Chem. Lett.*, **2017**, *8*, 3015-3019.
46. a) H. F. N. de Olivera, M. T. Clough, R. Rinaldi, *ChemSusChem*, **2016**, *9*, 3324-3329. b) A. J. Holding, A. Parviainen, I. Kilpelainen, A. Soto, A. W. T. King, H. Rodriguez, *RSC Advances*, **2017**, *7*, 17451-17461.
47. a) K. E. Gutowski, G. A. Broker, H. D. Willauer, J. G. Huddleston, R. P. Swatloski, J. D. Holbrey, R. D. Rogers, *J. Am. Chem. Soc.*, **2003**, *125*, 6632-6633. b) N. J. Bridges, K. E. Gutowski, R. D. Rogers, *Green Chem.*, **2007**, *9*, 177-183. c) V. Najdanovic-Visak, J. N. C. Lopes, Z. P. Visak, J. Trindade, L. P. N. Rebelo, *Int. J. Mol. Sci.*, **2007**, *8*, 736-748. d) C. L. S. Louros, A. F. M. Cláudio, C. M. S. S. Neves, M. G.Freire, I. M. Marrucho, J. Pauly, J. A. P. Coutinho, *Int. J. Mol. Sci.*, **2010**, *11*, 1777-1791.
48. a) M. M. Hossain, L. Aldous, *Aust. J. Chem.*, **2012**, *65*, 1465-1477. b) D. Glas, C. V. Doorslaer, D. Depuydt, F. Liebner, T. Rosenau, K. Binnemans, D. E. de Vos, *J. Chem. Technol. Biotechnol.*, **2015**, *90*, 1821-1826. c) T. Rashid, C. F. Kait, I. Regupathi, T. Murugesan, *Industrial crops and products*, **2016**, *84*, 284-293.
49. Y. Fukaya, K. Hayashi, M. Wada, H. Ohno, *Green Chem.*, **2008**, *10*, 44-46.
50. A. Romero, A. Santos, J. Tojo, A. Rodríguez, *Journal of Hazardous Materials*, **2008**, *151*, 268-273.
51. a) R. C. Remsing, R. P. Sawtloski, R. D. Rogers, F. Moyna, *Chem. Commun.*, **2006**, 1271-1273. b) R. C. Remsing, G. Hernandez, R. P. Swatloski, W. W. Massefski, R. D. Rogers, G. Moyna, *J. Phys. Chem. B*, **2008**, *112*, 11071-11078. c) J. Zhang, H. Zhang, J. Wu, J. Zhang, J. He, J. Xiang, *Phys. Chem. Chem. Phys.*, **2010**, *12*, 1941-1947; *Phys. Chem. Chem. Phys.*, **2010**, *12*, 14829-14830. d) Y. Zhao, X. Liu, J. Wang, S. Zhang, *Chem Phys Chem*, **2012**, *13*, 3126-3133.
52. a) T. G. A. Youngs, J. D. Holbrey, M. Deetlefs, M. Nieuwenhuyzen, M. F. C. Gomes, C. Hardacre, *ChemPhysChem*, **2006**, *7*, 2279–2281. b) T. G. A. Youngs, C. Hardacre, J. D. Holbrey, *J. Phys. Chem. B*, **2007**, *111*, 13765–13774. c) T. G. A. Youngs, J. D. Holbrey, C. L. Mullan, S. E. Norman, M. C. Lagunas, C. D'Agostino, M. D. Mantle, L. F. Gladden, D. T. Bowron, C. Hardacre, *Chem. Sci.*, **2011**, *2*, 1594–1605.
53. a) H. B. Liu, G. Cheng, M. Kent, V. Stavila, B. A. Simmons, K. L. Sale, S. Singh, *J. Phys. Chem. B*, **2012**, *116*, 8131–8138. b) F. Huo, Z. P. Liu, W. C. Wang, *J. Phys. Chem. B*, **2013**, *117*, 11780–11792. c) B. D. Rabideau, A. Agarwal, A. E. Ismail, *J. Phys. Chem. B*, **2014**, *118*, 1621–1629.
54. a) B. Lu, A. Xu, J. Wang, *Green Chem.*, **2014**, *16*, 1326-1335. b) R. S. Payal, S. Balasubramanian, *Phys. Chem. Chem. Phys.*, **2014**, *16*, 17458–17465. c) H. F. N. de Oliveira, R. Rinaldi, *ChemSusChem*, **2015**, *8*, 1577-1584. d) E. Hassan, F. Mutelet, M. Bouroukba, *Carbohydr. Polym.*, **2015**, *127*, 316–324.
55. A. W. T. King, A. Parviainen, P. Karhunen, J. Matikainen, L. K. J. Hauru, H. Sixta, I. Kilpeläinen, *RSC Adv.* **2012**, *2*, 8020.

56. a) S.-K. Ruokonen, C. Sanwald, M. Sundvik, S. Polnick, K. Vyavaharkar, F. Duša, A. J. Holding, A. W. T. King, I. Kilpeläinen, M. Lämmerhofer, P. Panula, S. K. Wiedmer, *Environ. Sci. Technol.*, **2016**, *50*, 7116-7125. b) J. Witos, G. Russo, S.-K. Ruokonen, S. K. Wiedmer, *Langmuir*, **2017**, *33*, 1066-1076.
57. a) M. Jelínková, J. Briestenský, I. Santar, B. Říhová, *Int. Immunopharmacol.*, **2002**, *10*, 1429-1441. b) D. S. Zimnitsky, T. L. Yurkshtovich, P. M. Bychkovsky, *J. Colloid. Interf. Sci.*, **2006**, *1*, 33-40. c) S. Fischer, K. Thümmler, B. Volkert, K. Hettrich, I. Schmidt, K. Fischer, *Macromol. Symp.*, **2008**, *262*, 89-96. d) B. Belhalfaoui, A. Aziz, E. H. Elandaloussi, M. S. Ouali, L. C. De Ménorval, *Journal of Hazardous Materials*, **2009**, *169*, 831-837. e) A. A. Vaidya, M. Gaugler, D. A. Smith, *Carbohydr. Polym.*, **2016**, *136*, 1238-1250. f) W. Shang, Z. Sheng, Y. Shen, B. Ai, L. Zheng, J. Yang, Z. Xu, *Carbohydr. Polym.*, **2016**, *141*, 135-142.
58. a) T. Heinze, T. F. Liebert, K. S. Pfeiffer, M. A. Hussain, *Cellulose*, **2003**, *10*, 283-296. b) M. Jebrane, G. Sèbe, *Holzforschung*, **2007**, *61*, 143-147. c) M. Jebrane, F. Pichavant, G. Sèbe, *Carbohydr. Polym.*, **2011**, *83*, 339-345. d) J. Chen, J. Xu, K. Wang, X. Cao, R. Sun, *Carbohydr. Polym.*, **2016**, *137*, 685-692.
59. a) J. Li, L.-P. Zhang, F. Peng, J. Bian, T. Q. Yuan, F. Xu, R.-C. Sun, *Molecules* **2009**, *14*, 3551-3566. b) C.-Y. Chen, M.-J. Chen, X.-Q. Zhang, C.-F. Liu, R.-C. Sun, *J. Agric. Food. Chem.*, **2014**, *62*, 3446-3452.
60. a) J. Wu, J. Zhang, H. Zhang, J. He, Q. Ren, M. Guo, *Biomacromolecules* **2004**, *5*, 266-268. b) M. Granström, J. Kavakka, A. W. T. King, J. Majoinen, V. Mäkelä, J. Helaja, S. Hietala, T. Virtanen, S.-L. Maunu, D. S. Agyropoulos, I. Kilpeläinen, *Cellulose* **2008**, *15*, 481-488. c) H. Nawaz, P. A. R. Pires, T. A. Bioni, E. P. G. Arêas, O. A. El-Seoud, *Cellulose*, **2014**, *21*, 1193-1204. d) O. Jogunola, V. Eta, M. Hedenström, O. Sundman, T. Salmi, J.-P. Mikkola, *Carbohydr. Polym.*, **2016**, *135*, 341-348.
61. T. Kakko, A. W. T. King, I. Kilpelainen, *Cellulose*, **2017**, *24*, 5341-5354.
62. a) R. Kakuchi, M. Yamaguchi, T. Endo, Y. Shibata, K. Ninomiya, T. Ikai, K. Maeda, K. Takahashi, *RSC Adv.*, **2015**, *5*, 72071-72074. b) R. Kakuchi, R. Ito, S. Nomura, H. Abroshan, K. Ninomiya, T. Ikai, K. Maeda, H. J. Kim, K. Takahashi, *RSC Adv.*, **2017**, *7*, 9423-9430.
63. M. C. Kuo, R. T. Bogan, *Process for the manufacture of cellulose acetate,* **1997**, US patent 5608050.
64. a) A. Isogai, Y. Kato, *Cellulose* **1998**, *5*, 153-164. b) T. Isogai, T. Saito, A. Isogai, *Cellulose* **2011**, 18, 421-431. c) H. Orelma, I. Filpponen, L.-S. Johansson, M. Österberg, O. J. Rojas, J. Laine, *Biointerphases* **2012**, *7*, 61-73. d) S. Fukui, T. Ito, T. Saito, T. Noguchi, A. Isogai, *Composites Science and Technology* **2018**, *167*, 339-345. e) X. Guo, L. Liu, Y. Hu, Y. Wu, *Carbohydr. Polym.*, **2018**, *197*, 524-530.
65. a) T. Kitaoka, A. Isogai, F. Onabe, *Nordic Pulp and Paper Research Journal*, **1999**, *4*, 279-284. b) M. Hirota, N. Tamura, T. Saito, A. Isogai, *Carbohydrate Polymers*, **2009**, *78*, 330-335 c) T. Saito, M. Hirota, N. Tamura, A. Isogai, *J. Wood. Sci.*, **2010**, *56*, 227-232.

66. P.-P. Xin, Y.-B. Huang, C.-Y. Hse, H. N. Cheng, C. Huang, H. Pan, *Materials*, **2017**, *10*, 526/1-526/14.
67. P. Huang, Y. Zhao, S. Kuga, M. Wu, Y. Huang, *Nanoscale*, **2016**, *8*, 3753-3759.
68. a) W. Czaja, A. Krystynowicz, S. Bielecki, R. M. Brown, *Biomaterials*, **2006**, *27*, 145-151. b) R. J. Moon, A. Martini, J. Nairn, J. Simonsen, J. Youngblood, *Chem. Soc. Rev.*, **2011**, *40*, 3941-3994. c) N. Shah, M. Ul-Islam, W. A. Khattak, J. K. Park, *Carbohydr. Polym.*, **2013**, *98*, 1585-1598. d) J. Huang, A. Dufrense, N. Lin, *Nanocellulose. From fundamentals to Advance materials*. Wiley-VCH, Weinheim, Germany, **2019**, Chapter 1, 1-20.
69. a) C. Yan, J. Wang, W. Kang, M. Cui, X. Wang, C. Y. Foo, K. J. Chee, P. S. Lee, *Adv. Mater.*, **2014**, *26*, 2022-2027. b) N. Lin, A. Dufresne, *European Polymer Journal,* **2014**, *59*, 302-325. c) Z. Shi, X. Gao, M. W. Ullah, S. Li, Q. Wang, G. Yang, *Biomaterials*, **2016**, *111*, 40-54. d) A. Jasmin, M. W. Ullah, Z. Shi, X. Lin, G. Yang, *Carbohydr. Polym.*, **2017**, *163*, 62-69.
70. S. Eyley, W. Thielemans, *Nanoscale*, **2014**, *6*, 7764-7779.
71. a) D. Trache, M. H. Hussin, M. K. M. Haafiz, V. K. Thakur, *Nanoscale*, **2017**, *9*, 1763-1786. b) S. Pirani, R. Hashaikeh, *Carbohydr. Polym.* **2013**, *93*, 357–363. c) Y. Li, G. Li, Y. Zou, Q. Zhou, X. Lian, *Cellulose* **2014**, *21*, 301–309.
72. a) L. Heux, G. Chauve, C. Bonini, *Langmuir*, **2000**, *16*, 8210-8212. b) J. Araki, M. Wada, S. Kuga, *Langmuir*, **2001**, *17*, 21-27. c) A. Pakzad, J. Simonsen, R. S. Yassar, *Composites Science and Technology*, **2012**, *72*, 314-319.
73. a) J. Bras, D. Viet, C. Bruzzese, A. Dufresne, *Carbohydr. Polym.*, **2011**, *84*, 211-215. b) J. P. S. Morais, M. Rosa, F. de, M. de Souza Filho, M. de sá, L. D. Nascimento, D. M. do Nascimento, A. R. Cassales, *Carbohydr. Polym.*, **2013**, *91*, 229-235.
74. J. Araki, M. Wada, S. Kuga, Okano, *Colloids and surfaces A: physicochemical and engineering aspects*, **1998**, *142*, 75-82
75. S. C. Espinosa, T. Kuhnt, E. J. foster, C. Weder, *Biomacromolecules*, **2013**, *14*, 1223-1230.
76. P. B. Filson, B.E. Dawson-Andoh, D. Schwegler-Berry, *Green Chem.*, **2009**, *11*, 1808-1814.
77. a) D. S. Perez, S. Montanari, M. R. Vignon, *Biomacromolecules*, **2003**, *4*, 1417-1425. b) A. C. W. Leung, S. Hrapovic, E. Lam, Y. Liu, K. B. Male, K. A. Mahmoud, J. H. T. Luong, *small*, **2011**, *7*, 302-305. c) X. Cao, B. Ding, J. Yu, S. S. Al-deyab, *Carbohydr. Polym.*, **2012**, *90*, 1075-1080.
78. a) M. Pääkkö, M. Ankerfors, H. Kosonen, A. Nykänen, S. Ahola, M. Österberg, J. Ruokolainen, J. Laine, P. T. Larsson, O. Ikkala, T. Lindström, *Biomacromolecules*, **2007**, *8*, 1934-1941. b) K. Abe, S. Iwamoto, H. Yano, *Biomacromolecules*, **2007**, *8*, 3276-3278. c) K. Uetani, H. Yano, *Biomacromolecules*, **2011**, *12*, 348-353. d) W. Chen, Q. Li, Y. Wang, X. Yi, J. Zeng, H. Yu, Y. Liu, J. Li, *ChemSusChem*, **2014**, *7*, 154-161.
79. T. Saito, S. Kimura, Y. Nishiyama, A. Isogai, *Biomacromolecules*, **2007**, *8*, 2485-2491.

80. L. Wågberg, G. Decher, M. Norgren, T. Lindström, M. Ankerfors, K. Axnäs, *Langmuir*, **2008**, *24*, 784-795.
81. W. Chen, H. Yu, S.-Y. Lee, T. Wei, J. Li, Z. Fan, *Chem. Soc. Rev.*, **2018**, *47*, 2837-2872.
82. M. W. Ullah, M. UI-Islam, S. Khan, Y. Kim, J. K. Park, *Carbohydr. Polym.*, **2016**, *136*, 908-916.
83. a) C. Castro, R. Zuluaga, C. Álvarez, J.-L. Putaux, G. Caro, O. J. Rojas, I. Mondragon, P. Gañán, *Carbohydr. Polym.*, **2012**, *89*, 1033-1037. b) M. Ul-Islam, T. Khan, J. K. Park, *Carbohydr. Polym.*, **2012**, *89*, 1189-1197.
84. a) P. Lu, Y.-L. Hsieh, *Carbohydr. Polym.*, **2010**, *82*, 329-336. b) A. Dufresne, *Materials today*, **2013**, 16. 220-227.
85. a) A. Dufresne, D. Dupeyre, M. R. Vignon, *Journal of Applied Polymer Science* **2000**, *76*, 2080-2092. b) M. E. Malainine, M. Mahrouz, A. Dufresne, *Composites Science and Technology* **2005**, *65*, 1520–1526. c) R. Zuluaga, J.-L. Putaux, A. Restrepo, I. Mondragon, P. Gañán, *Cellulose* **2007**, *14*, 585– 592. d) S.-Y. Lee, S.-J. Chun, I.-A. Kang, J.-Y. Park, *Journal of Industrial and Engineering Chemistry* **2009**, *15*, 50–55. e) Y. Chen, C. Liu, P. R. Chang, X. Cao, D. P. Anderson, *Carbohydr. Polym.*, **2009**, *76*, 607-615. f) I. Siro, D. Plackett, *Cellulose* **2010**, *17*, 459–494. g) M. F. Rosa, E. S. Medeiros, J. A. Malmonge, K. S. Gregorski, D. F. Wood, L. H. C. Mattoso, G. Glenn, W. J. Orts, S. H. Imam, *Carbohydr. Polym.*, **2010**, *81*, 83-92. h) A. Ferrer, I. Filpponen, A. Rodríguez, J. Laine, O. J. Rojas, *Bioresource Technology* **2012**, *125*, 249–255. i) Y. Xu, J. Salmi, E. Kloser, F. Perrin, S. Grosse, J. Denault, P. C. K. Lau, *Ind. Crops Prod.*, **2013**, *51*, 381-384. j) H. Lu, Y. Gui, L. Zheng, X. Liu, *Food Res. Int.*, **2013**, *50*, 121-128. k) N. A. Rosli, I. Ahmad, I. Abdullah, *BioResources*, **2013**, *8*, 1893-1908. l) Y.-L. Hsieh, *J. Mater. Sci.*, **2013,** *48*, 7837-7846.
86. a) A. Chakraborty, M. Sain, M. Kortschot, *Holzforschung*, **2005**, *59*, 102–107. b) T. T. T. Ho, K. Abe, T. Zimmermann, H. Yano, *Cellulose*, **2015**, *22*, 421–433.
87. P. Satyamurthy, N. Vigneshwaran, *Enzyme Microb. Technol.*, **2013**, *52*, 20-25.
88. a) Q. Xu, Y. Gao, M. Quin, K. Wu, Y.Fu, J. Zhao, *Int. J. Biol. Macromol.*, **2013**, *60*, 241-247. b) T. Q. Hu, R. Hashaikeh, R. M. Berry, *Cellulose*, **2014**, *21*, 3217-3229.
89. a) A. C. W. Leung, S. Hrapovic, E. Lam, Y. Liu, K. B. Male, K. A. Mahmoud, J. H. T. Luong, *small*, **2011**, *7*, 302-305. b) X. Cao, B. Ding, J. Yu, S. S. Al-deyab, *Carbohydr. Polym.*, **2012**, *90*, 1075-1080.
90. E. Kontturi, A. Meriluoto, P. A. Penttilä, N. Baccile, J.-M. Malho, A. Potthast, T. Rosenau, J. Ruokolainen, R. Serimaa, J. Laine, H. Sixta, *Angew. Chem. Int. Ed.*, **2016**, *55*, 14455-14458.
91. G. Zhu, N. Lin, Surface chemistry of nanocellulose. In: *Nanocellulose: From Fundamentals to Advance Materials.* Wiley-VCH Verlag GmbH & Co. KgaA. Weinheim, Germany, **2019**, *chapter 5*, p 115-153.
92. M. Wojdyr, *J. Appl. Cryst.*, **2010**, *43*, 1126-1128.

93. a) M. Mazza, D.-A. Catana, C. Vaca-Garcia, C. Cecutti, *Cellulose*, **2009**, *16*, 207-215. b) D. L. Minnick, R. A. Flores, M. R. DeStefano, A. M. Scurto, *J. Phys. Chem. B*, **2016**, *120*, 7906-7919.
94. A. D. French, *Cellulose*, **2014**, *21*, 885-896.
95. G. Zuckerstätter, G. Schild, P. Wollboldt, T. Röder, H. K. Weber, H. Sixta, *Lenzinger Berichte*, **2009**, *87*, 38-46.
96. H. Kono, H. Hashimoto, Y. Shimizu, *Carbohydr. Polym.*, **2015**, *118*, 91-100.
97. J.-F. Sassi, H. Chanzy, *Cellulose*, **1995**, *2*, 111-127.
98. J. Buffiere, P. Ahvenainen, M. Borrega, K. Svedström, H. Sixta, *Green Chem.*, **2016**, *18*, 6516–6525.
99. a) A. Villares, C. Moreau, B. Cathala, *ACS Omega*, **2018**, *3*, 16203-16211. b) F. Lin, F. Cousin, J.-L. Putaux, B. Jean, *ACS Macro. Lett.*, **2019**, *8*, 345-351.
100. H. Koskela, I. Kilpeläinen, S. Heikkinen, *Journal of Magnetic Resonance* **2005**, *174*, 237-244.
101. Z. Ling, T. Wang, M. Makarem, M. S. Cintrón, H. N. Cheng, X. Kang, M. Bacher, A. Potthast, T. Rosenau, H. King, C. D. Delhom, S. Nam, J. V. Edwards, S. H. Kim, F. Xu, A. D. French, *Cellulose*, **2019**, *26*, 305-328.
102. a) O. Hollóczki, *Inorg. Chem.* **2014**, *53*, 835-846. b) N. M.A.N. Daud, E. Bakis, J. P. Hallet, C. C. Weber, T. Welton, *Chem. Commun.* **2017**, *53*, 11154-11156. c) J. Dupont, J. Spencer, *Angew. Chem. Int. Ed.* **2004**, *43*, 5296-5297. d) Y. Chu, H. Deng, J-P. Cheng, *J. Org. Chem.* **2007**, *72*, 7790-7793. e) S. Sowmiah, V. Srinivasadesikan, M-C. Tseng, Y-H. Chu, *Molecules* **2009**, *14*, 3780-3813. f) A. J. III. Arduengo, J. R. Goerlich, W. J. Marshall, *J. Am. Chem. Soc.* **1995**, *117*, 11027-11028. g) M. N. Hopkinson, C. Richter, M. Schedler, F. Glorius, *Nature* **2014**, *510*, 485-496. h) E. Ennis, S. T. Handy, *Curr. Org. Syn.* **2007**, *4*, 381-389. i) B. Erwin. C. Omoshile, *Acc. Chem. Res.* **2000**, *33*, 672-678. j) R. A. Olofson, W. R. Thompson, J. S. Michelman, *J. Am. Chem. Soc.* **1964**, *86*, 1865-1866. k) M. Alcarazo, S. J. Roseblade, E. Alonso, R. Fernández, E. Alvarez, F. J. Lahoz, J. M. Lassaletta, *J. Am. Chem. Soc.* **2004**, *126*, 13242-13243. l) M. J. Earle, K .R. Seddon, *Imidazole carbenes*. U.K. Patent WO 2001077081, October 18, **2001**. m) A. J. III. Arduengo, J. R. Goerlich, D. Khasnis, *Preparation of relatively stable 1,3-disubstitutedimidazol-2-ylidene carbenes*. U.S. Patent WO 9827064, June 25, **1998**; n) Y. Zhang, J. Y. G. Chan, *Energy Environ. Sci.* **2010**, *3*, 408-417. o) W. A. Hermann, *Angew. Chem. Int. Ed.* **2002**, *41*, 1290-1309. p) H. Rodríguez, G. Gurau, J. D. Holbrey, R. D. Rogers, *Chem. Commun.*, **2011**, *47*, 3222-3224. q) G. Gurau, H. Rodríguez, S. P. Kelley, P. Janiczek, R. S. Kalb, R. D. Rogers, *Angew. Chem. Int. Ed.*, **2011**, *50*, 12024-12026. r) A. J. III. Arduengo, R. L. Harlow, M. Kline, *J. Am. Chem. Soc.* **1991**, *113*, 361-363. s) W. A. Herrmann, C. Köcher, *Angew. Chem. Int. Ed.* **1997**, *36*, 2162-2187. t) V. Kumar, R. Rai, S. Pandey, *RSC Adv.* **2013**, *3*, 11621-11627.
103. a) A. G. Avent, P. A. Chaloner, M. P. Day, K. R. Seddon, T. Welton, *J. Chem. Soc. Dalton. Trans.* **1994**, *23*, 3405-3413. b) S-T. Lin, M-F. Ding, C-W. Chang, S-S. Lue, *Tetrahedron* **2004**, *60*, 9441-9446. c) K. M. Jr.

Dieter, C. J. Dymek, N. E. Heimer, J. W. Rovang, J. S. Wilkes, *J. Am. Chem. Soc.* **1988**, *110*, 2722-2726.

104. S. Gehrke, O. Hollóczki, *Angew. Chem. Int. Ed.* **2017**, *56*, 16395-16398.

105. a) Q. Zhang, N. S. Oztekin, J. Barrault, K. D. O. Vigier, F. Jérôme, *ChemSusChem*, **2013**, *6*, 593-596. b) Y. Yang, L. Song, C. Peng, E. Liu, H. Xie, *Green Chem.*, **2015**, 17, 2758-2763. c) Z. Söyler, K. N. Onwukamike, S. Grelier, E. Grau, H. Cramail, M. A. R. Meier, *Green Chem.,* **2018**, *20*, 214-224.

106. H. Sehaqui, K. Kulasinski, N. Pfenninger, T. Zimmermann, P. Tingaut. *Biomacromolecules*, **2017**, *18*, 242-248.

107. B. A. Chan, S. Xuan, M. Horton, D. Zhang, *Macromolecules*, **2016**, *49*, 2002−2012.

108. S. Kobayashi et al. (**2012**) Water in Organic Synthesis. Chapter 6.3 β-cyclodextrin chemistry in water, pp 773-805. Georg Thieme Verlag KG, Stuttgart, New York.

109. J.-K. Kim, B. Choi, J. Jin, *Carbohydrate Polymers*, 2020, *249*, 116823-116830.

110. Z. Meng, D. Sawada, C. Laine, Y. Ogawa, T. Virtanen, Y. Nishiyama, T. Tammelin, E. Kontturi, *Biomacromolecules*, **2021**, https://dx.doi.org/10.1021/acs.biomac.0c01600.